Thermodynamics and Kinetics of CVD Processes of Si and GaAs

Hugo de Moor

THERMODYNAMICS AND KINETICS OF CVD PROCESSES OF Si AND GaAs

THERMODYNAMICS AND KINETICS OF CVD PROCESSES OF Si AND GaAs

PROEFSCHRIFT

TER VERKRIJGING VAN DE GRAAD VAN DOCTOR IN DE
WISKUNDE EN NATUURWETENSCHAPPEN AAN DE
KATHOLIEKE UNIVERSITEIT TE NIJMEGEN,
OP GEZAG VAN DE RECTOR MAGNIFICUS
PROF. DR. B.M.F. VAN IERSEL
VOLGENS BESLUIT VAN HET COLLEGE VAN DEKANEN
IN HET OPENBAAR TE VERDEDIGEN
OP WOENSDAG 28 JANUARI 1987
DES NAMIDDAGS OM 3.30 UUR

DOOR

HUGO HYPOLITE CORNELIS DE MOOR

GEBOREN TE TILBURG.

DRUK: SNELDRUK ENSCHEDE

PROMOTOREN:

PROF. DR. L. J. GILING

PROF. DR. P. BENNEMA

voor

mijn ouders

Lucie

in herinnering aan

Jan Bloem

Dankwoord

Dit proefschrift zou niet in deze vorm voor u liggen zonder de steun van velen. Hierbij wil ik dan ook iedereen bedanken die me gesteund heeft op het werk, maar ook thuis.

In het bijzonder wil ik de afdeling Vaste stof III en Chemie bedanken voor de prettige sfeer. Zowel het enthousiasme waarmee er gewerkt werd, de gezelligheid tijdens en tussen het werk, alsook de persoonlijke betrokkenheid. Met name denk ik hierbij aan de "eetclub". Ik vond er een ambiance om me als mens en wetenschapper te vormen en de kracht om dit proefschrift te voltooien.

Met name een woord van dank aan alle studenten die direkt een bijdrage hebben geleverd aan dit werk; Hans Buskes, Robert Pet, Hans Hanssen en Arie Saaman, voor de oven-experimenten, Arie Saaman en Wim Jacobs voor de adsorptieberekeningen en Theun Lourens, Hans Janssen en Karel van Bommel voor de ets-experimenten.

John Giling, Johan van de Ven en Jan Weyher, ik heb nooit vergeefs een beroep op jullie gedaan en vond er een goed wetenschappelijk klankbord.

De technische ondersteuning van Harrie v/d Linden en Jan van Oyen was onontbeerlijk om de apparatuur draaiende te houden.

De algemene en technische diensten van de fakulteit, met name de glasblazers en instrumentmakerij, hebben me nooit in de kou laten staan.

De komputers van het IVV hebben het mogelijk gemaakt om talloze berekeningen uit te voeren en dit manuscript te vervaardigen.

Voor het gereed maken van het boekje wil ik Lucie Nollen, Hans Janssen, Theun Lourens en Peter Bogers bedanken. Ondanks mijn kritische blik hadden zij het geduld om mooie illustraties en een goede lay-out te verzorgen.

Op dit voor mij heugelijke moment wil ik even stilstaan bij Jan Bloem, die dit helaas niet heeft mogen meemaken. Zijn opvatting dat eenvoud in de wetenschap van het grootste belang is heeft veel indruk op me gemaakt. Het is onvergetelijk, hoe hij tot het laatste moment belangstelling had voor mij en mijn werk.

The study presented in this thesis has been carried out as a part of the research program of the Netherlands Foundation for Chemical Research (SON) with financial aid from the Netherlands Organisation for the advance of Pure Research (ZWO).

The following chapters of this thesis are published, or submitted for publication:

Chapter 2

Adsorption on Si(111) during CVD of silicon from silane: the effect of temperature, bond strength, supersaturation and pressure.
L.J. Giling, H.H.C. de Moor, W.P.J.H. Jacobs and A.A. Saaman,
J. Crystal Growth 78 (1986) 303

Chapter 3

Adsorption and growth kinetics on Si(100) for CVD of silicon from silane: the effect of surface reconstruction.
H.H.C. de Moor and L.J. Giling,
J. Crystal Growth

Chapter 4

Epitaxial growth of silicon by CVD in a hot-wall furnace.
J. Bloem, Y.S. Oei, H.H.C. de Moor, J.H.L. Hanssen and L.J. Giling,
J. Electrochem. Soc. 132 (1985) 1973

Chapter 5

Near equilibrium growth of silicon by CVD.
II. The Si-I-H system.
J.H.L. Hanssen, A.A. Saaman, H.H.C. de Moor, L.J. Giling and J. Bloem,
J. Crystal Growth 65 (1983) 406

Chapter 6

Subsurface trapping during growth and doping of III-V compounds.
L.J Giling and H.H.C de Moor,
J. Crystal Growth

CONTENTS

CHAPTER 1

INTRODUCTION

The chemistry and physics of CVD

In this thesis the growth and etching by CVD of monocrystalline semiconductors is studied. Several aspects are encountered which are general for CVD, but also special features more appropriate to crystalline surfaces and semiconducting materials will be treated. The emphasis in this work is given to:

1. the thermodynamics of the chemical reactions in the gas phase, which will be the leitmotiv throughout this thesis
2. the mutual influence of the surface structure on the adsorption of reactants and impurities
3. the incorporation of dopants in the crystal lattice

The thermodynamic approach used in the first topic is applicable to all CVD processes and will be elaborated in section 4. The background of the crystalline aspects used in this thesis will be elucidated in a discussion on the surface properties of Si and GaAs; (5). The principles of the trapping of atomic impurities during growth are explained in the last part of this introduction (6). As all the studies are performed to gain more insight in the total CVD process of Si and GaAs, to start with, an introduction will be given to the process as a whole.

1. General aspects of CVD

Chemical Vapour Deposition is in principle a method to cover, from the gas phase, a substrate with a thin layer via chemical reactions. The reactants are introduced in the gaseous form, diluted in a carrier gas, such as hydrogen and nitrogen and then transported to the reaction

zone. There, because of an increase in temperature, the input becomes unstable and all kind of chemical reactions take place. Eventually this results in the formation of a deposit. As the substrate surface usually acts catalytically on the decomposition of the reactants, it is often the most preferable site for the deposition.

The deposited film can be in an amorphous, poly- or single-crystalline form and may be used for its electrical, optical, mechanical or chemical properties, which are usually complementary to the properties of the bulk [1,2]. The applications range from thick amorphous coatings on cutlery to atomically thin layers for solid state lasers.

For example amorphous TiC, TiN or Al_2O_3 layers are used as a wear and chemical resistant coating on cutting tools. CVD is also applied to deposit thin films of zirconia on turbine blades, as this isolates against heat. In ceramics, CVD of amorphous SiC and Si_3N_4 is of increasing importance, as this is the best method to obtain dense layers. In the field of telecommunication, deposition of doped SiO_2 on the wall of a quartz tube is applied in the fabrication of optical fibers. Last but not least CVD is an indispensible technique in semiconductor industry. Amorphous SiO_2 or oxynitrides are used as protective layers in masking, whereas polycrystalline deposits of WSi_2, $TaSi_2$ or Al are applied for ohmic contacts.

The main interest however is the growth of monocrystalline layers, as this is the electrical or electro-optical active heart of the device. Transistors, diodes, solid state lasers and more advanced structures are hard to imagine without the application of CVD techniques. Especially in the technology of III-V compounds enormous progress has been made the last few years. Whereas in silicon epitaxy the layer thickness is in the order of microns, for GaAs-$Al_xGa_{1-x}As$ quantum well lasers the active layers are typically 50 A with a transition width between two layers of only one atomic layer. This kind of technologically tour de forces are likely to open a new world for the physicists as structures with atomic dimensions become available and are a challenge for materials scientists to aim at the physically possible limits.

2. Outline of CVD on a crystalline substrate

Growth of an epitaxial (= monocrystalline) layer with CVD, which is relevant in this study, can be divided schematically, as indicated in fig. 1, in the following steps [3]:

1. mixing of reactants and transport to the hot zone
2. transport, by diffusion, through the hot zone coupled with chemical reactions in the gas phase
3. adsorption on the crystal surface
4. surface diffusion to the reactive sites
5. incorporation in the crystal lattice (via chemical reactions)
6. desorption of the products
7. transport of the products through the hot zone to the exhaust

In an analysis of a CVD process it is essential to characterize each step as good as possible, as one weak link in the chain of reactions can have an adverse effect on the whole process. Essential in such a study is the determination of the reaction step which proceeds most difficult and therefore demanding the greatest potential difference: the rate limiting step in the growth process. Roughly a division can be made between diffusion (mass transport) and surface (kinetically) controlled processes. The potential difference between in- and output is in the first case needed to diffuse reactants to the surface and products away from the crystal, in the second case it is all needed to overcome an energy barrier on the crystal surface; fig.2

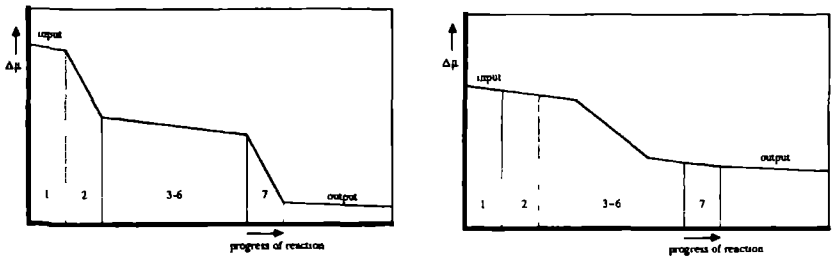

Fig.2

A) Potential drop for a diffusion limited process (step 2 and 7).

B) Potential drop, in case one of the surface steps (3,4,5 or 6) is rate limiting.

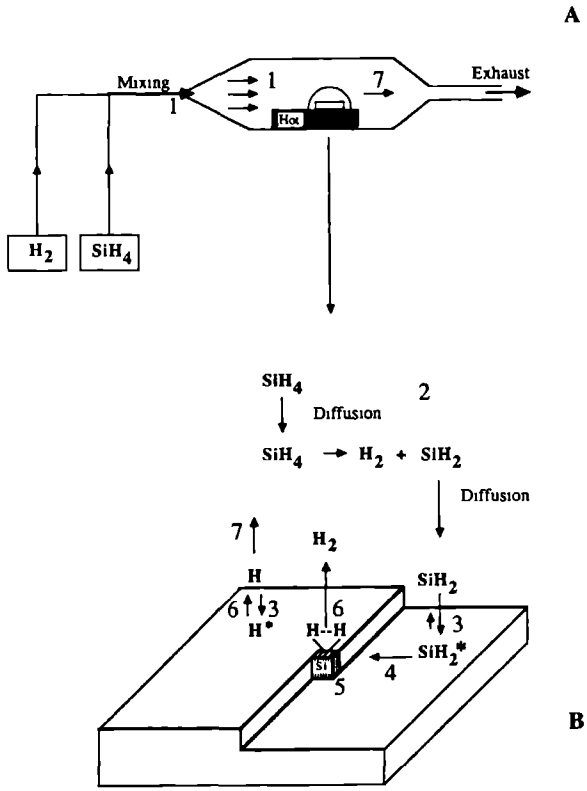

Fig.1 Schematic view of the growth of silicon from silane by CVD, indicating the different steps in the process.
A) An overall view of the reactor system.
B) An outline of the transport and reactions near and at the crystal surface.

To distinguish between the two processes, and eventually analyse the kinetics on the surface, demands a careful examination of the overall growth kinetics and study of the surface morphology. In principle, in epitaxial growth, diffusion limited processes show a good crystalline perfection of the layers, a low temperature dependence of the growth rate, but as a disadvantage a layer thickness, which varies as a function of place, because the gas depletes, and which depends on the shape of the substrate. Surface controlled processes usually give rise to an imperfect morphology and features like growth hillocks, bunches and even polycrystalline growth can be observed.

3. Transport of reactants and products

It is recognized more and more that control of the gasflow pattern in the reactor tube is of great importance when sharp junctions are desired [4,5]. Ideally gasflows brought together at a certain time, with a specific composition, should not mix with portions introduced earlier or later. This can be achieved best by reducing the time the flow needs to reach the hot zone and by working with a laminar flow. The piping, leading the mixed gas to the reactor should be as short as possible, and dead volumes in valves should be avoided absolutely. To minimize the residence time of the gas in the reactor tube it is profitable to work under reduced pressures. It is especially important to prevent return flow effects in the entrance region. There the gas expands due to the greater cross-section and to a sudden increase in temperature caused by the hot susceptor. This means an optimization of the shape of the reactor cell and susceptor, for specific temperature and flow settings.

Though often given too little attention, it is also important what happens with the reactants after the deposition zone, both with respect to the process as to the environment. For the former it is essential that the exit of the reactor does not cause return flows and that the products do not interfere with the growing crystals. For example in MOCVD of GaAs the formation of solid arsenic on cold parts of the reactor tube can give rise to dust on the crystal surface. Last but not least, CVD is often carried out with aggressive, poisonous, chemicals. As oxygen, or water is notorious in ruining the process, it is obvious to prevent any leakage before the reactor, however disposal of the reaction products is also a responsibility of the operator, though it is not always an easy task.

In case the gas flow is laminar and turbulence as well as convection is absent, the reactants are transported to (and the products from) the crystal surface via diffusion (vertical) and gas flow (horizontal). The fluxes to and from the crystal can be described with a diffusion model, which contains Fick's law [5]. During their transport to the crystal surface the reactants are heated up, so all kind of chemical reactions are likely to occur.

4. Gas phase chemistry

In a CVD system the driving force for crystallization ($\Delta\mu$) is mainly caused by the chemical instability of the reactants. A distinction can be made between systems where the reactants are far from equilibrium and the chemical reactions cause a large potential drop and those, which are more equilibrium related and were the supersaturation is only small. Examples of the first type of processes are the growth of Si from SiH_4 and GaAs from $(CH_3)_3Ga$ and AsH_3. To the second group belong the growth of Si and GaAs via $SiHCl_3$, and via $AsCl_3$ and GaAs, respectively.

As the difference in equilibrium and input partial pressures is large in systems with a large $\Delta\mu$, a study on the gas phase chemistry is then best performed by an evaluation of the chemical kinetics. Unfortunately this is only possible for some simple systems [6], as the propagation of the reactions depends on temperature and flow profile and the reaction kinetics. So, it is in most systems common practice to make the assumption that ultimately chemical equilibrium is established near the crystal surface. Then two extreme situations can be considered: the gas phase is also in equilibrium with the crystal (heterogeneous equilibrium) or only internally (homogeneous equilibrium) [7]. The first situation is representative for a diffusion controlled proces, fig. 2A, the supersaturation, $\Delta\mu$, is all needed to transport the reactants and products, to and from the crystal surface. As the diffusion can give a difference in chemical composition, e.g. Cl/H ratio, between input and surface region, in some systems, where a detailed study makes sense, it could be wise to correct for this difference [8]. The case of homogeneous equilibrium is the extreme situation that the process is completely surface controlled (fig. 2B). In practice always an intermediate condition is present and the supersaturation of the gas phase near the crystal surface is in between these two limits.

For a near-equilibrium system, such as the growth of GaAs or Si in the chloride system, the difference between hetero- and homogeneous equilibrium is small, so a good description of the process can be obtained, by a thermodynamic analysis, in any case [9,10]. To illustrate the use of thermodynamics in CVD, the Ga-As-Cl-H system is, as an example, worked out in detail.

One of the methods to grow GaAs is via the Effer process [11]. $AsCl_3$ is introduced into a furnace, where at high temperatures solid gallium arsenide is present. There the arsenic chloride decomposes and reacts:

(1) $AsCl_3 + 3\ GaAs(s) \rightarrow 3\ GaCl + As_4$

The equilibrium mixture of gallium monochloride and arsenic formed in this way is transported with a hydrogen carrier gas to a zone where the temperature is lower and where the gallium arsenide is deposited again:

(2) $GaCl + \frac{1}{4}\ As_4 + \frac{1}{2}\ H_2 \rightarrow GaAs(s) + HCl$

In this system the transport of gallium via chlorine is determining the amount of GaAs, which will be grown. The release of arsenic from the gallium arsenide in the first hot zone is relatively easy, at these high temperatures, due to the great tendency of arsenic to evaporate. To predict under what conditions the transport of gallium with chlorine is most efficient, the following thermodynamic approach is applied.

Suppose 1% $AsCl_3$ in H_2 is able to achieve equilibrium with solid GaAs. The composition of the gas phase after the establishment of that equilibrium is determined by the stability (μ°) of all possible gas phase species. For example for GaCl the following relations can be deduced:

(3) $Ga(l) + \frac{1}{2}\ Cl_2 \rightleftarrows GaCl \qquad \frac{P_{GaCl}}{(P_{Cl_2})^{\frac{1}{2}}} = \exp\left\{\frac{-\Delta\mu^\circ_{GaCl}(T)}{RT}\right\} = K_{P,GaCl}$

$\Delta\mu_i^\circ(T)$: the standard chemical potential of 1 mol of species i with respect to the elements in their most stable state, all at 1 atm pressure, for the given temperature.

$K_{P,GaCl}$: Equilibrium constant for the formation of GaCl out of liquid gallium and chlorine, for pressures in atm.

For each species in the system a similar equation can be formulated. Their relative stability $\Delta\mu_i^\circ$, which is for 1 mol equal to $\Delta G_{f,i}^\circ$, i.e. the Gibbs free energy it costs to form species i out of the elements (all at 1 atm), is often tabulated in thermochemical data books [12-15]. (For 298 K μ of the elements is 0, so that then $\Delta\mu_i = \mu_i$) As shown in chapter 2 and 7, evaluation of ΔG° of a reaction, is also possible by evaluation of ΔH°, the standard enthalpy, or ΔS° the standard entropy. The thermodynamic data needed to perform calculations in the Ga-As-Cl-H system are extensively discussed in ch. 7.

The equilibrium gas phase composition of the system can be calculated using the fact that ΔG is minimal. The relation between the Gibbs free energy of a system and the stability of its components is given by:

$$(4) \qquad G = \sum_i n_i \mu_i$$

$$\mu_i = \mu_i^\circ + RT \ln P_i$$

where n_i: mol of species i

According to the Gibbs phase rule, a system consisting of a gas phase containing x compounds and 4 elements, has 5+x degrees of freedom. For every compound an equation such as eq. (3) can be written down, if the temperature is specified, which fixes 1+x parameters, so that only the partial pressures of the 4 elements are left as unknown quantities. Thus for a given total pressure and 1 condensed phase, which determines the product of P_{Ga} and P_{As}, only 2 parameters are left to choose. This can be for example the molar ratio of Cl/H and (Ga - As)/Cl.

In fig. 3 the equilibrium gas phase composition of 1% $AsCl_3$ in H_2 is shown in the temperature range from 800 to 1200 K. The incoming $AsCl_3$ is totally decomposed at all temperatures. Chlorine is preferably attached to hydrogen at low temperatures, but changes rapidly for gallium (GaCl) at increasing temperatures. Arsenic is at low T most stable in the form of As_4. The dimer gains importance at higher temperatures. The total arsenic pressure ($2 P_{As_2} + 4 P_{As_4}$) is rising with temperature, as the gallium content increases.

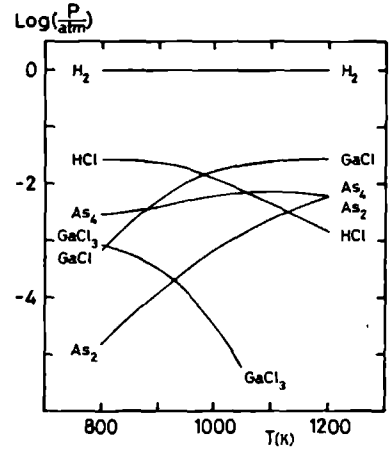

Fig.3 Gas phase composition of GaAs(s) in equilibrium with 1% $AsCl_3$ in H_2 at 1 atm total pressure as a function of temperature.

In the deposition model, the incoming gas etches the solid gallium arsenide and achieves equilibrium at T_1. The mixture, with a known composition, flows, without intermediate deposition, to a zone at T_2, where the excess GaAs can be used for epitaxial growth, and ultimately equilibrium is reached again. The amount of gallium (n_{Ga}) which is transported from the hot (T_1) to the deposition zone (T_2) is given by:

$$(5) \qquad n_{Ga}(T_1) = \left\{ \sum_{x,y,z} x\, n_{Ga_xCl_yH_z} - n_{GaCl} + n_{GaCl_3} \right\} (T_1)$$

The number of moles which can be deposited is the difference between the input and the amount which should remain in the gas phase:

$$(6) \qquad (n_{Ga})_{dep} = n_{Ga}(T_1) - n_{Ga}(T_2)$$

This is linked with the partial pressures as indicated in fig. 3 via the perfect gas law:

$$(7) \qquad P = n\,(RT/V)$$

So it would seem straightforward to replace the number of moles by the summation over the partial pressures. However one problem arises, (RT/V) is only constant when the number of species in the system does not change. In general this is not true and the total number of gas phase molecules are unequal before and after the reactions. Therefore a relative gallium content, to compare with the solubility (L), as used in chapters 4 and 5, should be introduced. The sum of the partial pressures as used there is formally not correct, though it is of little importance for a system where the change in the number of moles is only small. A correct approach would be to relate the content to the number of moles of an element which is constant during the whole process, such as hydrogen, chlorine, or the sum of both. In the chlorine system it is most logical to relate the gallium content to the chlorine input, as this takes care of almost the entire gallium transport. Then the solubility represents, more or less, the efficiency of chlorine to transport the gallium.

$$(8) \qquad L_{Ga\text{-}Cl} = \frac{n_{Ga}}{n_{Cl}} = \frac{\Sigma P_{Ga}}{\Sigma P_{Cl}}$$

$$\text{where } \Sigma P_{Ga} = \sum_{x,y,z} x \; P_{Ga_xCl_yH_z}$$

The advantage of this definition of the relative solubility is that changes in the number of moles caused by the chemical reactions affect the sum of the partial pressures of chlorine the same as the sum of the gallium pressures. On the other hand the relation between the number of moles gallium present in the gas phase and the solubility is clear as the moles of chlorine at any temperature is equal to the amount in the input.

The difference in relative solubility at T_1 and at T_2 is called the excess of gallium: ε

$$(9) \qquad \varepsilon = L_{Ga\text{-}Cl}(T_1) - L_{Ga\text{-}Cl}(T_2)$$

So finally we end with:

$$(10) \qquad (n_{Ga})_{dep} = \varepsilon \; n_{Cl}$$

The excess of gallium can be deduced from fig. 3 and n_{Cl} is three times the number of mol $AsCl_3$ introduced in the reactor.

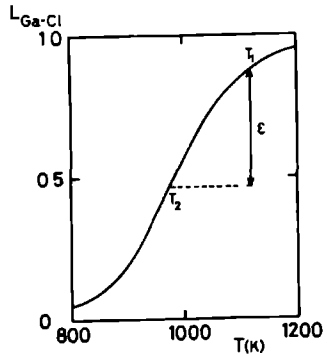

Fig.4 Solubility (L) curve for 1% $AsCl_3$ in H_2 at 1 atm total pressure as a function of temperature.

$L_{Ga-Cl} = \frac{\Sigma P_{Ga}}{\Sigma P_{Cl}}$; the partial pressures of gallium and chlorine species can be derived from fig. 3.

The excess, ε, is the difference in solubility between two temperatures.

In fig. 4 the relative solubility of gallium is plotted as a function of temperature. As indicated, when the source is at T_1 and the deposition zone at T_2, an excess (ε) of gallium is present in the gas phase, which can be used to form GaAs(s). Experimental evidence [10,16] indicates that the growth rate is proportional to ε. This means that all, or a constant fraction, of the gallium which can be released from the chlorine is deposited as gallium arsenide after reacting with arsenic. A similar behaviour is found in the Si-H-Cl system, nicely illustrated in fig. 8 of chapter 4 of this thesis. As indicated in that chapter the excess is at a given deposition temperature proportional to the supersaturation Δμ. Strictly the relation between ε and Δμ is only valid for a one-component system, but as can be seen in fig. 3 is reasonable for the Ga-As-Cl-H system at high temperatures.

In chapter 4 and 5 the use of solubility curves is extensively treated, so here only briefly the most important aspects will be discussed. It can be seen in fig. 4 that in the whole temperature region the source should be at a higher temperature than the deposition

zone. As the curve flattens at high temperatures it makes little sense to go higher than 1200 K with T_1. With a T_2 around 1000 K it makes little difference whether the source is at 1100 or 1200 K. The steeper the curve the smaller the temperature difference needs to be to obtain a certain growth rate. In this case, going down with the deposition temperature to 900 K is hindered by the occurence of a rate limiting step on the crystal surface, the desorption of chlorine, reducing the growth rate and the quality of the epitaxial layers.

As will be shown in this thesis, calculations of the gas phase composition can be used also in predicting the incorporation of dopants (ch. 6). The subsystem of the dopant element usually is internally in equilibrium in the gas phase and the partial pressure of the monatomic dopant is then a measure for the amount, which is built in [17,18].

As shown in chapters 2 and 3, in order to predict the surface coverage, it is essential to establish the gas phase composition. It is in this respect good to realize that radicals are most eager to adsorb on a silicon surface, as they can form chemical bonds. As they can be of only minor importance in the gas phase, it is better not to restrict the gas phase calculations to the most important species only.

Even for systems which are known, or expected, to be far from equilibrium, it is useful to calculate what the equilibrium situation would be. One should of course try to use knowledge on kinetics as far as possible, but the result of an equilibrium calculation already gives a good idea about the relative stability of the different possible species. In chapter 7 thermodynamical calculations are used to get an idea of the reactivity of gallium versus arsenic with respect to various reactants which may be present in the gas phase.

5. Adsorption and surface structure

After transport of the reactants and all kind of gas phase reactions the growth units have to adsorb onto the crystal surface. As, up to now, little attention was paid to the adsorption process, which is therefore poorly understood, it is one of the main issues of this thesis.

Experimentally, adsorption under conditions relevant for CVD processes, is hardly accessible. So, instead a theoretical study is carried out, but as far as possible based on experimentally observed phenomena. Essential in this respect is the fact that crystal growth of GaAs or Si on (111), (100) and (110) surfaces proceeds via steps. Growth species adsorb on the crystal surface and diffuse to the steps were they can be incorporated. Adsorption calculations can give information whether step growth is likely or not. Full coverage with impurities will hinder the movement of growth species and can even prevent proper attachment leading to polycrystalline growth. Accumulation of growth species can lead to two dimensional nucleation, creating new steps, therewith bypassing growth via the presented steps.

The view as presented here is not consistent with available adsorption models, which predict a high surface coverage [19,20]. In these papers, step growth on the (100) surface of GaAs is explained, assuming an overlayer of adsorbates, which stabilizes the surface [21]. In our view step growth is an intrinsic property of a (100) face, related with surface reconstruction. In the world of ultra-high vacuum experiments, this is a well-established phenomenon [22], in the field of epitaxial growth by CVD the impact of reconstruction is hardly recognized [23]. It will be shown in this thesis that, in general, reconstruction will not be removed by adsorbates in the high temperature region where epitaxial, step growth is observed. An atomistic picture will be presented which is able to explain step growth on a (100) silicon surface, in case of a low surface coverage. As the structure of the bare surface plays an essential role in this model, a short review will be given on the most important faces of Si and GaAs. Thereafter the adsorption model used will be elucidated briefly, as well as the implications for crystal growth.

As to be seen in fig. 5a and b both silicon and gallium arsenide consist of tetrahedrally bonded atoms, in the first case all identical ones in the latter alternately gallium and arsenic. This results for both in a face-centered cubic lattice, for silicon in the diamond structure, space group Fd3m, and for GaAs, which has a lower symmetry in the zinc blende structure, $F\bar{4}3m$. In the crystal structure clearly the

close packed (111) face can be discerned, as well as the {001} cube faces and a chain of tightly bonded atoms running in the [$\bar{1}$10] direction.

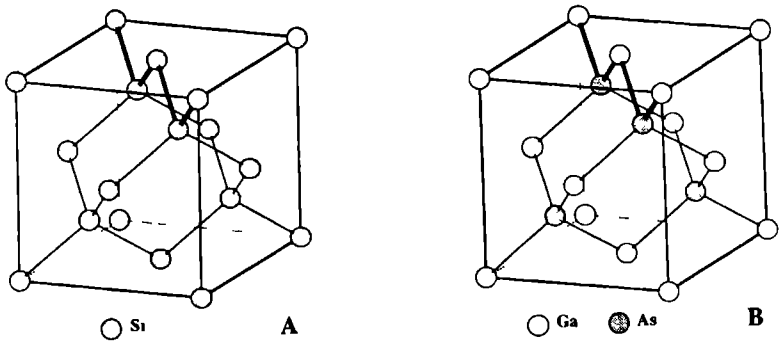

Fig 5
A) Crystal structure of silicon, indicated is the [$\bar{1}$10] PBC in the upper part of the cube.
B) crystal structure of gallium arsenide, indicated is the [$\bar{1}$10] PBC in the upper part of the cube.

In this study the structure of the surface is important, which is, in a first approximation, a reflection of the crystal structure. With respect to the growth behaviour, the stability of a crystal face, which is determined by the strength and the arrangement of the bonding in the surface layer, is essential. To obtain more insight in the bonding structure of a crystal face it is very useful to carry out a PBC-analysis [24]. This means a determination of the number of Periodic Bond Chains which are present in the surface layer. According to the Hartman Perdok theory, a PBC is an uninterrupted path of bonds having an overall periodicity of the crystal lattice. When in the surface layer of a crystal face two, or more, intersecting PBC's are present, the bonds between the atoms form a two-dimensional connected net and growth is only possible via steps; a (flat) F-face. When only one PBC is present, the surface is built up of strong chains, which are stable in the perpendicular direction, but with easy attachment lengthways; a (stepped) S-face. If no PBC is present, the surface is rough. It is a (kinked) K-face, with easy attachment at any site.

Essential in the analysis whether a PBC is present or not, is the thickness of the surface layer. This is according to the PBC theory determined by the crystallographic extinction conditions, as determined by the bulk properties. It is a serious matter of discussion, whether this is a proper criterium in case of semiconductors with a zinc blende or diamond structure. As will be evident from the following paragraph the structure of the surface layer can differ considerably from the bulk structure.

As for GaAs and Si only the first neighbours are strongly bonded in the crystal lattice, a PBC should contain two of the four sp^3 bonds of an atom, which are pointing in a <111> direction, as indicated in fig. 5a,b. Therefore all PBC's should run in <110> directions. With this information it can be derived that for silicon as well as gallium arsenide only one crystal face is flat: {111}. As can be seen in fig. 6 this surface contains 3 intersecting PBC's.

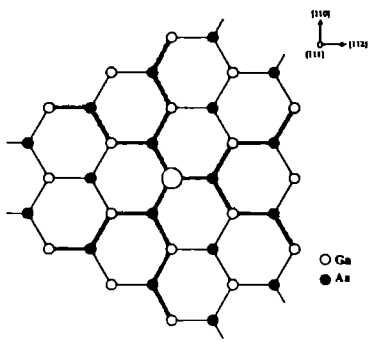

Fig.6 The three intersecting PBC's for the (111) surface of GaAs (or Si).

In fig. 7 a (110) surface is shown. It contains only 1 PBC and so should be stepped. Fast growth and etching is possible in the $[1\bar{1}0]$ direction. Growth experiments on GaAs and Si spheres however, indicates that {110} faces are present as small facets [25,26]. This could point to a stabilization in the [001] direction. As shown in chapter 7 the $[1\bar{1}0]$ chains are polarized, the arsenic being negative and gallium positive. This could give a Coulomb interaction in the [001] direction strong enough to account for the stability of the (110) face.

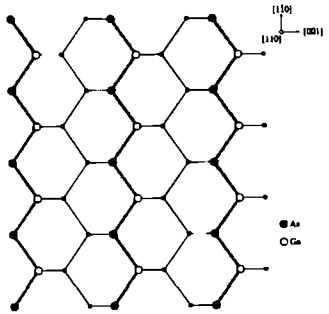

Fig.7 The [1$\bar{1}$0] PBC for the (110) surface of GaAs (or Si)

However the most notorious stabilization is observed for the (100) face. According to a PBC-analysis this face is kinked for silicon, fig. 9A, and stepped for gallium arsenide, fig. 9B. The latter is a consequence of the greater thickness of the (100) slice for GaAs. To obtain a periodicity for both gallium and arsenic, formally a slice should be taken containing both elements. This is analogous to the chemical view that in etching or growing, Ga and As is removed or attached as one unit. It will be shown in chapter 7 that with respect to hydrogen, both have a nearly equal reactivity and could also etch independently. This makes the difference between GaAs and Si vague.

Obviously the observed step growth is not in accordance with the K- and S-character of silicon, respectively gallium arsenide. For GaAs the picture changes radically when surface reconstruction is taken into account. In the absence of interactions with gas phase species it is well-known that two dangling bonds pointing towards each other form a new bond. This connects two surface atoms; fig. 8.

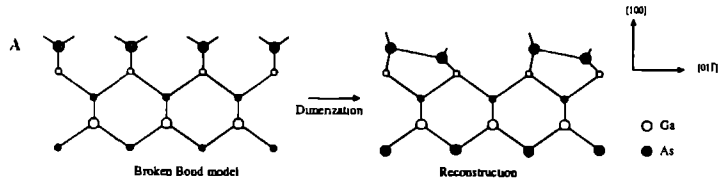

Fig.8 Cross-section of a (100) surface of GaAs, indicating the bond formation in the surface layer by the dimerization process.

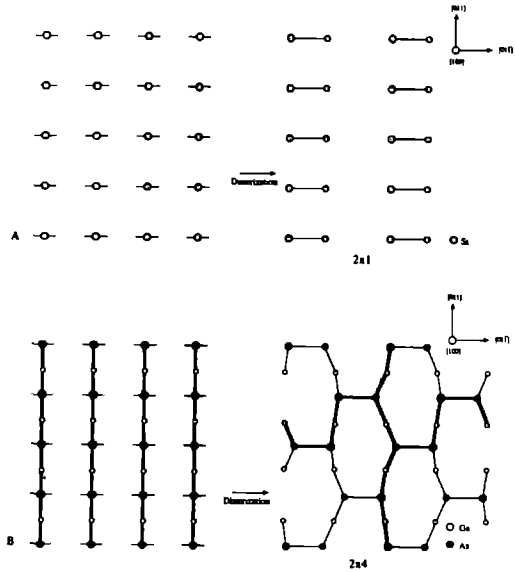

Fig.9 A) The (100) surface of silicon.
In the broken bond configuration no PBC can be constructed (left part).
Though dimerization stabilizes the surface,
no long order interaction (PBC) is formed.
B) The (100) surface of gallium arsenide.
Due to its binary character, GaAs has 1 PBC per slice.
For arsenic in the top layer it is the [011] PBC,
in case of gallium, it is the perpendicular [01$\bar{1}$] PBC.
After dimerization to a (2x4)As structure
two intersecting PBC's can be constructed.

For silicon this results in principle in a (2x1) structure, although more complicated ordering can not be excluded [27]. Though an interaction is introduced in the [011] direction it does not give a long order stabilization required to give an F- or an S-face. As will be shown in chapter 3, the assumption that adjacent to a double-bonded silicon species no dimer bond is possible, is sufficient to explain why attachment is preferable in the direction of the dimer bond. This results in an stepped face. As silicon contains a fourfold screw axis in the <001> direction, the dimerization in a subsequent layer is rotated 90°, resulting in an F-like growth.

For GaAs reconstruction can result in a (2x4) arsenic stabilized structure; fig. 9D. It can be seen directly that a connected net is formed (the choice of the new PBC is a bit arbitrary), so that independent of the growth kinetics, (100) is expected to be an F-face for GaAs. So in this case it is obvious that an analysis starting from the bulk structure of the crystal is not sufficient; the distortion of the surface, which is quite general for semiconductors (chapter 7), should be taken into account.

Only now that the structure of the bare surface is specified it is appropriate to introduce adsorption. As large adsorption energies can be involved the structure of the surface layer can be affected and obviously one of the intriguing questions now is, whether the surface reconstruction is removed by the adsorbates on (100).

To calculate the surface coverage a Langmuir model is applied. This implies that all adsorbates attach to a well-defined site by forming a chemical bond. In principle all sites are equal and the adsorbates do not interact. As pointed out in chapter 3 the resulting surface coverage gives information on the tendency of gas phase species to attach to the surface, for a given gas phase composition. It predicts which growth species will be dominant on the crystal surface and therefore will be the most probable species to be incorporated, and tells whether the growth is likely to be interfered by impurities.

For (111) the Langmuir model can be applied in its unmodified form, for a reconstructed (100) surface an interaction is introduced by the dimer bonds. Two different sites can be identified, but more important, the adsorption becomes dependent on the local environment. Therefore an energy correction must be introduced, which takes into account the coverage of the immediate surrounding; a mean-field approximation. An important result which comes out of the calculations, chapter 3, is that reconstruction is very difficult to remove by adsorption. Species are most likely to form only a single bond, therewith giving (100) the character of the (111) surface. The kinked character, for silicon the possibility to form two bonds, has disappeared. On the basis of the stability of the dimer bonds for GaAs a behaviour similar to that for silicon is expected. Probably this can be generalized to all

semiconductors with a zinc blende structure, namely that at high temperatures the reconstruction of a (100) surface is not removed by adsorbates and step growth will be observed.

6. Incorporation and subsurface trapping

After adsorption onto the crystal surface, growth units diffuse over the surface and are incorporated at a step site. A point which has given attention to in this thesis is the final incorporation in the bulk. This is discussed on the basis of doping in III-V compounds. It is shown in chapter 6 that the concentration of dopant which is finally built in, is very sensitive to the incorporation mechanism. The process can be divided in 3 steps, where basicly the dopant is transformed from an adsorbed species to a bulk atom. Most important is that the bonding situation changes, at the surface only one (maybe two) bonds with the crystal are present, finally in the bulk four bonds with the lattice are formed.

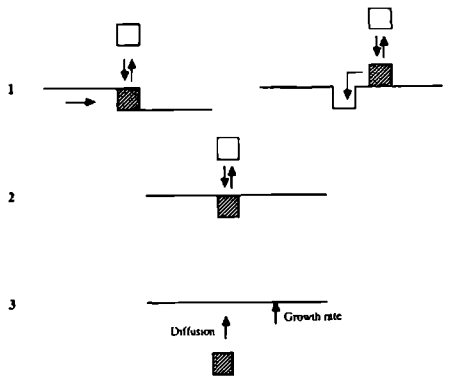

Fig.10 Incorporation of dopants.

1. incorporation of the adsorbed atoms in the surface layer by:
   a propagating step, or a surface vacancy.
2. exchange of a surface atom with the gas phase,
   to remove any excess, e.g. formed by the kinetics of step 1.
3. exchange of a subsurface atom with the surface by diffusion.
   this step is often too slow compared with the growth rate: subsurface trapping

In fig. 10 the three steps are illustrated. First the adsorbed species is either incorporated by a step, or tumbles in a surface vacancy. Though for Si and GaAs, growth on (100), (110) or (111) proceeds via steps, the concept of subsurface trapping can be applied for both normal and step growth. As incorporation by a step causes a change in chemical potential, either during the incorporation, or afterwards (2) a large portion of the dopant may be rejected and desorb. As the crystal grows, new layers are deposited on top of the dopant atom. It will be buried, unless it is able to migrate through the crystal. In fig. 10 it is indicated that in step 3 the incorporated dopant is eager to diffuse out of the crystal. This is due to the fact that the equilibrium concentration is in general lower in the subsurface than in the surface.

It will be shown in chapter 6 that it is a quite common phenomenom in the growth of III-V compounds that step 3 is hindered. In other words the velocity of the incorporated atoms, caused by diffusion, to the growing gas-solid interface, is lower than the lateral growth velocity of that surface, so that the dopant is buried.

As already discussed the excess of dopant in the subsurface is caused by the difference in environment, between the surface and the subsurface; situation 2 and 3 in fig. 10. However in many experiments it is likely that also the desorption equilibrium at the step is not established (left part of 1 in fig. 10). This is called step trapping. It should be realized that this is only effective when the subsequent desorption and diffusion processes are also hindered, else equilibrium between subsurface and gas phase can be restored.

7. Conclusion and lay-out of this thesis

As already indicated in this thesis, several aspects of the CVD process, are studied experimentally as well as theoretically. As in the world of epitaxial growth of silicon and gallium arsenide, too little attention is paid in explaining the process in terms of both chemistry and surface structure, the emphasis in this work is on those two topics.

In part 1, chapter 2 and 3, the adsorption is studied in two simple systems, containing only two elements, silicon and hydrogen, and their compounds. Already there it is evident that it is essential to have a good notion of the surface structure and the way the adsorbates are attached to the surface.

In part 2, chapters 4 and 5, another aspect of silicon growth is considered: the importance of the gas phase composition in determining the growth velocity and therefore the power of thermodynamic calculations. The theoretical knowledge of the gas phase composition is used to control the growth in a furnace with a great precision.

In the third part of this thesis some aspects relevant in the growth and etching of GaAs are elaborated. In chapter 6 the incorporation of dopants is theoretically studied from which it is possible to predict when equilibrium incorporation is no longer possible and trapping will occur. In the last chapter (7) of this work the surface structure of GaAs is studied. The underlying idea being that an understanding of the bare surface should form the basis for a detailed crystal growth description in CVD processes. As GaAs is a binary compound it is essential to control the III/V ratio during growth or etching in the surface layer. The reactivity and stability of gallium versus arsenic is studied in order to better understand the influence of the ambient gas phase on the composition of the solid.

REFERENCES

[1] Proceedings of EuroCVD 5 (1985), Ed. J.-O. Carlsson and J. Lindström (Uppsala, Sweden)

[2] Proceedings of the Ninth Intern. Conf. on CVD (Cincinnati, Ohio, USA, 1984), Ed. McD. Robinson, C.H.J. van den Brekel, G.W. Cullen, J.M. Blocher Jr. and P. Rai-Choudhury, (Electrochem. Soc. 84-6, Pennington, NJ, USA)

[3] J. Bloem and L.J. Giling, in: Current Topics in Materials Science Vol. 1 ch. 4, Ed. E. Kaldis, (North-Holland, Amsterdam, 1978)

[4] K.F. Jensen, Proc. Ninth Intern. Conf. on CVD (Cincinnati, Ohio, USA, 1984), p. 3 (Electrochem. Soc. 84-6, Pennington, NJ, USA)

[5] J. van de Ven, G.M.J. Rutten, M.J. Raaymakers and L.J. Giling, J. Crystal Growth 76 (1986) 352

[6] M.E. Coltrin, R.J. Kee and J.A. Miller, J. Electrochem. Soc. 131 (1984) 425

[7] F. Langlais, F. Hottier and R. Cadoret, J. Crystal Growth 56 (1982) 659
[8] P. van der Putte, L.J. Giling and J. Bloem, J. Crystal Growth 31 (1975) 299
[9] J. Bloem, Y.S. Oei, H.H.C. de Moor, J.H.L. Hanssen and L.J. Giling, J. Electrochem. Soc. 132 (1985) 1973
[10] J.L. Gentner, Philips J. Res. 38 (1983) 37
[11] D. Effer, J. Electrochem. Soc. 112 (1965) 1020
[12] JANAF Thermochemical Tables 2nd ed., NSRDS-NBS 37 (Natl. Bur. Std. US, Washington, DC, 1971)
[13] D.D. Wagman, W.H. Evans, V.B. Parker, R.H. Schumm, I. Halow, S.M. Bailey, K.L. Churney and R.L. Nuttal, "NBS tables of chemical thermodynamic properties", J. Phys. Chem. Ref. Data 11 (1982) supplement 2
[14] I. Barin, O. Knacke and O. Kubaschewski, "Thermochemical Properties of Inorganic Substances" (Springer, Berlin, 1973)
[15] O. Kubaschewski, E. LL. Evans and C.B. Alcock, "Metallurgical Thermochemistry" 4th ed., (Pergamon, Oxford, 1967)
[16] D.W. Shaw, J. Phys. Chem. Solids 36 (1975) 111
[17] H.T.J.M. Hintzen, J. Bloem and L.J. Giling, J. Electrochem. Soc. 131 (1984) 1900
[18] M.W.M. Graef, B.J.H. Leunissen and H.H.C. Moor, J. Electrochem. Soc. 132 (1985) 1942
[19] A.A. Chernov and M.P. Rusaikin, J. Crystal Growth 45 (1978) 73
[20] R. Cadoret in: Current Topics in Materials Science Vol. 5 ch. 2 Ed. E. Kaldis, (North-Holland, Amsterdam 1980)
[21] R. Cadoret, L. Hollan, J.B. Loyau, M. Oberlin and A. Oberlin, J. Crystal Growth 29 (1975) 187
[22] A. Kahn, Surface Sci. Reports 3 (1983) 193
[23] L.J. Giling and W.J.P. van Enckevort, Surface Sci. 161 (1985) 567
[24] P. Hartman in: "Structure and Morphology in Crystal Growth: an introduction" Ed. P Hartman, (North Holland, 1973, Amsterdam) p 367
[25] J.G.E. Gardeniers, private communication, 1986
[26] J.B. Loyau, M. Oberlin, A. Oberlin, L. Hollan and R. Cadoret, J. Crystal Growth 29 (1975) 176
[27] W. Mönch, Surface Sci. 86 (1979) 672

PART 1

ADSORPTION AND CRYSTAL GROWTH ON SILICON

CHAPTER 2

ADSORPTION ON Si(111) DURING CVD OF SILICON FROM SILANE: THE EFFECT OF TEMPERATURE, BOND STRENGTH, SUPERSATURATION AND PRESSURE

ADSORPTION ON Si(111) DURING CVD OF SILICON FROM SILANE: THE EFFECT OF TEMPERATURE, BOND STRENGTH, SUPERSATURATION AND PRESSURE

Abstract

In a theoretical study of the growth of silicon from SiH_4, we calculated the coverage of a Si(111) surface with all species existing in the Si-H system. These calculations are based on the Langmuir model for adsorption in which estimated standard Gibbs free energies for adsorption are used for all these species, together with their equilibrium partial pressures in the gas phase. The coverages are calculated as a function of temperature, supersaturation of the gas phase, enthalpy of adsorption and total H_2 pressure. It is shown that the coverage strongly depends on the adsorption energy. Because some species are bonded stronger to the surface than others, the composition of the adsorbed layer is quite different from that of the gas phase. It is shown that monatomic hydrogen is the most important adsorbate. Despite the great sensitivity of the coverage on the enthalpy of adsorption used in the calculations it is concluded that at the higher temperatures where monocrystalline growth is observed the surface is barely covered with H, on the other hand at low temperatures the coverage with H is almost complete. It is also demonstrated that at lower hydrogen pressures the surface coverage with monatomic hydrogen is strongly reduced, extending the growth regime for monocrystalline growth to about 900 K for a total pressure of 10^{-3} atm. SiH_2 is the most abundant growth species at 1 atm H_2 pressure, with a coverage ranging from 10^{-6} to 0.02, dependent on the supersaturation. However at high temperatures and low H_2 pressures monatomic silicon is more abundant on the surface than SiH_2 and is the first species to be considered in a growth mechanism. Silane is unimportant as an adsorbed growth unit as it can not form a chemical bond.

1. Introduction

Crystal growth is a process in which growth units adsorb on the crystal surface and are incorporated in the lattice. It will be clear that when various components can adsorb on the crystal surface, they will compete for each free surface site. Since only the adsorbed growth units can contribute to the growth rate, all other adsorbed species, impurities, may reduce the growth rate because of a blocking of available surface sites, thus diminishing surface concentration and diffusion of growth species. A high concentration of adsorbed impurities hinders the advancement of steps, which may result in step bunching, two dimensional nucleation and even the outgrowth of hillocks [1]. Moreover when these impurities are built in, they may cause imperfections in the grown layer. So knowledge of the composition of the adsorbed layer is important for a better understanding of crystal growth phenomena.

Despite its fundamental importance, as well in experimental as in theoretical studies, little has been reported so far on adsorption in relation to crystal growth. Experimental studies mostly deal with crystal growth processes at room temperature in liquid solutions giving information about growth inhibitors or morphological consequences. Adsorption studies in ultra-high vacuum [2,3] give some information on the nature of the atomic species adsorbed on the surface at high temperatures. But also here, systematic studies on adsorption as a function of temperature and partial pressures of the adsorbed species are scarce or just starting. Even for the technologically important CVD processes of silicon and GaAs little is known in this respect. So far only few theoretical analyses are available, indicating the presence of dense adsorption layers on Si(111) [4], GaAs(100) and (111) [5-7] as well as on InAs [8].

In this paper it will be shown that only at low temperatures, where polycrystalline growth is observed, a dense adsorption layer is probable. However at high temperatures, where it is possible to grow epitaxial layers, the coverage with H will be low. This can be concluded from the calculations, despite a lack of knowledge on the

exact bond strength, if also crystal growth observations are considered. Adsorption calculations also have their value in an analysis of the surface kinetics, because they can be used to decide which particles are potentially important in determining the reaction rate and which species can be ruled out in explaining the kinetics. It tells in which regime impurities can be expected to play a role and how their surface concentrations can be minimized.

We have studied in detail the effect of various parameters on the adsorption of the gaseous Si-H system on a Si(111) surface, allowing all species to be competitive. The adsorption model which will be presented is intentionally kept as simple as possible because the uncertainty in the structure and energy of the surface and the adsorbates is so large that a refined model does not make sense.

A method will be presented to estimate the complete data set necessary to calculate the adsorption constants. After computing the gas phase composition for the Si-H system the coverage of the Si(111) surface is calculated, using the concepts of chemi- and physisorption. This will enable us to demonstrate the above mentioned sensitivity of the degree of coverage (θ) for small changes in ΔH_{ad} and the dependence of coverage on the total H_2 pressure and the supersaturation of the gas phase. The Si(100) surface during growth from SiH_4, the Si-H-Cl and the Ga-As-Cl-H systems will be the subjects of three forthcoming papers [9,10,11]. In two appendices an account is given of the parameters used in the calculations. After a discussion of the importance of several parameters a recipe is given how to get an impression of surface coverage in systems for which accurate thermodynamic data are absent.

2. The adsorption model

2.1. Chemisorption

In order to calculate the equilibrium coverage θ_i of species i on Si(111), following Langmuir, localized adsorption is assumed i.e. the adsorption enthalpies involved are much larger than kT. The surface is thought to consist of adsorption sites, of equal geometry and energy

content. This implies that a flat surface, without steps and kinks, is considered and that relaxation of the crystal surface is neglected for the time being. Each site can be occupied by one molecule; steric hindrance or strong dipolar interaction influencing adsorption on neighbouring sites is not taken into account in this paper but will be dealt with in a coming paper [10,11]. Every radical can only form one bond with the silicon surface, the bond always being perpendicular to the crystal surface.

The adsorption process may be considered as a chemical equilibrium: a certain species (e.g. H) in the gas phase reacts with a free silicon surface site (*) resulting in an adsorbed species (e.g. H^*).

(1) $\quad H + * \rightleftarrows H^*$

The equilibrium constant $K_{ad,H}$ for this reaction relates the partial pressure of H in the gas phase to the relative concentration of vacant sites (Θ_{Vac}) and adsorbed H^* (Θ_H):

$$(2) \qquad K_{ad,H} = \frac{[H^*]}{[*]\ P_H} = \frac{\Theta_H}{\Theta_{Vac}\ P_H}$$

Rewriting of this equation and taking into account that i species can adsorb:

$$(3) \qquad \Theta_{Vac} = 1 - \sum_i \Theta_i$$

leads to the familiar Langmuir isotherm:

$$(4) \qquad \Theta_H = \frac{K_{ad,H}\ P_H}{1 + \sum_i K_{ad,i}\ P_i}$$

According to thermodynamic theory the equilibrium constant is related to the difference in standard Gibbs free energy (ΔG°) by:

$$(5) \qquad RT\ \ln K = -\Delta G^\circ$$

So that for reaction (1) we can write:

$$(6) \qquad RT \ln K_{ad,H} = -(H^{\circ}_{H^*} - H^{\circ}_{*} - H^{\circ}_{H}) + T\,(S^{\circ}_{H^*} - S^{\circ}_{*} - S^{\circ}_{H})$$
$$= -\Delta H^{\circ}_{ad} + T\,\Delta S^{\circ}_{ad}$$

where H° and S° are the standard enthalpy and entropy respectively at temperature T. Eq. (6) shows that a high (negative) adsorption enthalpy (bond strength) and a small loss in entropy will result in a large equilibrium constant for adsorption and thus in a high surface coverage.

The main problem in discussing adsorption is the uncertainty in the enthalpy change in the formation of the new bond. No reliable experimental data are available for the adsorption enthalpy on a silicon surface. As an approximation the diatomic bond strength (DABS) is often used. This is a good starting point for diatomic molecules which contain a single bond, but in many other cases, where in the diatomic molecule double or triple bonds are present, it is essentially wrong. For instance, in the adsorption of Cl or Si on a (111) silicon surface a single bond is formed, whereas in the diatomic molecules, SiCl and Si_2, the bond order is 2½ respectively 2. For the Si-H system in appendix A an evaluation is given of the available data on bond strength and length, resulting in an adsorption enthalpy, at 298 K, of 54 kcal/mol for the Si or Si-H species and 70 kcal/mol for H on a Si(111) surface. The accompanying bond length for Si-Si is 2.35 A and for Si-H 1.52 A respectively.

From the given room temperature value of ΔH_{ad} its value at a temperature T can be calculated using:

$$(7) \qquad \Delta H^{\circ}_{ad}(T) = \Delta H^{\circ}_{298} + \int_{298}^{T} \Delta C_p \, dT$$

The correction term, $\int \Delta C_p \, dT$ is best evaluated using partition functions. Although generally this is complicated by the lack of accurate data, it is well possible for silicon, because the silicon system is thoroughly investigated [12]. In appendix B the relation between C_p and the partition function is worked out in detail.

The entropy content of the system is also calculated with the use of partition functions (appendix B). It is assumed that upon adsorption a

non-linear gas phase molecule looses 3 translational and 3 rotational degrees of freedom, whereas a gain is achieved of 1 stretch and 2 bending modes of the adsorbate as well as rotation along the bonding axis. A small contribution to S (and C_p) is given by some low lying electronic states of the molecules in the gas phase, of the dangling bonds on the surface and those of the adsorbed species. This leads for a Si(111) surface to an entropy change given by:

$$(8) \quad \Delta S^{\circ}_{ad} = S^{\circ}(vib + rot + elec)_{ads} - S^{\circ}(elec)_{*} - S^{\circ}(transl + rot + elec)_{g}$$

Table 1
Entropy gain and loss in adsorption on Si(111) at 1400 K (cal/mol K)

	Loss				Gain			Total
	$transl$	rot_g	$elec_g$	$elec_*$	rot_{ads}	vib_{ads}	$elec_{ads}$	ΔS°_{ad}
H	33.7	--	1.4	1.4	--	6.6	--	-29.9
Si	43.6	--	4.4	1.4	--	19.5	2.7	-27.2
Si_2	45.7	17.1	3.5	1.4	--	21.5	1.4	-44.8
Si_3	46.9	19.9	2.2	1.4	--	22.7	1.4	-46.2
SiH	43.7	11.7	2.7	1.4	6.7	19.6	2.1	-31.2
SiH_2	43.8	17.9	2.1	1.4	7.6	19.7	1.4	-36.6
SiH_3	43.9	18.4	1.4	1.4	5.8	19.8	--	-39.5

In table 1 all the terms which contribute to this change in entropy are listed. The data to perform the calculations on the gas phase species have been taken from JANAF [12-14], Glushko [15] and Noläng [16]. The vibrational frequency of the adsorbates is calculated using $\nu_{stretch}(Si\text{-}H) = 2057 cm^{-1}$ and $\nu_{bending}(Si\text{-}H) = 637\ cm^{-1}$ [17] (app. B, eq. (B.11)), whereas for the evaluation of the rotational contribution the following bond lengths and angles have been taken: Si-Si 2.35 Å and Si-H 1.52 Å, 120° for SiH (sp^2 hybridization) and 109°28' (sp^3) for SiH_2 and SiH_3. The bond between adsorbate and crystal is perpendicular to the surface for Si(111). The electronic levels in the adsorbed molecule are assumed to be the same as in the corresponding gas phase particle, to which one additional H is attached. A Si(111) surface consists of dangling bonds which, in a first approximation, have a double degenerated groundstate. The accompanying electronic contribution to

the entropy, 1.4 cal/mol K, which is lost during adsorption, is of minor importance, but still is taken into account. For the adsorbing molecule, as well as the crystal surface, it is further assumed that the internal vibration modes are not affected by the adsorption process.

From an inspection of table 1 it is obvious that for the entropy loss of the gas phase molecule S_{elec} is of little importance, the main contributions come from the translational and the rotational part. For the adsorbate the vibration, especially bending, contributes most to the entropy, for the non-linear molecules rotation also has to be taken into account.

Table 2

Temperature correction, ΔH°_{T-298}, for the adsorption enthalpy at 1400 K (kcal/mol) on Si(111)

H	-0.9	SiH	1.6
Si	1.0	SiH_2	-2.8
Si_2	-2.3	SiH_3	-1.1
Si_3	-1.1		

In table 2 it can be seen that the temperature dependence of the enthalpy of adsorption is small. The various contributions to C_p almost appear to cancel each other, so in eq. (7) this term is not significant.

Table 3

$LogK_{ad}$ for the adsorption on Si(111) at 1400 K

H	4.54	SiH	1.37
Si	2.34	SiH_2	0.87
Si_2	-1.00	SiH_3	-0.02
Si_3	-1.50		

From the enthalpy and entropy data as given in tables 1 and 2 and appendix A, the equilibrium constants for the adsorption of the gas phase radicals have been calculated and are given in table 3. If the partial pressures of the gas phase species are known, the surface coverage can be calculated using eq. (4).

2.2 Physisorption

SiH_4, Si_2H_6 and H_2 can not form chemical bonds with the substrate. Only physical interaction with the silicon surface is possible, so the adsorption is no longer localized and two degrees of translational freedom are maintained. In the calculation of S_{transl} of the physisorbed state it is assumed that all molecules occupy the same surface area as H_2, viz. 17 A^2. This value is derived from the density of liquid H_2, 70 g/l [18], assuming a cubic close-packed arrangement. For rotation most probably only 1 degree of freedom is preserved resulting in a rotational loss of one degree for H_2, a linear molecule, and two for SiH_4. Entropy gain resulting from vibration is not taken into account, the stronger the bonding to the surface the more important its contribution, however the gain is counteracted by the smaller translation contribution of the lateral movement. The enthalpy is estimated, using Chernov's results [19], to be 8 kcal/mol for H_2 and 10 kcal/mol for SiH_4. In table 4 the entropy and enthalpy data and the resulting equilibrium constants at 1400 K for physisorption of SiH_4 and H_2 are given; Si_2H_6 is omitted because its coverage will be far below the physically realistic limit.

Table 4
Physisorption on Si(111) at 1400 K

	ΔH°_{298}	ΔH°_{T-298}	S_{gas}		$S_{physisorp}$		ΔS°_{ad}	$LogK_{ad}$
	(kcal/mol)		transl	rot	transl	rot	(cal/mol K)	
H_2	-8	-2.2	35.8	6.2	14.0	2.4	-25.5	-3.99
SiH_4	-10	-3.3	44.0	16.6	19.5	3.0	-38.1	-6.24

For low coverage, using the Volmer approach, it can be derived that:

(9) $\quad \Theta_i = K_{ad,i}\, P_i$

Θ_i is the time averaged fraction of the surface covered with species i.

3. Calculation of partial pressures, effect of supersaturation

For the determination of the gas phase composition equilibrium calculations have been performed. For many cases this method has given satisfactory results [1,20]. This is especially true when growth and etching go hand in hand, as in the $SiCl_4$ and $SiHCl_3$ systems. One must be careful however if the system is far from equilibrium, as is the case in the growth of Si from SiH_4, which is relevant for this paper, because here kinetic factors will play an important role too. For instance the temperature distribution and the residence time in the reactor may determine the degree of decomposition of silane. Therefore, in order to obtain an apparatus independent view on adsorption, two limiting situations will be considered, representing the limiting cases for the supersaturation:

(i) Heterogeneous equilibrium, when equilibrium is established between gas phase and solid silicon; only temperature and pressure determine the composition of the gas phase. In this case the supersaturation of the gas phase is essentially zero. In practice this corresponds to near-equilibrium growth, e.g. in a hot-wall reactor [20], or to a mass transport limited CVD process, where the reactions at the surface are faster than the diffusion towards the crystal. It must be realized that for this latter situation the concentration of growth species is low, the lower limit being the equilibrium situation.

(ii) Homogeneous equilibrium [21] if the rate limiting step is the incorporation of growth species in step or kink positions. The equilibrium between solid and gaseous silicon is not established, the gas phase is only equilibrated internally, so the supersaturation is maximal.

The last model will give an upper limit of the concentrations in the gas phase, the first a lower limit. However it should be realized that kinetic barriers can give rise to higher partial pressures of SiH_4 and intermediates, like SiH_2, and lower of the products, e.g. Si_2.

The above mentioned equilibrium calculations were performed using an iterative computer program based on minimization of the Gibbs free energy. Fig. 1a gives the composition of the gas phase in case of

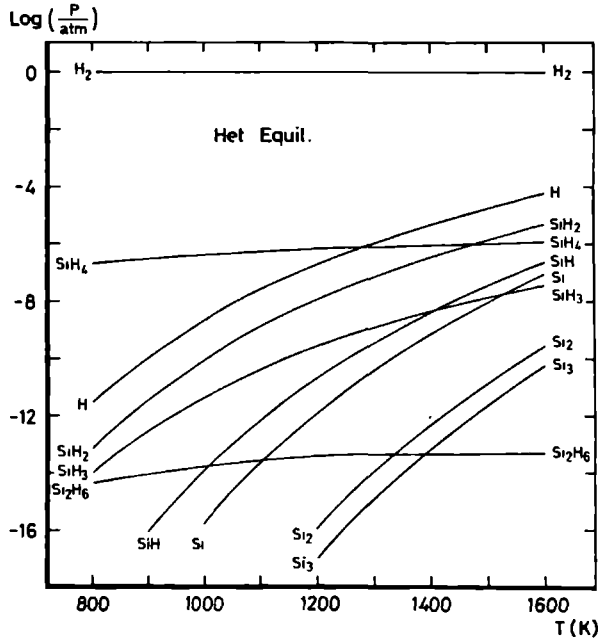

Fig. 1a Gas phase composition of the Si-H system as a function of temperature, using the heterogeneous equilibrium hypothesis, at 1 atm total pressure.

heterogeneous equilibrium. Apart from H_2, the most important species in the gas phase are SiH_4 and H at respectively low and elevated temperatures. SiH_2 and SiH_4 are the dominating silicon containing molecules.

In fig. 1b the homogeneous equilibrium mixture of 1% SiH_4 in H_2 is depicted. Omitting the presence of solid silicon, thus allowing a high supersaturation of growth species, results in an increase of the total silicon content in the gas phase of more than three decades. The partial pressures of SiH_x are increased similarly; the influence on Si_2H_6, Si_2 and Si_3 is evidently more drastical, resulting in the dominance of Si_3 over SiH_2 at high temperatures. This clustering of silicon is in fact the onset of the formation of solid silicon. If Si_4 or Si_5 were taken into account their concentration would also be high.

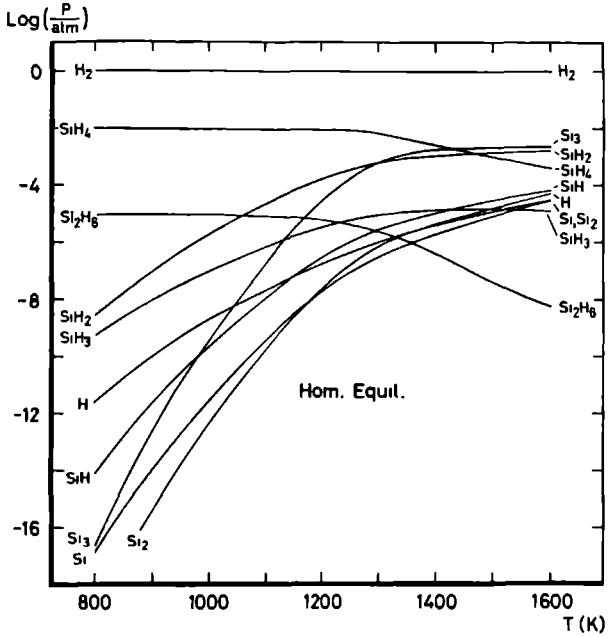

Fig. 1b Gas phase composition of 1% SiH_4 in H_2 as a function of temperature, using the homogeneous equilibrium hypothesis, at 1 atm total pressure.

Experimentally little is known about the structure of Si_3 and larger clusters. Recent theoretical calculations indicate that Si_3 is probably cyclic, with an apex bond angle of 78°, instead of linear as formerly assumed [12]. However the transformation of the triangular form to the linear form is easy, although the difference in stability is calculated to be 8 kcal/mol [22]. It is assumed that the linear form will be adsorbed, for the cyclic form probably will decompose on adsorption. So P_{Si_3}, and thus the coverage, can be a factor of 20 too high using the JANAF data, for these might be related with the cyclic form. The importance of Si_2, an intermediate in the formation of Si_3 and larger clusters, in the gas phase has been established recently [23].

With the given partial pressures and the equilibrium constants for adsorption as tabulated in tables 3 and 4, the surface coverages for chemi- and physisorption can be calculated using eqs. (4) and (9).

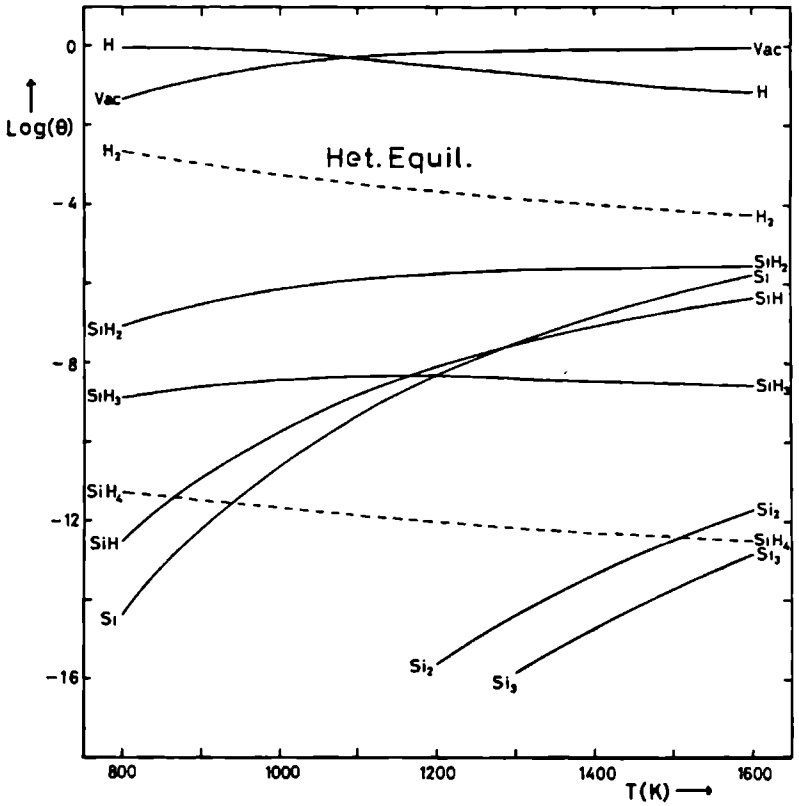

Fig. 2a Coverage of a Si(111) surface, in equilibrium with a "heterogeneous" gas phase at 1 atm total pressure, as a function of temperature. The dotted lines refer to physisorption.

Fig. 2a and b give the composition of the adsorption layer on a Si(111) surface as a function of temperature. Two processes constitute this layer: chemisorption and physisorption. All the radicals in the gas phase compete, with different probabilities, to form a bond with the dangling bonds of the silicon surface atoms. Over this layer of chemisorbed radicals, a submonolayer of physisorbed molecules is formed, which is transparant for the radicals in the gas phase and those present on the surface. Even if physisorption is substantial, chemisorption is hardly influenced by the presence of physisorbed species. Because also

with chemisorbed radicals van der Waals interactions are possible, in a first approximation, the surface area available for two-dimensional physisorption is independent of the coverage of the crystal surface with radicals. So the two layers can be described independently.

Both in the homo- and heterogeneous approach H is the dominating species in the chemisorbed layer. At a temperature of 1400 K, where the growth can be epitaxially, the coverage is 0.14. The only difference between hetero- and homogeneous equilibrium is found in the coverage of the silicon species. In the case of heterogeneous equilibrium SiH_2 is the most important silicon adsorbate, although at 1600 K Si adatoms also must be considered (fig. 2a). The coverage with growth species is for all temperatures very low; 8×10^{-8} at 800 K rising to 2×10^{-6} at 1300 K where it reaches an almost constant level. Comparing fig. 2a with 1a it is evident that the composition of the gas phase and the chemisorption layer are not identical. The surface is considerably enriched in H, Si, SiH and SiH_2, especially at lower temperatures. This is a direct consequence of differences in standard Gibbs free energies upon adsorption for these species.

In the homogeneous assumption, fig. 2b, SiH_2 is also the dominating growth unit. The concentration is evidently much higher, ranging from 0.1% to 2.5% with a maximum in θ_{SiH_2} at 1200 K. Evidently the increase of P_{SiH_2} with higher temperature is too small to counteract the decrease in K_{SiH_2}. Striking is the small coverage of Si_3 at high temperatures, although it is the most important silicon radical in the gas phase its surface coverage amounts to less than 1% of θ_{SiH_2}. In table 1 the reason can be found: the linearity of the Si_3-molecule gives for the adsorbed species no contribution to the rotational part of the entropy, which accounts for the entropy loss to be 10 cal/mol K higher than for SiH_2. This demonstrates that small changes in the standard Gibbs free energy can have an enormous effect on the coverage.

The physisorption layer is, as expected, very rarefied; van der Waals interactions lead only to substantial coverage near the condensation temperature of the adsorbing species. H_2 is the most important physisorbed species. The packing density of the physisorbed layer is at

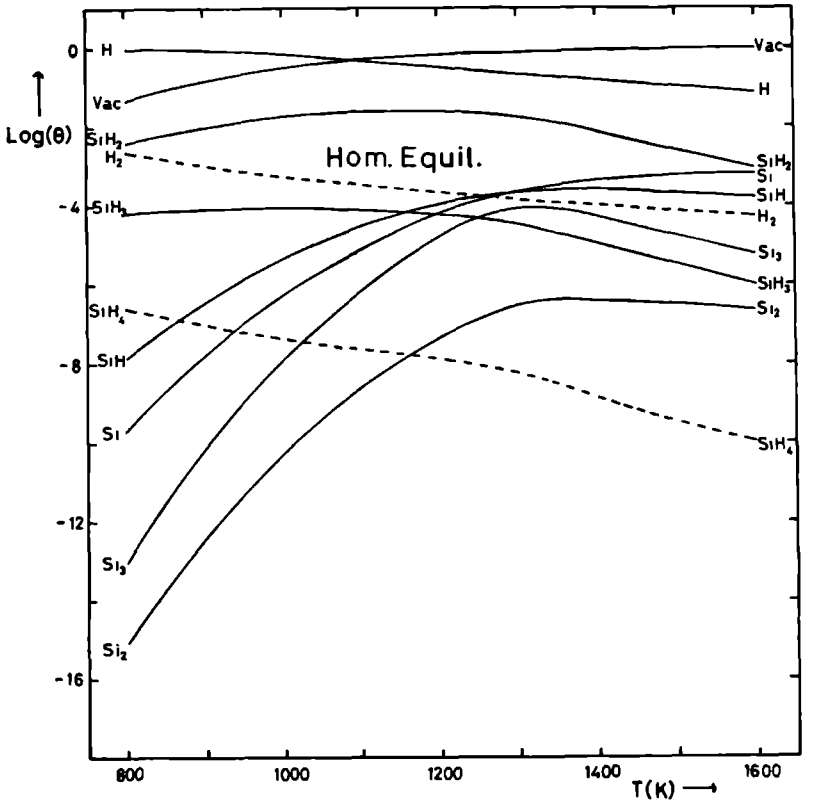

Fig. 2b Coverage of a Si(111) surface, in equilibrium with a "homogeneous" mixture of 1% SiH_4 in H_2 at 1 atm total pressure, as a function of temperature. The dotted lines refer to physisorption.

800 K comparable with the density of H_2 in the gas phase, at 1400 K the adsorption layer is already 2 decades more rarefied. So H_2 is repelled from the silicon surface at higher temperatures. Then the lower entropy going with confinement to a two-dimensional physisorption layer becomes evidently more important than the enthalpy gain.

For SiH_4 it is even less favourable to be present near the crystal surface; the rotational entropy loss is much larger than for H_2. As can be seen in fig. 2a and b at all temperatures the density in the physisorption layer is lower than in the gas phase. If the concentration of silane is compared with Θ_{SiH_2}, it can be seen that as a growth unit, its importance on the crystal surface is negligible at all temperatures.

In the following physisorption will be omitted, because the coverage is always negligible compared with chemisorption. For the crystal growth process of silicon obviously the chemisorbed radicals on the crystal surface are far more important.

4.1. The influence of bond strength on the surface coverage

It has been stated various times that the accuracy in the bond strength is not very high. Several factors can be mentioned that make ΔH_{ad} uncertain: relaxation and reconstruction of the silicon surface, the influence of the lower lying silicon layers and a poor knowledge of even the isolated bond. Therefore it is interesting to see how small changes in the thermodynamic values can influence the adsorption curve.

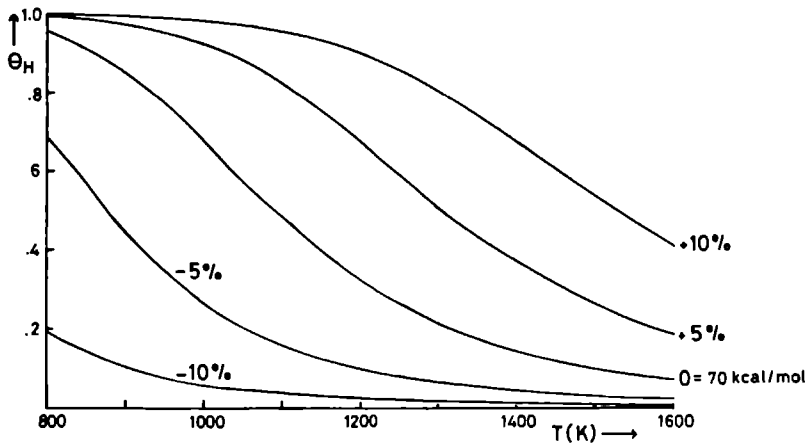

Fig. 3 Hydrogen coverage of a Si(111) surface, in equilibrium with a "heterogeneous" gas phase at 1 atm total pressure, as a function of the Si-H bond strength. Si-Si bond strength is 54 kcal/mol.

To this end it has been calculated how a change of 5 and 10% in the strength of the Si-H bond affects the coverage on a Si(111) surface. The results are given in fig. 3. From this figure it can be seen that at e.g. 1300 K a 10% more stable Si-H bond (with respect to 70 kcal/mol) gives an increase in H-coverage from 21 to 80%. Destabilizing the bond

with 10%, which amounts to a difference of only 7 kcal/mol, results in a θ_H of 2%. The assumption of homogeneous instead of heterogeneous equilibrium in the gas phase only gives minor changes in this pattern. So within the limits of uncertainty the surface is calculated to be almost bare or fully covered with monatomic hydrogen.

The question now is which coverage corresponds to the real situation. Because of the sensitivity of the coverage for small changes in the data, the problem can not be solved theoretically, only experiments can give the final answer. In the literature available to us, we have not been able to find any case where experimental conditions could safely guarantee the near-equilibrium situation required for comparison with our calculations. It is possible to measure the enthalpy with flash desorption, but this technique is too inaccurate to elucidate this situation; the most sensitive method would be in situ determination of the equilibrium coverage. Because UHV analyzing techniques cannot be applied in these high pressure growth systems, no direct information is available yet. As a compromise, indirect information can be obtained studying crystal growth phenomena as a function of gas phase composition, e.g. bunching, pit formation and growth rate, because impurities affect these processes.

The dramatic effect in the change of H-coverage, as described above, of course reflects itself in the adsorption of the other species. In fig. 4a and b the coverage of SiH_2 is shown as a function of T for small changes in the Si-H bond strength, i.e. in the H-coverage, assuming a constant ΔH for the Si-Si bond, viz. 54 kcal/mol. Compared with fig. 2a and 2b the main characteristics of the θ_{SiH_2} vs T plots are preserved in fig. 4a and b. Decreasing the Si-H strength from 77 to 63 kcal/mol in general results in an increase of θ_{SiH_2}. This is an obvious result; $Si-SiH_2$ becomes relatively more stable. At high temperatures a lower Si-H bond strength can also result in a lower θ_{SiH_2}, which is best seen in fig. 4a. This effect is due to a change in the vibration entropy of SiH_2, which is coupled to ΔH_{Si-H}, since the known frequencies of Si-H are used to calculate the stretch and bending frequencies of SiH_2 (eq. (B.11)).

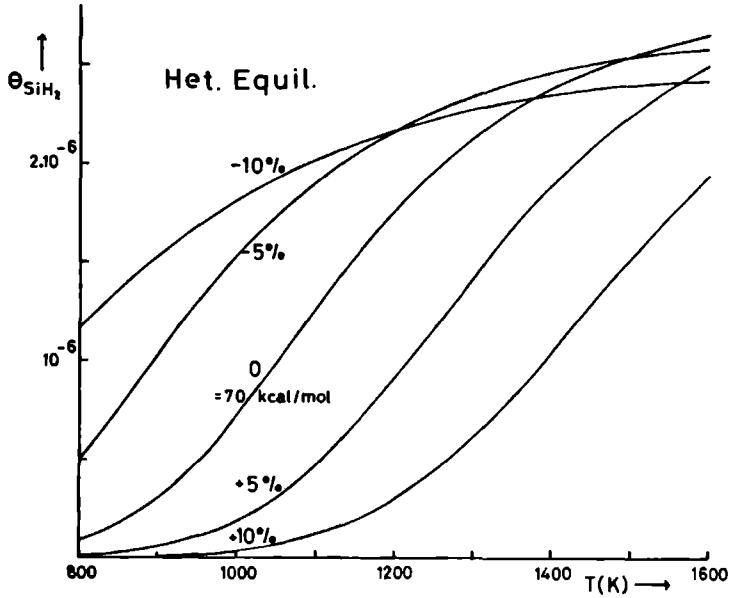

Fig. 4a SiH_2 coverage of a Si(111) surface, in equilibrium with a "heterogeneous" gas phase at 1 atm total pressure, as a function of the Si-H bond strength. Si-Si bond strength is 54 kcal/mol.

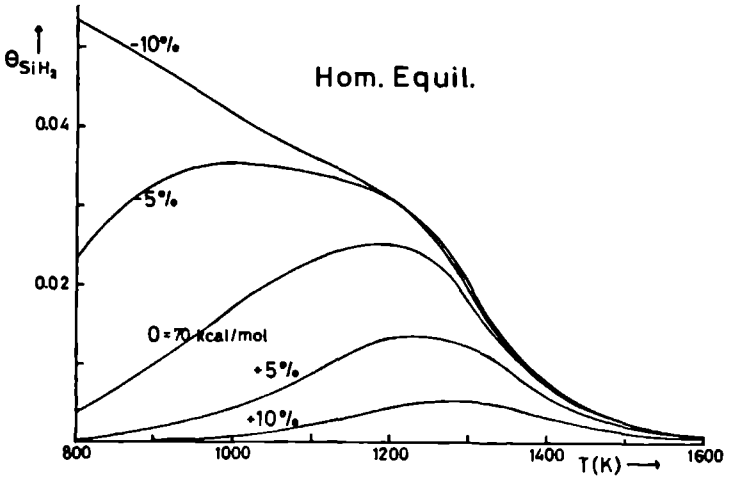

Fig. 4b SiH_2 coverage of a (111) surface, in equilibrium with a "homogeneous" mixture of 1% SiH_4 in H_2 at 1 atm total pressure, as a function of the Si-H bond strength.
Si-Si bond strength is 54 kcal/mol.

In case of heterogeneous equilibrium the coverage of SiH_2 increases as a function of rising temperature for all values of ΔH_{Si-H}, fig. 4a, but the effect is more pronounced for higher Si-H enthalpies. In the homogeneous equilibrium assumption the relation between θ_{SiH_2} and temperature is completely different (fig. 4b), which was already apparent in fig. 2b. When here the Si-H bond is taken to be 10% less stable than in the diatomic molecule, θ_{SiH_2} is continuously decreasing with rising temperature, while for higher bond strengths a maximum in the coverage is found, as in fig. 2b. So only for a very weak Si-H bond SiH_2 can effectively compete with H at low temperatures.

In principle it should be possible to obtain an idea of the surface coverage from the growth rate, which is related with θ_{SiH_2}, but it may not be expected that this will result in a highly reliable picture of the surface; the number of unknown parameters is too large. Only if surface processes are rate limiting a dependence of the growth rate on the equilibrium coverage of SiH_2 is observed; in these cases a trend towards a homogeneous equilibrium situation is expected.

5. Influence of total pressure on surface coverage

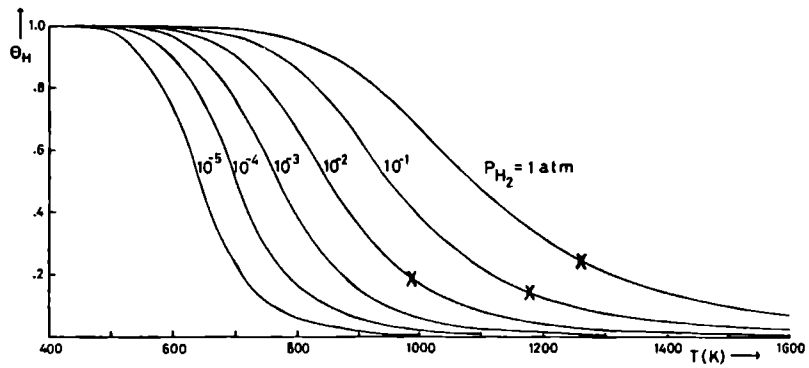

Fig. 5 Hydrogen coverage of a Si(111) surface, in equilibrium with a "heterogeneous" gas phase, as a function of temperature for different total H_2 pressures.
X: transition between mono and polycrystalline growth as experimentally observed by Duchemin [25].

Growth at reduced hydrogen pressures has been shown to be profitable with respect to the perfection of crystallinity of the epilayers [24-27]. It is possible to grow monocrystalline layers at much lower temperatures than at 1 atm, due to the lower coverage of impurities. Although oxygen is notorious in degrading the surface quality also hydrogen has a great influence on the transition between poly- and monocrystalline growth.

In fig. 5 the hydrogen coverage is shown as a function of pressure and temperature, using again for the bond strength of H on Si(111) the value of 70 kcal/mol. It is obvious that lowering the pressure results in an enormous decrease in H-coverage, for the gas phase consists almost entirely of hydrogen. A hundred fold reduction in pressure results at 1300 K in a change in Θ_H from 0.21 to 0.026 and at 1000 K from 0.68 to 0.17 due to a decrease in the partial pressure of monatomic H with a factor of 10.

From this calculation it is clear that working under reduced H_2 pressures gives a less covered surface and thus an increased surface mobility of the growth species. More important is, that it also gives

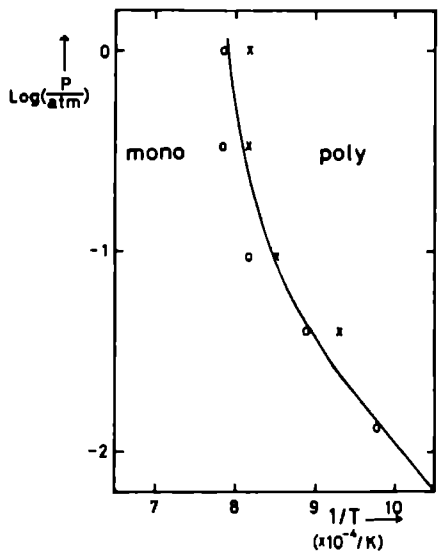

Fig. 6 Transition temperature between mono and polycrystalline growth as a function of total H_2 pressure for silane growth according to Duchemin [25].
o: monocrystalline growth
x: polycrystalline growth

less chance that as a result of a high coverage large amounts of adsorbates are trapped, the epitaxial feeling gets lost and monocrystalline growth becomes polycrystalline growth. A similar effect can be obtained when hydrogen as a carrier gas is replaced by an inert gas. However this has the disadvantage that the influence of oxygen becomes more important; hydrogen is a better agent to diminish the effect of trace amounts of this impurity [28].

The transition between mono- and polycrystalline growth illustrates the influence of impurities. In fig. 6 the results as obtained by Duchemin et al. [25] for SiH_4 growth are plotted. The corresponding transition points are also indicated in fig. 5. It can be seen that,

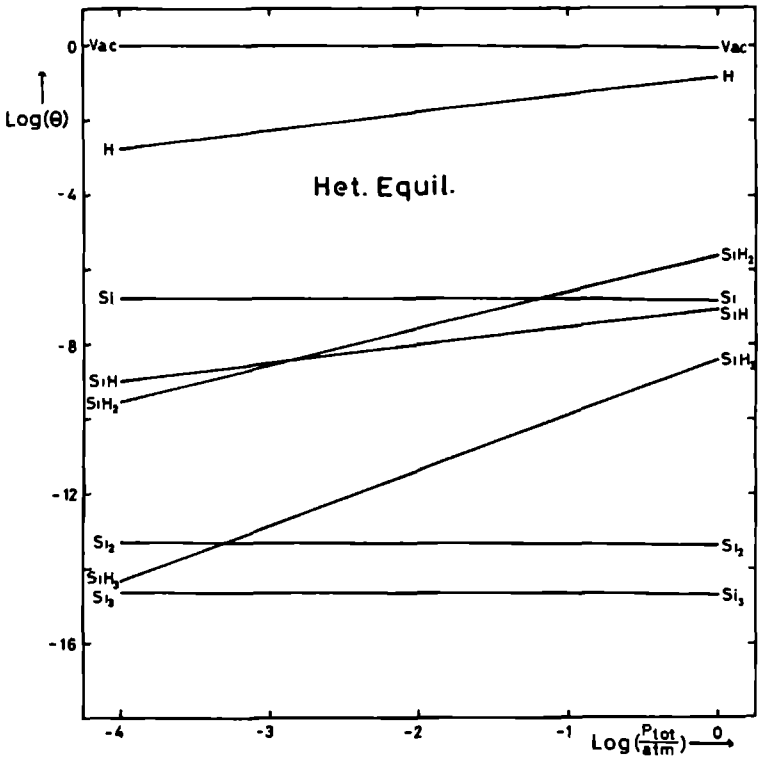

Fig. 7a Coverage of a (111) surface at 1400 K, in equilibrium with a "heterogeneous" gas phase, as a function of the total H_2 pressure.

for the three pressures lying in the range measured by Duchemin, the hydrogen coverage is 20 ± 5%. It must be remembered though, that this figure strongly depends on the value of ΔH°_{Si-H} used in the calculation of θ_H versus T (fig. 3). The point is that the maximum coverage of H where epitaxial growth is possible is remarkably constant.

For the heterogeneous Si-H equilibrium the surface coverages of all chemisorbed species have been calculated at 1400 K as a function of total pressure on a Si(111) surface; fig. 7a. It appears that at high pressures SiH_2 is the main growth species, at lower pressures Si adatoms are the most important growth units. In the homogeneous equilibrium

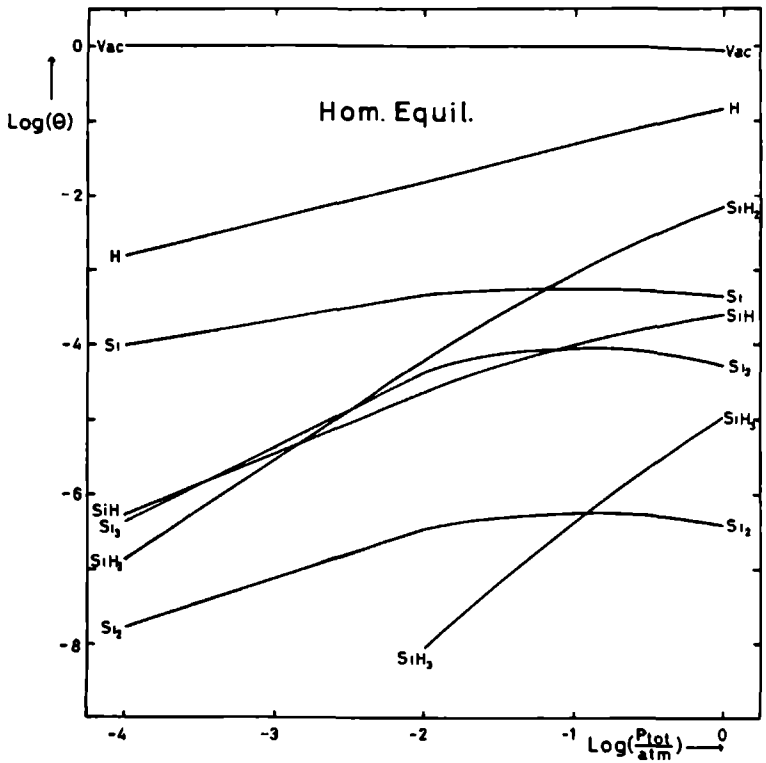

Fig. 7b Coverage of a (111) surface at 1400 K, in equilibrium with a "homogeneous" equilibrium mixture of 100% SiH_4 if $P_{tot} < 10^{-2}$ atm and with a constant partial pressure of SiH_4 of 10^{-2} atm in H_2 for all $P_{tot} > 10^{-2}$ atm, as a function of the total H_2 pressure.

assumption a similar behaviour is found; fig. 7b. The only difference is a much higher SiH_2- and Si-coverage and a greater probability for the existence of silicon clusters, e.g. Si_3, on the surface. Note that in both cases the H-coverage drops with the square root of the H_2 pressure.

6. Discussion

The present analysis has demonstrated that, within the limits of accuracy, it is hard to calculate the impurity coverage better than within one order of magnitude for most temperatures (fig. 3). Despite this uncertainty it can be argued from crystal growth considerations, that a coverage of more than 80% at temperatures higher than 1300 K is very unlikely, in agreement with the conclusions of Claassen [29], but in contrast with the observations of Cadoret and Hottier [30]. The basic requirement for good epitaxial growth is that each growth unit can easily find a correct lattice place at the crystal surface. This implies a surface mobility for growth units which is not hindered by adsorbed impurity atoms, kink sites which are not blocked by these impurities and steps which can propagate freely without bunching on each other, as is the case when a low concentration of impurity atoms is adsorbed on the surface. In addition the concentration of adsorbed growth units must be reasonably high to explain the fast growth processes at the surface.

In our opinion the absence of step bunching, stacking faults and growth pyramids, is direct evidence that for the growth of silicon at T > 1300 K, the silicon surface is reasonably free of chemisorbed impurities. It has been shown above that when 54 and 70 kcal/mol are used for the Si-Si and Si-H bond strength respectively, which directly followed from an analysis of the bond strength, a surface coverage is calculated which is in fair agreement with the above given crystal growth criteria (figs. 2a and b). In addition the concentration of growth species on the surface is high enough to make sure that adsorption and subsequent surface diffusion are not rate limiting at temperatures where gas phase diffusion is known to limit the growth rate. The amount of hydrogen on the surface on the other hand is

low enough not to hinder the motion of steps at temperatures where epitaxial growth is observed. This gives confidence that the calculated adsorption curves are representative for the actual situation, although some uncertainty will remain up to the moment that the coverage has been determined experimentally.

In this paper it is shown that for the growth of silicon from silane, at one atmosphere, SiH_2 is potentially the most important growth species, in agreement with Claassen's assumptions [31]. If the presence of hydrogen is reduced in the gas phase the importance of atomic silicon as a growth unit increases at higher temperatures. SiH_4 is despite the relative high partial pressure in the gas phase of no importance as an adsorbed species: it is not capable to attach properly to the surface. It is however of prime importance as supplier of SiH_2, what can be formed in the gas phase in equilibrium with silane. However it is also possible that the crystal surface acts catalytically on the decomposition of SiH_4; chemical reactions transform physisorbed species in chemisorbed ones, because they are bound stronger to the surface. In the approach presented here this can not be distinguished, only the equilibrium concentrations are calculated.

For the crystal growth process primarily the radicals which are chemisorbed on the crystal surface should be considered; in this study H, Si and SiH_2. This will often give results which are not expected from an analysis of the gas phase composition, it even may be that species which are only present in small concentrations can determine the process.

In the calculations presented above not only all the species present in the Si-H system are taken into account, but also all possible contributions to the entropy have been calculated. This is not always necessary, because it can be seen in table 1 that not all entropy terms are equally important. Therefore if for a system the data to determine the entropy are not as easily accessible as for the silicon-hydrogen system, to a first approximation it will be sufficient just to take the translational part as the entropy loss. This is easy to calculate for all molecules, knowing the molecular weight. It can be verified in

table 1 that the agreement with the more precisely calculated entropy loss is good for H, Si_2, Si_3, SiH_2 and SiH_3. Only for Si and SiH the difference is large.

The best recipe for a correct estimate of the adsorption enthalpy is to take the bond strength of a bond resembling the adsorption bond with respect to bond order and, if possible, configuration. With these data the equilibrium constant for adsorption can be calculated, so that after calculating the partial pressures of the species in the gas phase and using eq. (4) a first impression on the composition of the adsorption layer is obtained. In the above given illustration of adsorption on a Si(111) surface it is seen that hydrogen is the dominating adsorbate. So if only the total coverage is of interest the problem can be simplified by taking only H into account. For this species it is worthwile to evaluate more contributions to the entropy, however an approximation which can be made in any case is to neglect the electronic contribution and the temperature correction for the adsorption enthalpy (table 2). If information is desired regarding the nature of the growth species, then the initial calculations will give an indication which particles can be omitted in a more rigorous evaluation. In the above given example this concerns, Si, SiH, Si_2 and Si_3 at low temperature and Si_2, Si_3 at high temperature in the heterogeneous equilibrium assumption. Especially if the gas phase contains many species this considerably simplifies the calculations.

7. Conclusion

It has been shown that calculations on the degree of adsorption are very sensitive to small variations in the heat of adsorption, or small changes of the entropy, indicating that the utmost care must be taken in using these data for the interpretation of crystal growth phenomena.

The calculations also revealed a high sensitivity to the total hydrogen pressure, demonstrating in this way the benefit of working under reduced H_2 pressures.

Finally it has been shown that the composition of growth species on the silicon surface is completely different from that calculated for the

gas phase. This phenomenon will also remain true when the actual bond strength is smaller or larger than suppossed, and is therefore of general interest for an understanding of the chemistry and the mechanism of the CVD process. Since on the crystal surface only radicals are of interest, in discussing crystal growth, it is important to consider their concentration in the gas phase too.

Acknowledgements

The present investigations have been carried out under the auspices of the Netherlands Foundation for Chemical Research (SON) with financial support from the Netherlands Organization for the advancement of pure Research (ZWO). I would like to thank Professor L.J. Giling for the indispensable discussions, Drs. A.A. Saaman and Mr. W.P.J.H. Jacobs for performing the computer calculations and Dr. R.Z.C. v. Meerten for critically reading the manuscript.

Appendix A Bond strength and length

- Si-Si

  The best correspondence is found with the bonding in a silicon crystal; so half the sublimation enthalpy [12] should be taken: 53.85 kcal/mol. In view of the uncertainties involved a round value of 54 kcal/mol is used. The accompanying bond length is 2.35 Å.

  For all silicon species adsorbing on the silicon surface the same values are used, it should be realized though, that small differences due to the substituents are to be expected.

- Si-H

  As a first approximation it is possible to take the reaction enthalpy of the decomposition of the diatomic molecule in the gaseous elements:

  (A.1) $SiH \rightarrow Si + H$

With the use of data from the JANAF tables [12,14] the enthalpy amounts to 70 ± 2 kcal/mol. In compounds such as SiH_2, SiH_3 and SiH_4, the average Si-H bond strengths are 77, 71 and 77 kcal/mol respectively [15,13]. Clearly hybridization and substituents have a significant effect on the enthalpy of formation.

In this paper we have chosen the lower value of the diatomic bond strength, DABS, because implicitly with adsorption, the small (but certainly present) surface relaxation has to be taken into account.

The bond length varies from 1.52 A, SiH, to 1.48 A, SiH_4; the more substituents the shorter the atomic distance. Following the choice of the DABS, 1.52 A is the Si-H bond length in the present calculations.

Appendix B The partition function related to entropy and heat capacity

In general the relation between the entropy and the canonical partition function (Q) of a system with volume (V) at pressure (P) is given by:

$$(B.1) \quad S = k\left[T \left[\frac{\partial \ln Q}{\partial T}\right]_{V,N} + \ln Q \right]$$

If the system is ideal and consists of N indistinguishable molecules with independent modes of motion the molecular partition function (q) can be written as the product of translational, rotational, vibrational and electronic contributions.

$$(B.2) \quad Q = \frac{(q_t\, q_r\, q_v\, q_e)^N}{N!}$$

Using Stirling's approximation:

$$(B.3) \quad \ln Q = N \ln(q_t\, q_r\, q_v\, q_e) - N \ln N + N$$

$$S = kN\left\{ T \left[\frac{\partial \ln q_t}{\partial T} + \frac{\partial \ln q_r}{\partial T} + \frac{\partial \ln q_v}{\partial T} + \frac{\partial \ln q_e}{\partial T}\right]_{V,N} + \{\ln q_t - \ln N + 1\} + \ln q_r + \ln q_v + \ln q_e \right\}$$

The entropy can be written as a sum of independent contributions.

The influence of the partition function on the heat capacity is given by:

$$(B.4) \quad C_p = C_v + T \left[\frac{\partial V}{\partial T}\right]_{P,N} \left[\frac{\partial P}{\partial T}\right]_{V,N}$$

$$(B.5) \quad C_v = \frac{1}{kT^2} \left[\frac{1}{Q} \frac{\partial^2 Q}{\partial \beta 2} - \frac{1}{Q^2} \left[\frac{\partial Q}{\partial \beta}\right]^2 \right]_{V,N}$$

$$\beta = \frac{1}{kT}$$

The last term in eq. (B.4) is for 1 mol of an ideal gas equal to the gasconstant R. For C_v, the different contributions to the molecular partition function, are also additive, considering that eq. (B.5) is in fact the second derivative of ln Q.

- Translational contribution

  If for the entropy the N! term is included and for the heat capacity the second term of eq. (B.4), it can be derived that for n mol of an ideal gas, with mass m and three degrees of translational freedom:

$$(B.6) \quad q_t = (2\pi mkT/h^2)^{3/2}\, V$$

$$S_t = nR \ln\left[e^{5/2}(2\pi mkT/h^2)^{3/2}\, (kT/P)\right]$$

$$C_{p,t} = \frac{5}{2} nR$$

- Rotational contribution

Assuming that there is no coupling between vibrational and rotational levels in the molecules (the rigid rotator approximation) and that the temperature is high enough to give a continuous distribution of states, it can be derived for a linear molecule, with symmetry factor σ and moment of inertia I, that:

$$(B.7) \quad q_r = \frac{8\pi^2 kT\, I}{\sigma h^2} = \frac{T}{\sigma\theta_r}$$

$$S_r = nR\left(1 + \ln\left\{\frac{T}{\sigma\theta_r}\right\}\right)$$

$$C_{p,r} = nR$$

When spectroscopic data are available it is useful to write the rotational temperature θ_r as a function of the rotational constant B:

$$(B.8) \quad \theta_r = \frac{Bhc}{k}$$

$$B = B_e - \frac{\alpha_e}{2}$$

In JANAF [12-14] the equilibrium rotational constant B_e, and α_e, the rotational vibrational interaction constant, are tabulated.

For polyatomic and adsorbed molecules with F degrees of rotational freedom:

$$(B.9) \quad q_r = \frac{\sqrt{\pi}}{\sigma} \prod_{i=1}^{F} \left\{\frac{8\pi^2 kT}{h^2} I_i\right\}^{1/2} = \frac{\sqrt{\pi}\, T^{F/2}}{\sigma\theta_r}$$

$$S_r = nR\left(\frac{F}{2} + \ln\left\{\frac{\sqrt{\pi}\, T^{F/2}}{\sigma\theta_r}\right\}\right)$$

$$C_{p,r} = \frac{F}{2} nR$$

It should be reminded that for gas phase molecules rotation along 3 axes is possible, for adsorbates rotation is only possible along 1 axis.

- Vibrational contribution

In the harmonic oscillator rigid rotator approximation, after separation of the zero-point energy, the partition function is given by:

$$(B.10)\quad q_v = \frac{1}{1 - \exp\left\{\frac{-h\nu}{kT}\right\}} = \frac{1}{1 - \exp\left\{\frac{-\theta_v}{T}\right\}}$$

$$S_v = nR \left[\frac{(\theta_v/T)\exp(-\theta_v/T)}{1 - \exp(-\theta_v/T)} - \ln\{1 - \exp(-\theta_v/T)\} \right]$$

$$C_{p,v} = nR \left[\frac{(\theta_v/T)^2 \exp(-\theta_v/T)}{\{1 - \exp(-\theta_v/T)\}^2} \right]$$

For adsorbed molecules the vibrational frequency ν, to calculate the vibrational temperature θ_v, is usually unknown so an approximation has to be made. For a harmonic oscillator it is known that ν is proportional to μ, the reduced mass (which equals for an adsorbed molecule its mass), and k_e, the force constant:

$$(B.11)\quad \nu = A \left\{\frac{k_e}{\mu}\right\}^{\frac{1}{2}}$$

$$k_e = \frac{2D_e}{R_e^2}$$

The dissociation energy D_e and bond length R_e are often known. Still missing is knowledge about the proportionality factor A. This can be determined if for a molecule with known D_e and R_e the vibrational frequency is known.

- Electronic contribution

For a molecule with g-fold degenerated excited states, with an energy E above the ground state:

$$(B.12) \quad q_e = \sum_i g_i \exp\left\{\frac{-E_i}{kT}\right\}$$

$$S_e = nR \left[\ln\left\{\Sigma g_i \exp(-E_i/kT)\right\} + \frac{\Sigma(E_i/kT)\, g_i \exp(-E_i/kT)}{\Sigma\, g_i \exp(-E_i/kT)} \right]$$

$$C_{p,e} = nR \left[\frac{\Sigma(E_i/kT)^2\, g_i \exp(-E_i/kT)}{\Sigma\, g_i \exp(-E_i/kT)} - \left[\frac{\Sigma(E_i/kT)\, g_i \exp(-E_i/kT)}{\Sigma\, g_i \exp(-E_i/kT)}\right]^2 \right]$$

REFERENCES

[1] J. Bloem and L.J. Giling in: Current Topics in Materials Science Vol. 1 ch. 4, Ed. E. Kaldis, (North-Holland, Amsterdam 1978)

[2] T. Sakurai and H.D. Hagstrum, Phys. Rev. B14 (1976) 1593

[3] M.L. Yu and B.S. Meyerson, J. Vac. Sci. Techn. A2 (1984) 446

[4] A.A. Chernov and N.S. Papkov, Sov. Phys. Dokl. 21 (1976) 300

[5] A.A. Chernov and M.P. Rusaikin, J. Crystal Growth 45 (1978) 73

[6] R. Cadoret in: Current Topics in Materials Science Vol. 5 ch. 2 Ed. E. Kaldis, (North-Holland, Amsterdam 1980)

[7] J. Korec and M. Heyen, J. Crystal Growth 60 (1982) 297

[8] A.A. Chernov and M.P. Rusaikin, J. Crystal Growth 52 (1981) 185

[9] H.H.C. de Moor and L.J. Giling, this thesis, ch. 3

[10] J.G.E. Gardeniers, H.H.C. de Moor and W.P.J.H. Jacobs, to be published

[11] J.G.E. Gardeniers, H.H.C. de Moor, W.P.J.H. Jacobs and L.J. Giling, to be published

[12] JANAF Thermochemical Tables 2nd ed., NSRDS-NBS 37, (Natl. Bur. Std. US, Washington, DC. 1971)

[13] JANAF Thermochemical Tables, 1978 Supplement, J. Phys. Chem. Ref. Data 7 (1978) 793

[14] JANAF Thermochemical Tables, 1982 Supplement, J. Phys. Chem. Ref. Data 11 (1982) 695

[15] V.P. Glushko, Ed. of Thermodynamic Properties of Individual Substances Vol. II (Nauka, Moscow 1979)

[16] B.I. Nolång and M.W. Richardson, University of Uppsala, private communication

[17] H. Kobayashi, K. Edamoto, M. Onchi and M. Nishijima,
J. Chem. Phys. 78 (1983) 7429
[18] Handbook of Chemistry and Physics, 58th ed.,
Ed. R.C. Weast (CRC Press, Cleveland, OH, 1977-'78)
[19] A.A. Chernov, J. Crystal Growth 42 (1977) 55
[20] J. Bloem, Y.S. Oei, H.H.C. de Moor, J.H.L. Hanssen and L.J. Giling,
J. Electrochem. Soc. 132 (1985) 1973
[21] F. Langlais, F. Hottier and R. Cadoret, J. Crystal Growth 56 (1982) 659
[22] K. Raghavachari, J. Chem. Phys. 83 (1985) 3520
[23] P. Ho and W.G. Breiland, Appl. Phys. Lett. 44 (1984) 51
[24] G.W. Cullen and J.F. Corboy, J. Crystal Growth 70 (1984) 230
[25] J.P. Duchemin, M. Bonnet and F. Koelsch, J. Electrochem. Soc. 125 (1978) 637
[26] T. de Jong, W.A.S. Douma, L. Smit, V.V. Korablev and F.W. Saris,
J. Vac. Sci. Techn. B1 (1983) 888
[27] T.J. Donahue and R. Reif, J. Appl. Phys. 57 (1985) 2757
[28] H.J. Rijks, J. Bloem and L.J. Giling, J. Crystal Growth 47 (1979) 397
[29] W.A.P. Claassen and J. Bloem, J. Crystal Growth 51 (1981) 443
[30] R. Cadoret and F. Hottier, J. Crystal Growth 61 (1983) 259
[31] W.A.P. Claassen, J. Bloem, W.G.J.N. Valkenburg and C.H.J. van den Brekel,
J. Crystal Growth 57 (1982) 259

CHAPTER 3

ADSORPTION AND GROWTH KINETICS ON Si (100) FOR CVD OF SILICON FROM SILANE: THE EFFECT OF SURFACE RECONSTRUCTION

ADSORPTION AND GROWTH KINETICS ON Si(100) FOR CVD OF SILICON FROM SILANE: THE EFFECT OF SURFACE RECONSTRUCTION

Abstract

The coverage of a Si(100) surface with growth units and impurities is calculated, within the Langmuir adsorption model and derivations thereof, for a broken bond as well as for a (2x1) reconstructed surface. It is shown that for the broken bond model, where every silicon atom has two dangling bonds, the coverage with growth species is far too high to be acceptable. A better agreement with the experimentally observed step growth on Si(100) can be attained if surface reconstruction is taken into account. Then adsorption can occur in two ways: (i) directly on the remaining dangling bonds, or (ii) after breaking of the dimer bond. It is shown that double-bonded silicon adsorbates are only present at low concentrations, for the dimer bonds have to be broken, reducing the gain in adsorption energy considerably. So a reconstructed (100) surface is mainly covered by single-bonded species (hydrogen), just like a (111) surface. Combining this result with a kinetic crystal growth model leads - at high temperatures and low supersaturations - to diffusion of single-bonded silicon adsorbates to steps, where they are incorporated two by two, after simultaneous breaking of one dimer bond. The model explains why a (100) surface grows as if it were an F-face, like (111). Nevertheless at high supersaturations, in contrast with Si(111), the silicon coverage on Si(100) becomes high, making direct condensation probable. It is shown that monatomic Si dominates at $T > 1375$ K, below this temperature SiH_2 is the main growth unit.

1. Introduction

During the growth of silicon from the gas phase impurities as well as growth units adhere to the surface and diffuse over the surface to step and kink sites where they can be incorporated in the lattice. A high surface coverage retards the movement of species on the surface; the concentration of growth species can become too high leading to two dimensional nucleation and eventually growth hillocks. A high coverage with impurities can hinder the movement of the steps resulting in bunching and can result in incorporation into the lattice [1,2]. So for a good understanding of crystal growth it is of great importance that the composition and density of the adsorption layer on a crystal surface is studied; experimentally as well as theoretically.

According to UHV studies the top layers of a (100) surface of a diamond-like crystal are distorted compared to the bulk [3,4]. The dangling bonds pointing towards each other overlap and an extra bond is formed between two surface atoms. Essential in the model presented in this study is that the resulting stabilization of the surface will hinder adsorption, if this causes breaking of dimer bonds. Therefore hydrogen is favoured to adsorb compared with silicon species: double-bonded adsorbates are more likely to remove the reconstruction.

In a previous paper adsorption has been studied on Si(111) [5]. A model has been given how to calculate the coverage of a crystal surface if all gas phase species are allowed to be competitive in the adsorption process. It could be concluded that hydrogen is the main adsorbate and that the concentration of growth units is between 10^{-6} and 2.5% depending on the supersaturation and temperature. The presence of a dense adsorption layer, under conditions where epitaxial growth is possible, as predicted by other authors [6,7], could not be confirmed. Unfortunately direct measurements of the surface coverage during chemical vapour deposition at atmospheric pressure are not available, yet. Experiments on the nature of the adsorbates in UHV [8,9] are valuable but extrapolation to conditions normally applied in CVD is not straightforward.

In this paper at first the gas phase composition is calculated for minimal and maximal supersaturation. The adsorption constants needed to calculate the surface coverage are evaluated in appendix A. Then adsorption is discussed for a (100) surface with two dangling bonds at each site: the broken bond model. It will be shown that this model inevitably leads to an unrealistic high coverage of growth species. Reconstruction of the bare surface, which is subsequently assumed, results in much lower surface coverages, which are in better agreement with the experimentally observed step growth [10]. Under conditions where epitaxial growth is found, the surface reconstruction is hardly removed, mainly small amounts of hydrogen are attached to the dangling bonds not involved in the dimerization. Linked with this equilibrium model a kinetic theory is developed based on the assumption that a growth unit is preferably attached adjacent to another double-bonded silicon species in the direction of the dimer bond. This explains that because of the (2x1) reconstruction the silicon surface no longer is a kinked, but becomes a stepped face. As silicon possesses a fourfold screw axis perpendicular to (100), the dimerization in the succeeding layer is rotated 90°. This effectively results in a (100) surface which appears to be flat and step growth, as well as square facets, are likely to be observed.

2. Adsorption on an unreconstructed (100) surface

2.1. Model

In a previous paper a model to calculate Langmuir chemisorption has been discussed [5]; the silicon surface is in chemical equilibrium with the gas phase containing all kind of Si-H species. Each gas phase species reacts with a free silicon surface site (*) to an adsorbed species; e.g. for SiH_2:

$$(1) \qquad SiH_2 + * \rightleftarrows SiH_2^* \qquad K_{ad,SiH_2} = \frac{\theta_{SiH_2}}{\theta_{Vac}\, p_{SiH_2}}$$

The equilibrium constant K_{ad,SiH_2} relates the relative concentration of adsorbed SiH_2 (θ_{SiH_2}) and vacant sites (θ_{Vac}) to the partial pressure of

SiH_2 in the gas phase. This leads to the familiar Langmuir isotherm if competition with all other species is taken into account.

$$(2) \qquad \theta_{SiH_2} = \frac{K_{ad,SiH_2}\, P_{SiH_2}}{1 + \sum_i K_{ad,i}\, P_i}$$

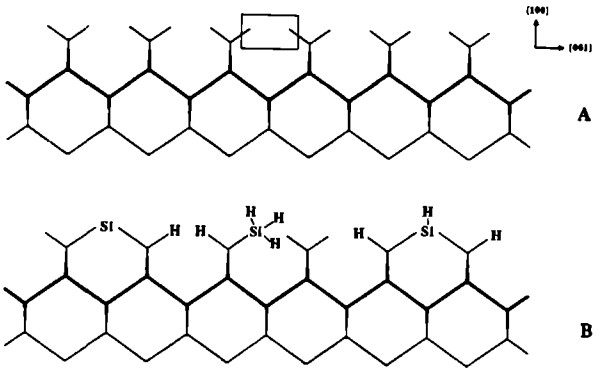

Fig. 1 A) Bare broken bond Si(100) surface
□ An adsorption site consisting of two dangling bonds belonging to different silicon atoms.
B) Broken bond surface covered with silicon species, H and HH.

Every adsorption site consists of two dangling bonds, directed towards each other and making an angle of 35° with the crystal surface, if the broken bond model is applied for a (100) surface; fig. 1A. The possibility to form two bonds permits the accommodation of two H atoms in one site [8]. Silicon species on the other hand are so large that per site only one adsorbate can be present; fig. 1B. So in contrast with a (111) surface the action of a free surface site will depend on the nature of the adsorbates, i.e. for H eq. (1) must be extended with:

$$(3) \qquad H^* + H \rightleftarrows H^*H \qquad K_{ad,2H} = \frac{\theta_{HH}}{\theta_H\, P_H} = \frac{\theta_{HH}}{K_{ad,H}\, \theta_{Vac}\, P_H^2}$$

Assuming that the two H atoms do not interact mutually, when they are attached to the same site, they adsorb independently ($K_{ad,2H} = K_{ad,H}$).

$$(4) \qquad \theta_{HH} = \frac{K_{ad,HH}(P_H)^2}{1 + \sum_i K_{ad,i}\, P_i + K_{ad,HH}\, P_H^2} \qquad K_{ad,HH} = (K_{ad,H})^2$$

Note that the Langmuir isotherm now is no longer linear in hydrogen pressure. H plays a role in two equilibria; adsorption of two H atoms per site is favourable to only one, if $K_{ad,H} P_H > 1$ (or $\theta_H > \theta_{Vac}$), which corresponds to low temperatures or high pressures of hydrogen [8].

Using eqs. (2) and (4) the coverage of a crystal surface can be calculated if the equilibrium constants for adsorption and the partial pressures in the gas phase are known.

2.2. Gas phase composition

The partial pressures of the gas phase species in contact with the surface are determined assuming equilibrium [1,5]. Depending on the rate determining step in the process two limiting situations can be considered:

(1) Heterogeneous equilibrium: between gas phase and solid silicon equilibrium is established, the supersaturation ($\Delta\mu$) of the gas phase is zero. The gas phase composition is only determined by temperature and pressure. The supersaturation of silicon introduced in the reactor is fully needed to overcome the diffusion barrier, the CVD process is mass transport limited representing the growth of epitaxial silicon at high temperatures. The concentrations of growth species at the surface are in principle at the lower limit, being in equilibrium with silicon.

(2) Homogeneous equilibrium [11]: only internally the vapour phase is equilibrated. There is no contact with solid silicon; the silicon content in the gas phase is equal to the input value. $\Delta\mu$ of the gas phase near the crystal surface is maximal, it is all needed to diffuse growth species, over the crystal surface, to step or kink sites, where the incorporation, which is probably rate limiting [12], occurs after a chemical reaction. The growth of polycrystalline silicon at low temperatures is represented by this assumption. In this case the upper limit of the concentrations of growth species in the gas phase and at the crystal surface is calculated.

In fig. 2a the composition of the gas phase using the heterogeneous equilibrium assumption is given. The thermodynamic data used to perform the calculations have been discussed in the paper on Si(111) [5]. The

gas phase mainly consists of H_2, only at very high temperatures the radical H is formed in appreciable amounts. The efficiency of the silicon deposition is high, about 99.99% when an input of 1% SiH_4 in H_2 is used, because in equilibrium the silicon content of the gas phase is only 10^{-6}. Of the unreacted silane a large part will be decomposed to SiH_2 only at very high temperatures.

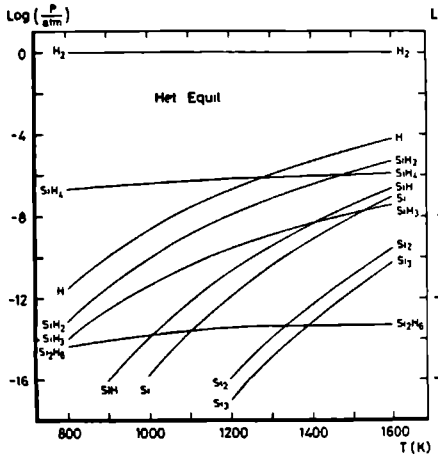

Fig. 2a
Gas phase composition of the Si-H system as a function of temperature, using the heterogeneous equilibrium hypothesis, at 1 atm total pressure.

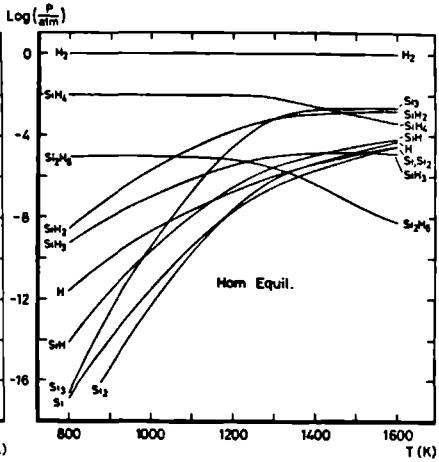

Fig. 2b
Gas phase composition of 1% SiH_4 in H_2 as a function of temperature, using the homogeneous equilibrium hypothesis, at 1 atm total pressure.

Fig. 2b represents the homogeneous equilibrium mixture of 1% SiH_4 in H_2. When the silicon introduced in the system is not able to react to solid silicon, the silicon content of the gas phase is increased by more than three decades. The partial pressures of SiH, SiH_2, SiH_3 and SiH_4 are increased almost proportionally; the influence on Si_2H_6, Si_2 and Si_3 is evidently more drastical, resulting in the dominance of Si_3 over SiH_2 at high temperatures. This clustering of silicon is in fact the onset of the formation of solid silicon, homogeneous nucleation caused by the enormous supersaturation. At low temperatures little silane will be decomposed and the concentration of silicon radicals is low, despite the high silicon content of the gas phase.

2.3. Adsorption constants

The equilibrium constants for adsorption are calculated using a chemical approach. In principle the standard enthalpy (H°_{ad}) and entropy of adsorption (S°_{ad}), constituting the Gibbs free energy (G°_{ad}), are evaluated from known thermochemical data and statistical thermodynamics.

$$(5) \qquad RT \ln K_{ad} = -\Delta H^{\circ}_{ad} + T \Delta S^{\circ}_{ad}$$

In a previous paper [5] the determination of the adsorption constants of Si-H species on a (111) surface is extensively studied. They are discussed in appendix A for an unreconstructed Si(100) surface. The resulting enthalpy gain, entropy loss and adsorption constants are presented in table 1.

Table 1
Adsorption on an unreconstructed Si(100) surface at 1400 K

	ΔH°_{ad} (kcal/mol)	ΔS°_{ad} (cal/mol·K)	log K_{ad}
-H	-70.9	-29.9	4.54
>Si	-105.4	-32.2	9.42
$>Si_2$	-110.3	-50.5	6.17
$>Si_3$	-109.1	-52.0	5.67
>SiH	-109.2	-43.0	7.66
$>SiH_2$	-111.9	-50.0	6.56
$-SiH_3$	-55.1	-39.5	-0.02

All the silicon radicals, apart from SiH_3, are able to form two bonds with the surface. Energetically this is by far more favourable than single-bond adsorption: the extra enthalpy gain, 54 kcal/mol, is by far not compensated by the extra entropy loss (at most 14 cal/mol·K). This results in adsorption constants for double-bonding, which are more than 6 orders of magnitude higher at 1400 K. Therefore the coverage with single-bonded silicon species will be negligible.

Hydrogen adsorption is, apart from the possibility of twofold adsorption per site, identical for a (111) and unreconstructed (100) silicon surface.

2.4. Coverage

Fig. 3a represents the coverage of a Si(100) surface in the broken bond approximation, in equilibrium with a "heterogeneous" gas mixture (fig. 2a); the adsorption constants at 1400 K are presented in table 1. It is striking that the surface is almost fully covered with growth species, the concentration is more than 5 orders of magnitude higher than on a Si(111) surface. Θ_{SiH_2} is more than 0.9 until 1170 K, diminishing rapidly at higher temperatures. If T > 1375 K Si becomes the principal adsorbate. Si is, compared with SiH_2, far more important on a (100) than on a (111) surface. This is caused by the removal of the possibility to rotate for SiH_2 on (100), which raises the entropy loss with 8 cal/mol·K and diminishes K_{ad}.

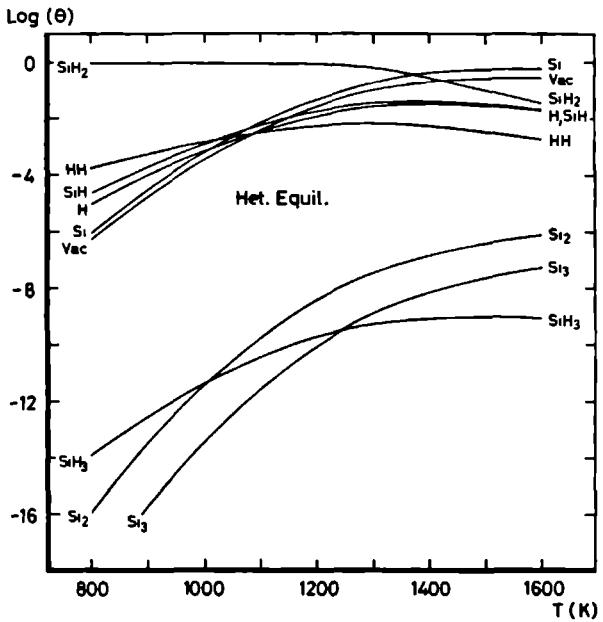

Fig. 3a Coverage of a broken bond Si(100) surface, in equilibrium with a "heterogeneous" gas phase at 1 atm total pressure, as a function of temperature.

In the temperature range of 800 to 1600 K θ_{Si}/θ_{Vac} is almost constant; $K_{ad,Si}\ P_{Si}$ has only a small temperature dependence. Since Si(100) is a rough, kinked, face in the broken bond model, the enthalpy needed to remove a silicon atom out of a perfect surface, which is related with P_{Si}, is exactly counteracted by the gain achieved when a silicon atom is attached to the surface. So the Gibbs free energy is minimal when the configuration entropy is maximal: $\theta_{Vac} = \theta_{Si}$. However the motion of Si on the surface, i.e. vibration, is less restricted than in the bulk, therefore the entropy contribution for adatoms is at 1400 K 16.5 cal/mol·K, instead of 13.5. So θ_{Si}/θ_{Vac} is slightly higher than 1, namely 2, increasing a little with temperature.

Hydrogen is not able to compete effectively with the silicon species, although it is also able to react with the two bonds available per adsorption site. The equilibrium constant $K_{ad,HH}$ (10^9 at 1400 K) is comparable with $K_{ad,Si}$ (3×10^9), however the quadratic dependence on P_H makes an effective adsorption impossible. Until 1100 K it is favourable to have two hydrogen atoms, HH, adsorbed on one site.

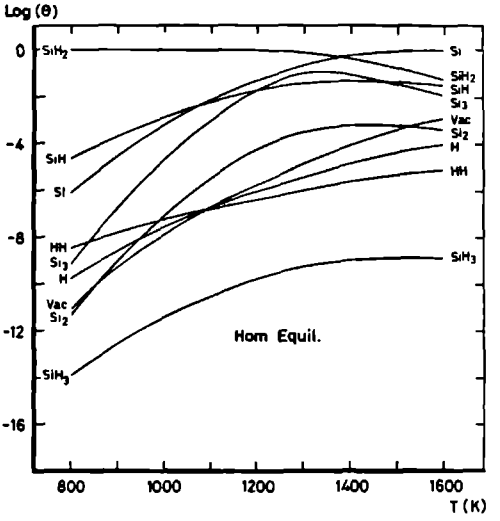

Fig. 3b Coverage of a broken bond Si(100) surface, in equilibrium with a "homogeneous" mixture of 1% SiH_4 in H_2 at 1 atm total pressure, as a function of temperature.

A gas mixture of 1% SiH_4 in H_2, which is in homogeneous equilibrium, of course does not give a significant increase in the total coverage, fig. 3b, since the surface is already fully covered with growth species at zero supersaturation. Because of the much lower concentration of vacant sites, hydrogen is only present on the surface in very small amounts; at most 10^{-4}. Si_2 and Si_3 become relatively more important compared with a "heterogeneous" gas phase, but despite the high P_{Si_3}, because of the higher entropy loss and temperature correction, Si_3 is still less abundant on the surface than SiH_2.

Compared with Si(111) it is most striking that instead of hydrogen, SiH_2 and Si are the dominating adsorbates on Si(100). At first sight this difference could be considered a matter of semantics. As (100) is a rough surface in the broken bond approximation, a silicon adatom is bonded identically to the surface as a surface atom to the bulk. Two adatoms, neighbouring in the direction of their dangling bonds, form one new surface site. Therefore, in such a site, the hydrogen atoms of two neighbouring SiH_2^* are indistinguishable from $^*HH^*$. This view, though correct, is limited as it is a static, momentary one, neglecting the processes preceding the final state.

In this study the growth of a silicon surface is of interest, which means that the equilibrium situation is used to gain knowledge on the dynamics of the process. Especially the tendency of a gas phase species to adsorb, is important in a discussion of the growth kinetics. So, not only the final situation is important, but also the way this is achieved. Therefore the Langmuir model is used, as this implies that the state before and after equilibration is well-defined; an initially bare surface is covered to not more than a monolayer. The composition of the adsorption layer is a measure for the relative probability of the different species to adsorb on the surface, for given partial pressures in the gas phase. The monolayer coverage gives also information on the behaviour to be expected for further outgrowth. If the coverage with growth species is high, the area of "new" surface is large and the growth becomes rough, as the ratio of new to original surface is high.

In this dynamic view a (111) surface is eager to attract H, whereas on (100) preferentially SiH_2 and Si, which are growth species, will be

adsorbed. On (111), rough growth is improbable, because of the low concentration of growth species. Instead, silicon species are likely to diffuse over the surface to steps and kink sites, where they can be incorporated: step growth. On a (100) surface, in the broken bond model, the concentration of growth species is so high that two dimensional nucleation will be very easy and normal, rough, growth will be observed. The adsorbed growth species are bonded very strongly and will have little tendency to move over the surface. Experimentally however it is observed that on (100) as well as (111) surfaces growth species diffuse to steps [10,13]. So in contrast to the results for (111), the present adsorption calculations conflict with crystal growth experiments and a better model to describe the (100) surface must be looked for.

Of course it is not really surprising that for a surface which is rough, step growth is concluded to be unlikely. Yet the calculations on the broken bond surface have their value as they act, in this study, as starting point for the quite complex calculations on a reconstructed surface. The model which will be derived in section 3.3 basicly uses the broken bond model; a correction is applied to calculate the coverage of a reconstructed surface.

3. The effect of surface reconstruction on adsorption

3.1. Reconstruction energy

In UHV a (2x1) LEED pattern is commonly observed for a bare Si(100) surface [3], which is best described by the buckled dimer model [14]. A multiple bond is formed, with a bond order of ~1.4, between two silicon atoms, which are subjected to Jahn-Teller distortion; one of the silicon atoms has moved out of the surface and is negatively charged, the other is displaced inwards and is positive; fig. 4A. On the basis of minimization of Hellmann-Feynman forces it has been calculated that this (2x1) reconstruction stabilizes the surface 39 kcal/mol dimer [15]. A cluster model however indicates only a stabilization of 26 kcal/mol [16]; if subsurface relaxation is taken into account 35 kcal/mol dimer has been reported [17]. On the basis of these results the

reconstruction enthalpy is chosen to be 30 kcal/mol dimer in the present paper. As will be shown in the discussion, the general picture of adsorption on (2x1) reconstructed Si(100) does not depend on the exact choice of the reconstruction energy.

Little is known about the loss of entropy. Intuitively it is expected that formation of an extra bond diminishes the motion of the surface atoms, resulting in a lower vibrational entropy. In contrast Mönch [3] reported that the mean square displacement, in other words the motion, is larger for a (2x1) reconstructed than for a (1x1) truncated surface. The Debye temperature is 240 K for the former surface and 480 K for (1x1) resulting in an entropy which is 4 cal/mol·K larger for the (2x1) structure at 1400 K [18]. The entropy difference, whatever it really is, will be relatively unimportant compared with the large $\Delta H_{reconstr}$. So, in view of the large uncertainty in ΔH°, in our calculations ΔG° of the transition (2x1)→(1x1) will be taken equal to ΔH°: 30 kcal/mol dimer.

It should be realized that for a bare Si(100) surface, reconstruction is stable up to the melting point. This can be understood as follows. For a (2x1) dimerized surface the vibrational entropy is at least 14.8 cal/mol·K at 1685 K: the entropy of the bulk [19]. (Since surface atoms are only bound to three neighbours instead of four, the motion is less restricted and thus S_{vib} will actually be greater than in the bulk.) The vibrational entropy for an unreconstructed surface is at the melting point, 1685 K, 15.5 cal/mol·K (T_D = 480 K). In this case also the electronic levels of the two dangling bonds contribute 2.7 cal/mol·K to the entropy. So reconstruction results in an entropy loss of at most 3.4 cal/mol·K and an energy gain which is at least 24 kcal/mol at the melting point.

This shows that surface reconstruction seriously has to be considered at the higher temperatures which are normal for chemical vapour deposition. In the gas phase radicals are present which can adsorb and may break the dimer bonds. However the tendency to adsorb is greatly reduced since the reconstruction energy must be raised by the adsorbing species.

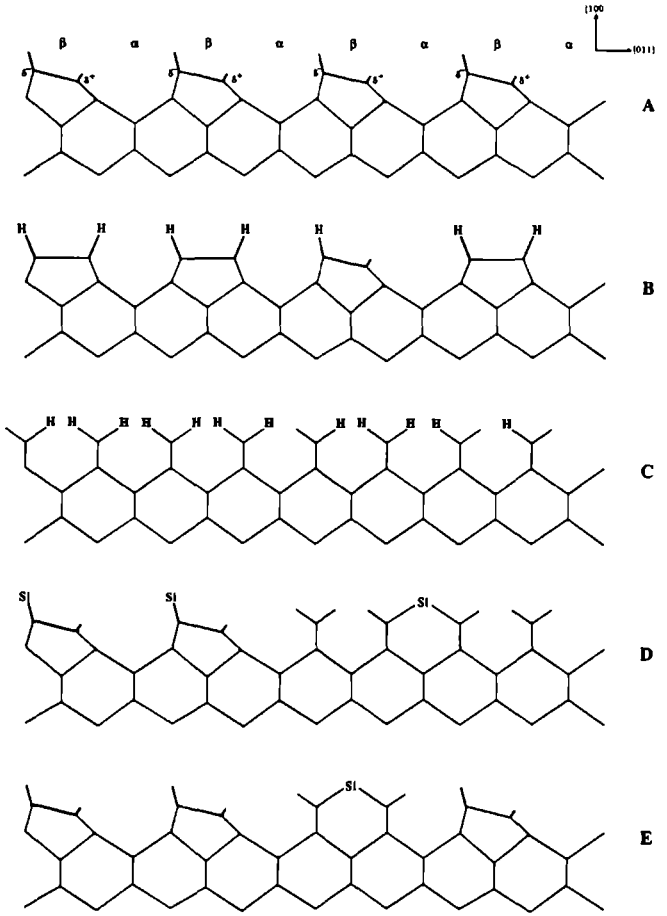

Fig. 4 A) Uncovered (2x1) reconstructed (100) surface with buckled dimers
B) Adsorption of H on α sites
C) Adsorption of H on β sites (and simultaneously on α sites)
D) Adsorption of single- and double-bonded silicon on α sites
E) Adsorption of double-bonded silicon on a β site

In figs. 4 and 5 schematically the structure before and after adsorption is depicted. As discussed, for energetic reasons, the surface will reconstruct in the absence of interactions with gas phase species, at all temperatures. This results in two different adsorption

sites, one, α, consisting of two dangling bonds, the other, β, containing a dimer bond; figs. 4-5A. An α site is, for single-bonded adsorbates, comparable with an adsorption site in the broken bond model: it also consists of two dangling bonds. However they differ considerably, one is protruding and has a high electron density, the other has a very low density and is difficult to access for an adsorbate, since the silicon surface atom, from which it is an orbital, is retroceded. A β site consists of a dimer bond, which has to be broken upon adsorption. Then the surface has locally a broken bond conformation. A β site can be screened by adjacent α sites covered with single-bonded adsorbates.

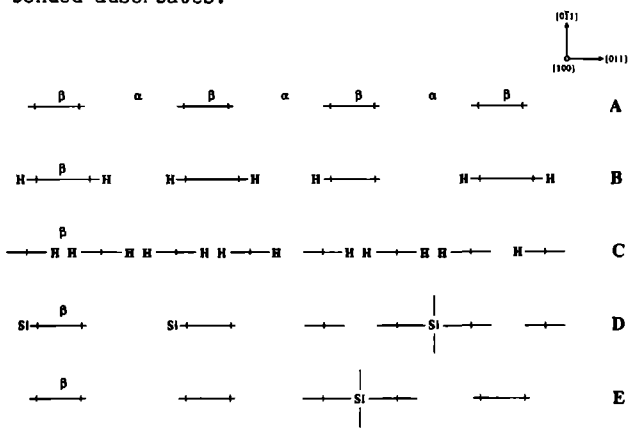

Fig. 5 Top view on a reconstructed (100) surface covered identically as fig. 4. Clearly visible is the (2x1) periodicity along the [011] and [01$\bar{1}$] axes resulting in a one-dimensional adsorption.

Hydrogen adsorbs preferably on α sites (fig. 4B), for at low exposure or elevated temperatures a (2x1)H structure is observed, indicating that reconstruction still is present. If two hydrogen atoms are attached to a dimer bond, the Jahn-Teller distortion is removed in favour of optimum bond lengths and angles, resulting in symmetrical dimers [8,20,21]. At low temperatures or high exposure a (1x1)2H structure is observed. Then hydrogen also adsorbs on β sites and breaks dimer bonds; fig. 4C.

Silicon radicals can attach to an α site and form only one bond, as on a (111) surface; fig. 4D. As opposed to a "broken bond" surface, formation of a second bond is not likely at low silicon coverage. As

indicated on the right-hand side of fig. 4D, this will result in breaking of two dimer bonds. This is because a double-bonded adsorbate connects two adjacent silicon surface atoms, causing them to move away from their other silicon neighbours towards their "bulk position". Thus the overlap with the dangling bonds of those atoms is not effective anymore and the two dimer bonds of the adjacent β sites will be broken. This means that at low silicon coverage double-bond adsorption will occur only at β sites. Only 1 dimer bond is broken and locally the (2x1) reconstruction is destroyed; fig. 4E. An analogous preference for adsorption on a β site is found for the reaction of N_2O with Si(100). The dimer bond is broken and the double-bonded oxygen is in a bridging position between two surface Si atoms [22].

3.3 Adsorption energy

The adsorption constants for a reconstructed surface can be calculated using the broken bond model, if a correction is applied for the broken dimer bonds. The attachment on β sites is identical for all species: one dimer bond must be broken. For α sites a distinction should be made between single- and double-bonded adsorbates.

As shown in figs. 4B and 4D adsorption of single-bonded silicon and hydrogen hardly affects the stability of the adjacent dimer bonds. In case of adsorption on both sides of a dimer bond, it is known that the Jahn-Teller distortion is removed. Since this costs only 6 kcal/mol [15,16], which is small compared with the reconstruction energy of 30 kcal/mol, this correction is not taken into account. Although it is expected that a single bond is less stable than on Si(111), because of the neighbouring dimer bond, in a first approximation, adsorption of single-bonded species on α sites can be treated as on Si(111). The results on this surface indicate that hydrogen is far more important than silicon [5], so in the subsequent discussion the hydrogen coverage on α sites will be taken equal to the total coverage with single-bonded adsorbates. It should be realized though, that single-bonded silicon is negligible in calculating the equilibrium coverage, but essential in a description of the crystal growth process.

Adjacent to double-bonded silicon no dimer bond can be present. Therefore, in contrast to single-bond adsorption, a mutual influence of double-bond adsorption on α sites on the stability of adjacent β sites will appear. So instead of dimensionless in space - it is inherent to the Langmuir model that all all adsorption sites are equal and independent of each other - adsorption of double-bonded species becomes one-dimensional. Due to the reconstruction, now in the [011] direction an interaction is present, which makes the attachment of adsorbates coherent in one direction. Therefore the surface can be thought to be composed of independent strings of alternating α and β sites, for whom the adsorption is connected (fig. 5). This poses great difficulties for the calculations on a reconstructed surface. If the surface is fully covered with silicon adsorbates, on the average they break half of a dimer bond, whereas for a bare surface, each silicon adsorbed on an α site breaks two bonds. Thus the energy gain of double-bonded adsorbates on α sites is in fact a function of the coverage of β sites and vice versa, resulting in complex equations. However in view of the large uncertainty in the reconstruction energy, the model is simplified as far as meaningful.

Essential in the calculations is that the reconstruction energy is divided over all the adsorbates involved in the breaking of a particular dimer bond. This can be done since the crystal surface is in equilibrium with the gas phase. Then the calculated surface coverage depends only on the total energy difference between the covered and the bare surface. It is irrelevant whether the breaking of a dimer bond is raised by the adsorbate on the β site, or by its α-neighbours, or all the adsorbates on the surface. This in contrast with a kinetic view, where in principle one adsorbate causes the breaking of the dimer bond and must overcome an energy barrier. In an equilibrium approach one must be careful to divide the reconstruction energy in a correct way over different species. In this respect a distinction has to be made only between single- and double-bonded species; henceforth indicated as hydrogen respectively silicon. As was shown in the preceding paragraph they adsorb differently on α sites.

It is a major problem in the calculations that the average number of dimer bonds broken per adsorbate, which is determined by the resulting coverage, must be used in the input as the correction to the broken bond model. To avoid an iterative procedure the coverage is calculated for well-defined limiting situations only. This means that beforehand in the calculations a specific surrounding is assumed for an adsorption site, which allows determination of the reconstruction correction and thus makes it possible to compute K_{ad} for the different adsorbates. Of course the "real" environment of an adsorbate can deviate from the choosen one. It is conceived that the average surrounding - hence the "real" coverage - is a combination of limiting situations.

In principle for α and β sites a limiting situation is reached when they are completely covered with hydrogen or silicon or completely empty. This results in 9 limiting conditions if α and β sites are considered to be independent. However, four situations are impossible: Si on α or β sites and vacant neighbouring β respectively α sites - if all dimer bonds are broken obviously the whole surface will be covered with silicon -; H on β sites and α sites bare or covered with silicon, since hydrogen prefers to adsorb on α and silicon on β sites. Energetically only three conditions are really different, as indicated in table 2. One limit obviously is a surface completely covered with silicon (I). A second one that the α sites will be covered with hydrogen and the dimer bonds of the β sites are broken by adsorbed silicon or hydrogen (II). In the last limit (III) the reconstruction will be completely preserved, so the surface will be bare, or it might be that the α sites are covered with hydrogen.

Table 2

Energy correction due to the reconstruction of Si(100) (kcal/mol)

		I	II	III
		$Si_\alpha Si_\beta$	$H_\alpha(Si,H)_\beta$	$(H,Vac)_\alpha Vac_\beta$
α	-H	0	0	0
	>Si	15	20	60
β	-H	15	30	30
	>Si	15	30	30

In table 2 the correction terms are given for adsorption of single-(-H) or double-bonded (>Si) species on an α or β site for these three limiting situations. For the attachment of H on α sites, the first row of table 2, no energy correction has to be applied, because adsorption of hydrogen on α sites does not influence the stability of the adjacent dimer bonds. In general, for all limiting as well as intermediate coverages, the adsorption energy of single-bonded species on α sites should never be corrected for the removal of the reconstruction and is the same as on a (111) surface. For the adsorption of double-bonded silicon on α sites the following corrections can be deduced. If the environment of an α site can be described with limit I ($Si_\alpha Si_\beta$), an energy correction of 15 kcal/mol can be credited to a silicon adsorbate, since on the average half of a dimer bond is broken. If silicon is attached to an α site, which has a surrounding resembling limit II ($H_\alpha(Si,H)_\beta$), the reconstruction energy can be shared with the two adsorbates on the β sites, so on the average two third of a dimer bond is broken (20 kcal/mol). If the reconstruction is still intact, III ($(H,Vac)_\alpha Vac_\beta$), silicon adsorption on an α site will be at the expense of two adjacent dimer bonds (60 kcal/mol).

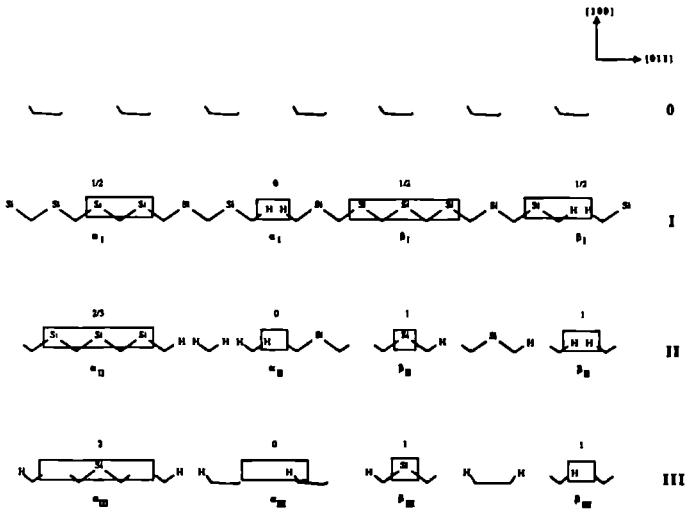

Fig. 6 Number of broken dimer bonds used in the calculations, starting from a bare surface (0), per adsorbate in one of the three different limiting environments.

Adsorption of double- and single-bonded species is equal at β sites: for both the dimer bond had to be broken to allow adsorption. Now only two limiting surroundings can be distinguished: α sites covered with silicon (I), or either with hydrogen or bare (II and III). In the first situation on the average half of a dimer bond is broken (15 kcal/mol) in the latter the adsorbate on the β site must raise the full energy of a dimer (30 kcal/mol). For β sites a surrounding II or III leads to the same energy correction, so in the following both situations are indicated with β_{II}.

In fig. 6 the number of broken dimer bonds per adsorbate and the possibility to divide the extra energy over more species is schematically indicated. In this figure an environment I for α sites is indicated with α_I. For the other limiting situations analogous expressions are used.

For the adsorption calculations it is assumed that adsorbates on α or β sites, feel an environment which can either be described by I, II or III; neglecting all intermediate situations. This means that only the local surrounding of an adsorption site is taken into account in the determination of the standard adsorption energy gain for a specific species; a mean-field approximation. In the approach followed here, for adsorption on an α site only the coverage of the adjacent β and subsequent α sites is considered (in the direction of the dangling bonds). For the adsorption on β sites it is assumed that only the coverage of the adjacent α sites is significant. So the adsorption on α as well as on β sites can be described as a linear combination of the limiting environments:

$$(6) \qquad \theta_{i,\alpha} = k\,\theta_{i,\alpha_I} + l\,\theta_{i,\alpha_{II}} + m\,\theta_{i,\alpha_{III}}$$

$$\theta_{i,\beta} = n\,\theta_{i,\beta_I} + p\,\theta_{i,\beta_{II}}$$

k is the probability that adsorbates on α sites have a surrounding resembling situation I. This chance is assumed to be equal to the product of the total coverage of the β sites and the total silicon coverage of the α sites: the probability that the adjacent β sites are covered and the subsequent α sites contain silicon. This assumption

implies that instead of $\{\theta_{tot,\beta}\ \theta_{Si,\alpha}\}^2$, the simpler expression $\theta_{tot,\beta}\ \theta_{Si,\alpha}$ is used in the calculations. This approximation is justified for a probability nearly equal to one. It should be remembered that only limiting situations are used in the present calculations. Because of this approximation the occurence of each limit is exaggerated, however as they are mixed again later, the intermediate coverage will not deviate much from a calculation where all possible intermediate states also have been taken into account. Following the same model, l is the probability that α sites are vacant or contain hydrogen and β sites are covered, m that β sites are vacant, n that α sites are covered with silicon and p the chance that α is vacant or filled with hydrogen.

Table 3

Log K_{ad} for adsorption on a reconstructed Si(100) surface at 1400 K

	α_I	α_{II}	α_{III}	β_I	β_{II}
-H	4.54	4.54	4.54	2.19	-0.15
-HH-	9.07	9.07	9.07	6.73	4.39
>Si	7.08	6.30	0.05	7.08	4.73
$>Si_2$	3.83	3.05	-3.19	3.83	1.49
$>Si_3$	3.33	2.54	-3.70	3.33	0.98
>SiH	5.32	4.54	-1.71	5.32	2.97
$>SiH_2$	4.22	3.44	-2.81	4.22	1.87
$-SiH_3$	-0.02	-0.02	-0.02	-2.36	-4.71

The calculation of the "real" coverage will proceed in the following way. Starting from a bare surface at first the partial coverages of the α and β sites are calculated assuming one of the three possible surroundings. Each environment has a different correction to the adsorption energy, as derived for the broken bond model, depending on whether the adsorbates are single- or double-bonded. In table 3 the equilibrium constants, for the double-bonded silicon species and single-bonded hydrogen, needed to perform these calculations are presented. With the results of these five calculations, α_I, α_{II}, α_{III}, β_I and β_{II} (equal to β_{III}), it is possible to determine the belonging weight factors k,l,m,n and p. This is possible because these five unknown parameters are given by the following five relations. If the partial coverage $\Sigma\theta_{>Si}$ in the α_I limit is called a, b for α_{II} and c for

α_{III} and the coverage of silicon plus hydrogen is d for β_I and e for β_{II}, it can be derived that the following relations are valid:

(7) $k = n\,(nd + pe)$ $\qquad k + l + m = 1$

$l = p\,(nd + pe)$

$n = ka + lb + mc$ $\qquad n + p = 1$

After calculation of k-p, these can be used in eq. (6), together with a-e, to determine the "real" composition of the adsorbed layer on a reconstructed (100) surface.

3.4 Coverage of a reconstructed (100) surface

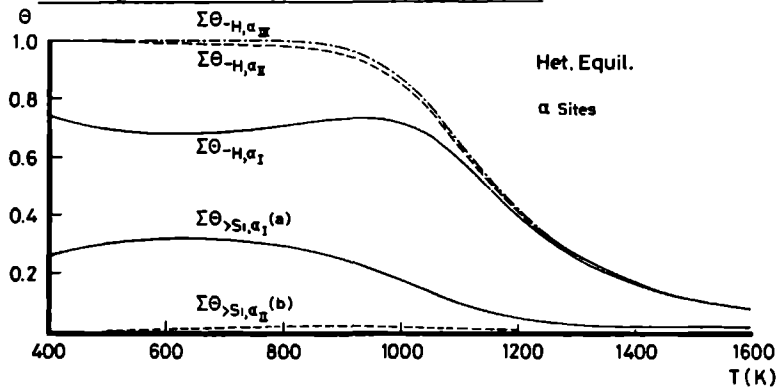

Fig. 7a Partial coverage of the α sites of a (100) surface, in equilibrium with a "heterogeneous" gas phase at 1 atm total pressure, as a function of temperature for the three different limiting environments.
——— α_I-limit - - - - α_{II}-limit ····· α_{III}-limit

The partial coverages of the α sites are calculated using the data of table 3 and fig. 2a and depicted in fig. 7a for the three limiting environments: α_I, α_{II} and α_{III}. Silicon species appear to be present only in fair amounts, ~0.3 from 400 to 900 K, if the neighbouring β and α sites also contain silicon (α_I). This is a significant difference with the silicon coverage in the broken bond model. A further decrease in energy gain with 5 kcal/mol ($\alpha_I \rightarrow \alpha_{II}$) already results in a negligible silicon coverage, illustrating the strong dependence of the surface coverage on the adsorption enthalpy [5]. In the limit III environment

for α sites the coverage with double-bonded silicon species is smaller than 10^{-8}, since adsorption costs the breaking of two dimer bonds. The composition of the adsorbed layer on this reconstructed surface is hardly affected by the stabilization, only the ratio of double- and single-bonded adsorbates has changed as compared with the broken bond model. As long as the same energy correction is used, the ratio of the coverage of the adsorbates is not altered. At low temperatures the total silicon coverage equals θ_{SiH_2}, at high temperatures θ_{Si} (fig. 3a). Hydrogen complements SiH_2 until 800 K, the "α surface" being fully covered with adsorbates, above 1000 K the hydrogen coverage diminishes and the α-vacancy concentration increases. Since the silicon coverage, only relevant for α_I, also decreases at high temperatures, above 1100 K the three hydrogen curves coincide. Then the coverage of the "α surface" is well known and resembles that of a (111) surface: the coverage is low and is mainly made up of hydrogen.

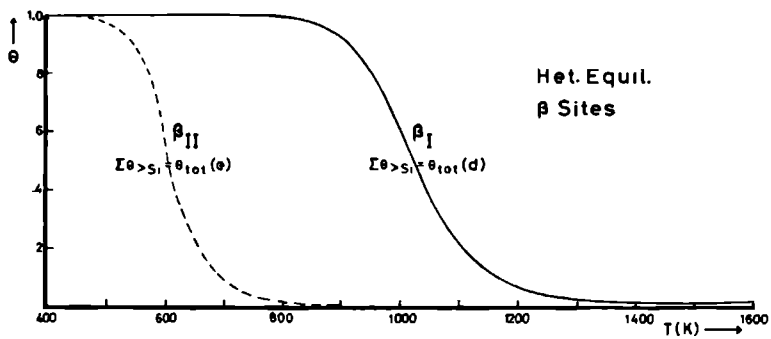

Fig. 7b Partial coverage of the β sites of a (100) surface, in equilibrium with a "heterogeneous" gas phase at 1 atm total pressure, as a function of temperature for the two different limiting situations.
——— β_I-limit - - - - β_{II}-limit

Fig. 7b represents the two limiting coverages of the β sites. The hydrogen coverage is very low for β_I, < 0.2%, as well as β_{II}, < 10^{-5}. Silicon is particularly eager to attach on β sites if the α sites are also filled with silicon species (β_I): silicon has a great tendency to cluster. Then the coverage is still a few percent above 1200 K, else silicon is only adsorbed at low temperatures, the surface being empty above 800 K (β_{II}).

It can be concluded from figs. 7a and b that hydrogen preferably will occupy the α positions whereas silicon, especially at lower temperatures, mainly is found on β sites. The difference in reactivity of α sites towards double- and single-bonded reactants apparently is that large that hydrogen now is favoured above silicon. The assumption that single-bonded adsorbates do not influence the stability of adjacent dimer bonds, whereas they are both broken when double-bonded silicon species are attached to an α site, can drastically influence the growth behaviour of a (100) surface. Adsorption of gas phase species on β sites is hindered for all equally, so the composition of the "β-surface" is the same as in the broken bond model, only the total coverage is lowered.

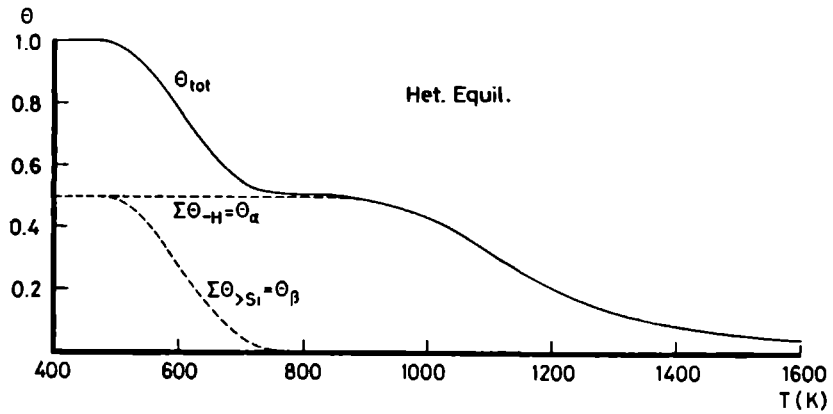

Fig. 8 Real coverage of a reconstructed (100) surface, in equilibrium with a "heterogeneous" gas phase at 1 atm total pressure, as a function of temperature.
——— total coverage
- - - - coverage with double- or single-bonded species

Since the partial coverages in the limiting situations now have been determined, it is possible to proceed to the next and final step in the calculation of the real coverage of the (100) surface, viz. the determination how much each limiting partial coverage contributes to the actual coverage. To this end the 5 unknown coefficients k, l, m, n and p in eq. (6) have to be calculated. This is realized by using the 5 relations as given in eq. (7), where the parameters a, b, c, d and e actually stand for the silicon curves as given and indicated in figs. 7a

and b. As depicted in fig. 8, at 400 K the β sites are fully covered with SiH_2, irrespectively of their surrounding. Since the silicon coverage in the α_{II}-limit (b) appears to be very low (7×10^{-4}), not compensated by a high one for α_I (a), it can be shown using eq. (7) that the α sites are mainly filled with hydrogen. This results in a limit II environment for α as well as β sites: l and p = 1. As for β sites β_{II} energetically equals β_{III}, the coverage can be described at all temperatures by β_{II}. The β sites are either empty or filled with silicon, the hydrogen coverage being negligible. Related with the rapidly increasing vacancy concentration on β, the surrounding of the α sites changes from limit II to limit III (l→0, m→1). Since both environments results in nearly the same coverage on α sites, a (100) surface seems to consist of two types of independent sites. For all temperatures α sites are mainly filled with single-bonded adsorbates (HH, H and a tiny fraction of silicon) and double-bonded silicon species are almost absent, so the coverage of β sites is not related to that of α sites. The α coverage nearly equals that of a (111) surface, since only single-bonded species are adsorbed. At very low temperatures β sites contain SiH_2, however the coverage decreases rapidly above 500 K (β_{II}). If T > 800 K the β sites are empty and the resemblance with (111) now applies to the whole (100) surface. At 1400 K the coverage with double-bonded silicon, on β sites, is only 4×10^{-5}, just slightly higher than on Si(111). The hydrogen coverage (HH + H) is 0.08 on (100), comparable with 0.14 on (111); the coverage with single-bonded silicon, adsorbed on α sites, is 10^{-6} [5]. It should be noticed that with respect to the α or β sites only, the (100) values as presented here should be doubled.

The results show that if reconstruction is taken into account, at low supersaturation, the silicon coverage is diminished enormously. So the probability of two adjacent silicon species with dangling bonds pointing towards each other - a nucleus on (100), as this forms a new surface site - has become so low that two dimensional nucleation, which was very probable in the broken bond model, becomes unlikely. Now silicon species are able to diffuse, preferentially via α sites, to steps. Since the coverage of α sites is comparable with the coverage on a (111) surface, growth on a (100) reconstructed surface will resemble growth on (111).

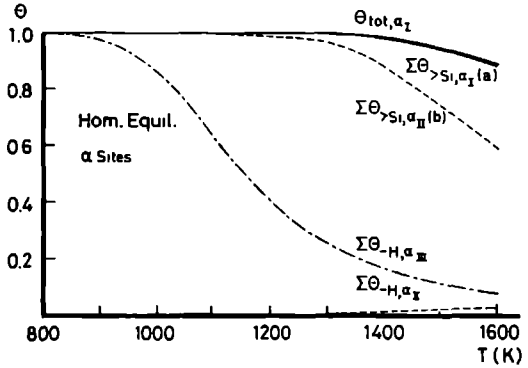

Fig. 9a Partial coverage of the α sites of a (100) surface, in equilibrium with a "homogeneous" mixture of 1% SiH_4 in H_2 at 1 atm total pressure, as a function of temperature, for the three different limiting environments.
——— α_I-limit - - - - α_{II}-limit -·-·-·- α_{III}-limit

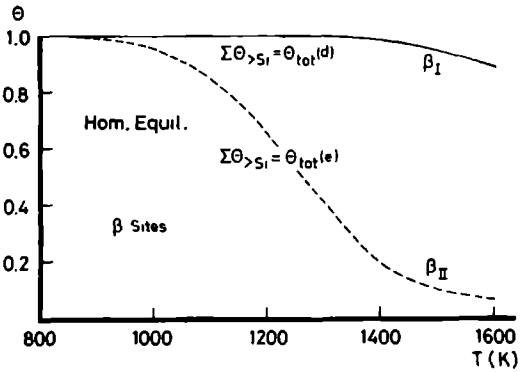

Fig. 9b Partial coverage of the β sites of a (100) surface, in equilibrium with a "homogeneous" mixture of 1% SiH_4 in H_2 at 1 atm total pressure, as a function of temperature, for the two different limiting situations.
——— β_I-limit - - - - β_{II}-limit

The situation is quite different for high supersaturations in the gas phase. The partial pressures of the silicon species are more than three decades higher if 1% SiH_4 in H_2 is only in equilibrium internally in the gas phase and of course with the adsorbed species on the crystal surface. This results for the α sites up to 1600 K in a high silicon coverage if the β sites are occupied: α_I and α_{II}; fig. 9a. Only in the α_{III} limit it is still very difficult for silicon to adsorb because this costs two dimer bonds, then only hydrogen is adsorbed. For the β sites, where only the adsorption of silicon is significant, the coverage is increased considerably as compared with zero supersaturation; fig. 9b. For β_{II} the total coverage with double-bonded silicon ($\Sigma\Theta_{>Si}$) is only smaller than 0.50 for T > 1260 K, instead of for T > 600 K at $\mu = 0$ (fig. 7b).

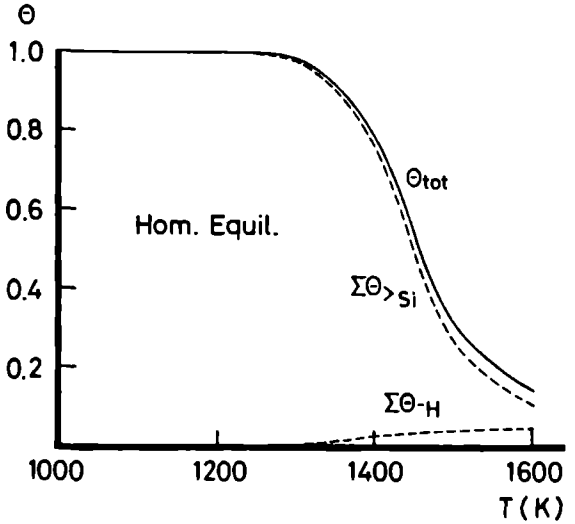

Fig. 10 Real coverage of a reconstructed (100) surface, in equilibrium with a "homogeneous" mixture of 1% SiH_4 in H_2 at 1 atm total pressure, as a function of temperature.
——— total coverage
- - - - coverage with double- or single-bonded species

The greater tendency of the α and β sites to be covered with silicon in homogeneous equilibrium is reflected in the resulting coverage; fig. 10. Up to 1200 K both α and β sites are fully covered with silicon and the coverage can be described with α_I and β_I. The small vacancy concentration at higher temperatures makes a limit III environment more

probable for α as well as for β sites. The lower coverage of β sites results in a greater contribution of α_{III}, the resulting smaller silicon coverage of α sites in a greater importance of β_{III} and vice versa. The higher hydrogen coverage on α sites favours initially also α_{II}. So the interaction between α and β sites, which is very strong when double-bonded silicon is adsorbed, is weakened rapidly at increasing temperatures.

At high supersaturations a (100) surface is, because of the high coverage with double-bonded growth species, even at high temperatures, very sensitive to two dimensional nucleation. So, compared with a (111) surface, for (100) the probability for two dimensional nucleation between steps is much higher [23]. Therefore to obtain step, instead of normal growth, one must always try to work in the diffusion limited regime, to be assured of a low supersaturation at the crystal surface. Only then defect free growth is to be expected for a (100) surface.

4. Influence of pressure on the coverage of a reconstructed surface

It is known that at reduced pressures the coverage with impurities can diminish drastically. The motion of growth units over the surface and the propagation of steps is less hindered and fewer kink sites, where growth takes place, are blocked. A lower coverage with growth units reduces the chance of two dimensional nucleation. Thus the crystalline perfection of the layers can improve considerably and the temperature where growth is monocrystalline can be lower [24,25].

In fig. 11a the coverage, as calculated with eqs. (6) and (7), is depicted for zero supersaturation. For all pressures the α sites only contain hydrogen and the β sites only silicon. The shape of the curves is similar to fig. 8. At low temperatures the α sites are fully covered, so the coverage of the β sites is $2*(\theta_{tot}-0.5)$. The silicon coverage is reduced drastically at lower total pressures. When the hydrogen coverage of the α sites starts to decrease, the β sites are already empty. Proper crystal growth is to be expected when the hydrogen coverage comes below 10% [5], the exact value depending on the

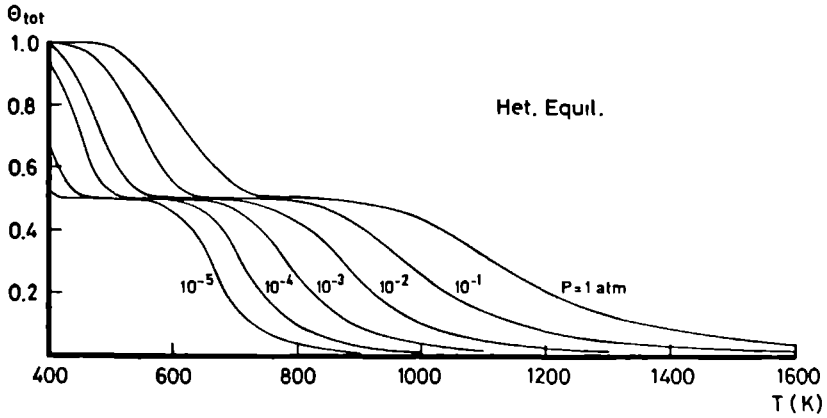

Fig. 11a Real total coverage of a reconstructed (100) surface, in equilibrium with a "heterogeneous" gas phase, as a function of temperature for different total pressures.

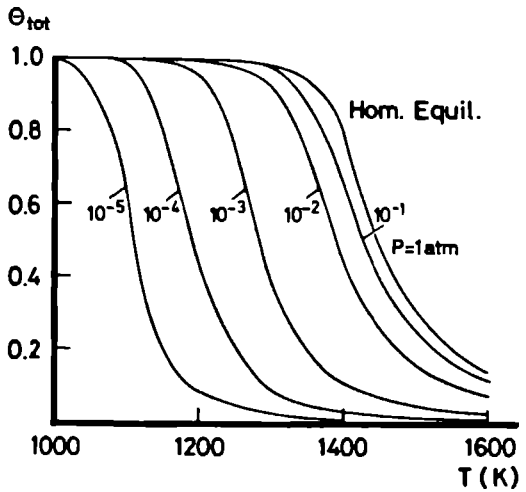

Fig. 11b Real total coverage of a reconstructed (100) surface, in equilibrium with a "homogeneous" equilibrium mixture of 100% SiH_4 if $P_{tot} < 10^{-2}$ atm and with SiH_4 in H_2, $P_{SiH_4} = 10^{-2}$ atm, for $P_{tot} > 10^{-2}$ atm, as a function of temperature for different total pressures.

mechanism of surface diffusion and step propagation. Then the diffusion of growth species is no longer seriously hindered and monocrystalline growth is possible. Since α sites resemble a (111) surface, the influence of pressure on the transition between poly- and monocrystalline growth is similar for a (111) and a reconstructed (100) surface at zero supersaturation.

At high supersaturations the improvement, which can be expected by lowering the pressure is quite different, compared with the heterogeneous case. At all temperatures the main adsorbate will be silicon instead of hydrogen, the contribution of hydrogen decreasing with pressure. The total coverage, which nearly equals $\Sigma\theta_{>Si}$, is depicted in fig. 11b. At low temperatures the tendency for silicon to adsorb is so great that β and α sites are fully covered. At elevated temperatures, too high for hydrogen adsorption to take over, the silicon coverage diminishes rapidly, strengthened by the accompanying shift from a limit I to a limit III surrounding for α as well as β sites. At low pressures the drop in silicon coverage occurs at lower temperature so two dimensional nucleation, preventing step growth in layers, becomes less probable reducing the limiting temperature for monocrystalline growth. From a comparison of figs. 11a and 11b it is clear that the total coverage is lower and the nature of the adsorbates is different in the heterogenous case. Therefore at small supersaturations epitaxial growth will be possible some hundreds of degrees kelvin lower than at high $\Delta\mu$. So it is also important to prevent a high supersaturation at low temperatures.

The partial pressures of the gas phase components and therefore also the composition of the adsorbed layer depends on the total pressure. For heterogeneous equilibrium the curve $\theta_{Si} = \theta_{SiH_2}$ shifts to lower temperatures at reduced total pressures, since P_{SiH_2}/P_{Si} is proportional to P_{tot}; fig. 12a. As can be deduced from that figure, at high temperatures where monocrystalline growth is possible, monatomic silicon can be an important growth species on a (100) surface, at all pressures.

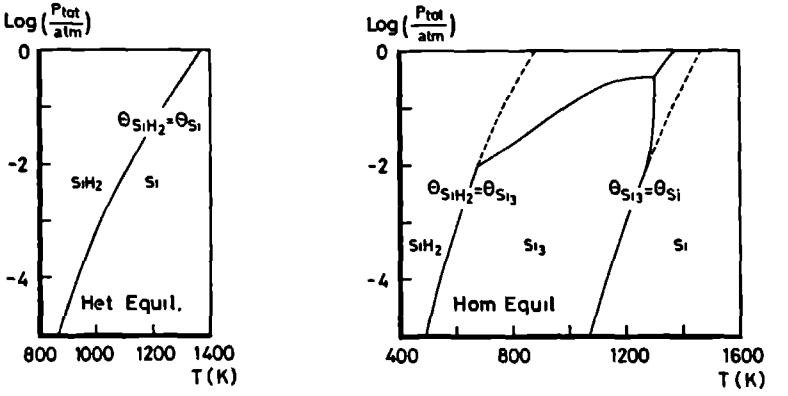

a adsorption layer in equilibrium with a "heterogeneous" gas phase

b adsorption layer in equilibrium with a "homogeneous" equilibrium mixture. For $P_{tot} < 10^{-2}$ atm 100% SiH_4, for larger pressures SiH_4 in H_2, $P_{SiH_4} = 10^{-2}$ atm The dashed lines refer to 100% SiH_4.

Fig 12 Most important adsorbed growth species on a (100) surface, as a function of temperature and total pressure.

For homogeneous equilibrium going to higher temperatures first SiH_2, then Si_3 and finally Si is the main silicon adsorbate; fig. 12b. For total pressures smaller than 10^{-2} atm (100% SiH_4), the curve $\theta_{SiH_2} = \theta_{Si_3}$ is proportional to P_{tot}^3, for SiH_4, Si_2H_6 and H_2 are most abundant in the gas phase, resulting in a larger contribution of Si_3 at low pressures. The transition $\theta_{Si_3} = \theta_{Si}$ has a pressure dependence of the power 2/3, since then Si_3 is the principal silicon gas phase species. The shape of the curves representing equal coverage of two species changes for $P > 10^{-2}$ atm. This is due to the varying Si-H ratio (%SiH_4 in H_2) as can be seen when it is taken constant (dashed lines). Increasing the hydrogen percentage suppresses the contribution of Si_3 considerably, herewith improving the crystalline perfection of the grown layers. Hydrogen reduces also the total silicon coverage as can implicitely be deduced from fig. 11b, where the influence of the total pressure on the coverage becomes much smaller, when for $P_{tot} > 10^{-2}$ atm H_2 is introduced into the system.

5. Crystal growth on a reconstructed (100) surface

The equilibrium coverage as calculated in the preceding sections provides a good start to discuss crystal growth on a Si(100) surface. So far only a few articles discuss the influence of surface reconstruction on crystal growth [10,26-28]. An atomistic picture explaining the preference for growth units to diffuse to step and kink sites, instead of sticking to the surface and forming two-dimensional nuclei, has not been presented yet. When the structure of the surface, as obtained from the adsorption calculations, is used in a kinetic model, it can be shown that it is quite obvious that steps are stable on a (100) surface and two dimensional nucleation improbable at low supersaturations.

In contrast to an equilibrium approach as used in the above given adsorption calculations, in crystal growth it is also important when the growth process a dimer bond is broken or formed and which adsorbate is causing it. Starting point for a good understanding of the crystal growth process must be the coverage of the crystal surface. This indicates the probability that a site is covered with growth units or impurities and the tendency that they will adsorb on a specific site. It gives an idea about the possibility of surface diffusion to steps versus the probability for two dimensional nucleation. For the incorporation of the growth units on step or kink sites the full energy of the bonds to be broken or formed has to be taken into account, instead of the average energy as in the adsorption calculations. The probability that a growth unit, which breaks for example 1 dimer bond upon incorporation, will attach to a kink, is given by the $\Sigma O_{>Si,\beta_{II}}$ curve: the coverage of double-bonded silicon species adsorbed at the cost of one dimer bond (figs. 7b and 9b).

The model which will be presented is based on a perfect (2x1) reconstructed surface. It should be realized that in fact regions will exist where the (2x1) pattern is alternated with areas with for example a (2x2) or a (4x2) structure. They are all based on asymmetric dimers, only the ordering is different. For the model it has basicly no consequences, only the regularity is affected. The dimerization of the surface is in the subsequent discussion taken in the [011] direction.

On a reconstructed (100) surface the coverage is low at zero supersaturation and high temperatures, so growth can proceed via diffusion of single- and double-bonded silicon species to steps and kinks. For $\Delta\mu = 0$ on β sites only double-bonded silicon is adsorbed: $\Sigma\theta_{>Si} = 3.7\times10^{-5}$ at 1400 K. The single-bonded silicon adsorbates are found only on α sites: $\Sigma\theta_{-Si} = 1.3\times10^{-6}$ [5], all coverages related to the entire surface. On a (111) surface, representative for α sites, an activation energy for diffusion of 25 kcal/mol has been reported [29], almost half of the adsorption enthalpy. For double-bonded species this results in 39 kcal/mol, if also $\frac{1}{2}\Delta H^{o}_{ads}$, corrected for the breaking of a dimer bond, is taken. Thus the probability to diffuse is 150 times larger for single-bonded silicon species. Since the coverage differs a factor of 30, the ratio of the single- to double-bonded silicon flux is 5 at 1400 K. However, if the dimer bond is not restored in the activated complex of the double-bonded adsorbate, which is quite probable, the flux ratio increases to 800. This means that single-bonded growth units will dominate the step growth.

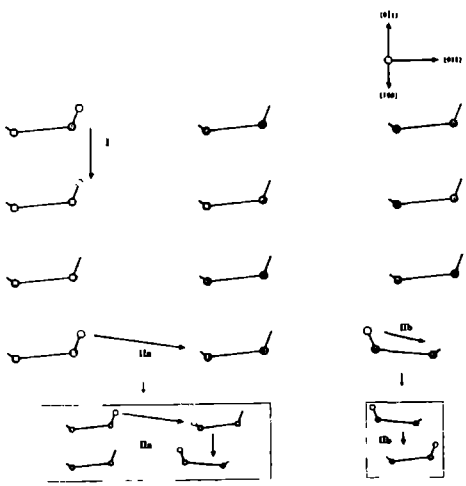

Fig. 13 Anisotropic diffusion on reconstructed Si(100); schematic view on a tilted (100) surface.
I: Jump from one α site directly to another
IIa: Jump from one dangling bond to another, within one α site
IIb: Jump from one α site to another via a β site

As can be seen in fig. 13 diffusion of single-bonded silicon adsorbates is anisotropic in the <011> direction. They can diffuse from α to α site directly (I), or via a β site (IIa and b). The second process involves a jump from a protruding dangling bond to a retroceded bond with a low electron density (IIb). The dimer bond will be distorted severely, but may not be broken, since then the silicon species could adsorb on the β site. Kinetically this step is unfavourable to diffusion via α sites, which involves two protruding dangling bonds, only. So like on a broken bond surface [30], diffusion is favoured in the $[0\bar{1}1]$ (and $[01\bar{1}]$) directions. In the next layer the dimers are rotated 90° and accordingly the diffusion path changes from $[0\bar{1}1]$ to [011]. Essential is that in each layer the diffusion is mainly limited to a linear motion. This is in contrast with a (111) surface where diffusion is not limited to a row of surface sites but is equivalent in 3 directions.

If in the diffusion process via a β site (IIb in fig. 13) the dimer bond is broken, the diffusing single-bonded species can attach to the β site and form two bonds. In principle this process is reversible: a double-bonded adsorbate on a β site also can jump out of the β site and attach to a dangling bond of the adjacent α site with simultaneous restoring of the dimer bond. So there is a possibility for silicon adsorbates to exchange between α and β sites. In equilibrium this exchange does not influence the population of single- and double-bonded growth species on the surface. However in the growth process local differences in the supersaturation can occur. As diffusion gives mainly a transport of single-bonded growth species towards the step, $\Delta\mu$ tends to be lower for α sites than for β sites near the step. As long as the kinetic barrier for the jump from α to β sites and vice versa is negligible, this results in a removal of double-bonded adsorbates from β sites and thus effectively a diffusion of these two dimensional nuclei to the step. If the energy barrier for exchange between α and β sites is high, it could be that the adsorbates on both sites behave independently. However silicon adsorbates could also be trapped predominantly on β sites, enhancing considerably two dimensional nucleation. If on the other hand the reverse jump from a β to an α site is easier, monatomic two dimensional nuclei can dissolve, promoting step

growth. At the α sites the supersaturation of especially monatomic silicon will increase. This can additionally promote the crystal growth at the steps since, as will be shown later, Si can form dimer bonds within the adsorbed layer.

5.2 Step propagation

The dimerization of a (100) surface leads to adsorption and crystal growth which is neighbour related in the [011] (and $[0\bar{1}\bar{1}]$) directions. If growth occurs next to one already occupied site in one of these directions, one dimer bond must be broken if the attachment is on an α site and no bond if it is on a β site. If the adjacent sites are unoccupied, formation of a double bond costs 1 dimer bond on a β site and two on an α site, just like adsorption on a bare surface. So the presence of one neighbour in the dimerization direction, as in case of a [011] step, reduces the number of bonds to be broken by one.

The adsorbates have the possibility to form dimer bonds in the $[0\bar{1}1]$ direction. This dimerization promotes the incorporation of growth species if it occurs simultaneously, thus reducing the activation energy. Of course this is only possible, if no hydrogen is attached to one of the dangling bonds involved in this dimerization process, for this must be desorbed first. So immediate formation of this dimer bond is not possible for SiH_2. This means that the incorporation could be different for Si and SiH_2, the two major growth species, favouring monatomic silicon.

On the basis of the possibility to form a new dimer bond in the adsorbed layer, the different growth sites can be divided into two groups (a,b,c) and (d,e,f). The first three sites having the possibility to form a new dimer bond, the latter not. As indicated in fig. 14 the most favourable site is (a) since no dimer bond has to be broken and the adsorbed silicon can form a new dimer bond with the adjacent silicon atom in the adsorbed layer. For (b) and (c) one, respectively two dimer bonds must be broken, compensated by the formation of a new one. Adsorption on (d), (e) and (f) results in breaking of respectively no, one, or two dimer bonds, yet no new one can be formed.

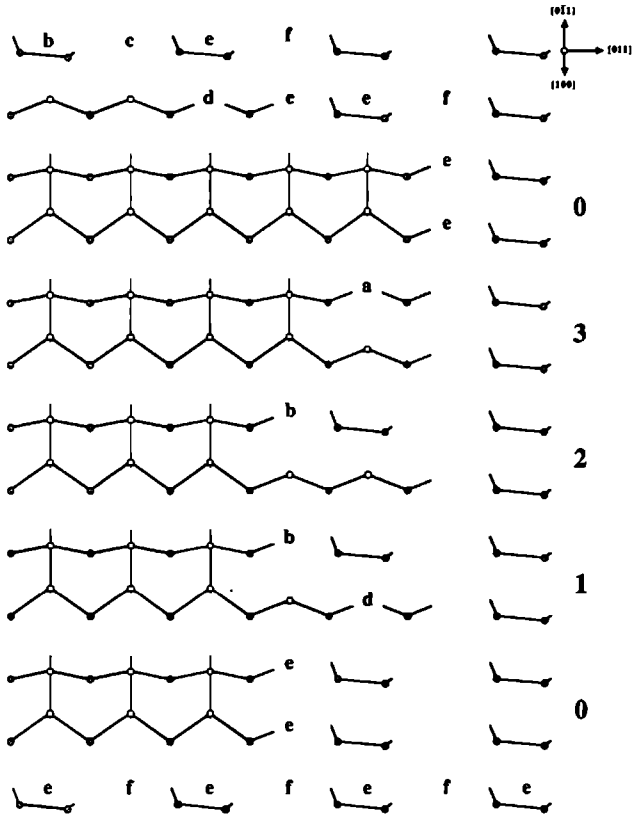

Fig. 14 Growth sequence of a step on a (2x1) reconstructed (100) surface. 0→3 indicate the different stages, however the surface as sketched could also be a momentary view.

Essential in step growth on a reconstructed (100) surface is the presence of a silicon neighbour in the [0$\bar{1}\bar{1}$] or [011] direction. In fig. 14 it is indicated how the growth process then proceeds. The rate limiting step is adsorption on an (e) site, which costs 1 dimer bond (0→1 in fig. 14). As indicated in the bottom of the figure two (e) sites are present, differing in the fact that the upper one has a neighbouring silicon adsorbate and the lower one has not. In principle the upper one could form a dimer bond with its neighbour. For energetic reasons however, it is preferable to proceed the existing dimer chain.

Dimer formation between adsorbates of different chains represents the formation of a "dislocation" in the (2x1) reconstruction. So both sites are real (e) sites with an equal attachment probability. The subsequent attachment to a (d) site is easy, since no dimer bond is present anymore (1→2). As will turn out later, it is very probable that these two steps often occur similtaneously, in this way reducing the energy barrier of the limiting step. After attachment of the two species the same process will be repeated again in the [011] direction. One of the neighbouring rows has the possibility to form dimer bonds with the already formed row, so it can proceed fast in the [011] direction. Thus adsorption on a (b) and on an (a) site will immediately follow (2→3→0). So if the supply of growth species is not rate limiting, a step will grow with four units at a time if dimerization occurs simultaneously with the incorporation, else with two.

If no double-bonded silicon neighbour is present in the [011] or $[0\bar{1}\bar{1}]$ direction attachment is only likely when a new dimer bond can be formed with an adsorbate. As shown in fig. 14, the top left β site is a (b) site, allowing adsorption with net no dimer bond breaking. Adsorption along a dimerized adsorbate chain, as depicted right from the centre in the upper part of fig. 14, is similar to two dimensional nucleation: at least one bond has to be broken, i.e. attachment on an (e) site. Although this is the same as the rate limiting step in the step propagation, it will be shown that adsorption on such a β site is unfavourable to attachment on an α site, which lies along a [011] step. So, as depicted in fig. 15, $[0\bar{1}1]$ and $[01\bar{1}]$ steps are smooth. Random adsorption along the step is unlikely as compared to attachment at a kink site. If two silicon adsorbates, forming a dimer bond, are considered to be one growth unit, [011] growth is rough, since adsorption on both sides of the growth unit, in the $[0\bar{1}1]$ direction, is independent of its presence. In the next layer this pattern has rotated 90°.

So the dimerization of the crystal surface results in a stepped (100) surface, in some respects comparable with Si(110). Both consist of chains which can grow and etch fast in one direction; in case of (100) the [011], for (110) the $[1\bar{1}0]$ direction. The propagation of the chains is independent in these directions. For (110) no in-plane bonding

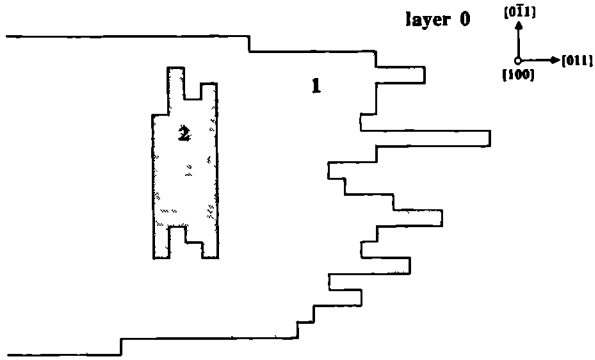

Fig. 15 Roughness of the steps on a (2x1) reconstructed (100) surface.
In two directions, [011] and [0$\bar{1}\bar{1}$] for layer 1, the growth is rough.
The perpendicular step is smooth.
In the next layer (2) this behaviour has rotated 90°.

between the chains is possible. On (100) the dimerization of the adsorbates does not result in a long order interaction, it only gives a double chain. As will be discussed later, only if a "dislocation" occurs in the dimerization of the adsorbed layer, a weak, but important, interaction appears in the [0$\bar{1}$1] direction. In contrast to (110) where attachment is the same for all growth units, for (100) a basic growth unit consists of 4 adsorbates, if dimerization occurs. However the main difference is that for (110) lower lying chains run parallel to the surface chain, whereas for (100) the dimer chain of the adsorbates is perpendicular to the surface dimerization. The adsorbed layer is in fact a new surface onto which new adsorption is possible. Though a (100) surface is only twofold symmetric, effectively for Si(100) fourfold symmetry is observed, as for every new layer a change of 90° occurs for the direction of steps and fast diffusion.

5.3. Step growth versus two dimensional nucleation

The kink sites needed to obtain [0$\bar{1}$1] growth - which remains in the discussion the slow growth direction - can be produced by a misorientation, dislocations or two dimensional nucleation. To obtain smooth step growth, preferably the kink sites should be created by an applied misorientation.

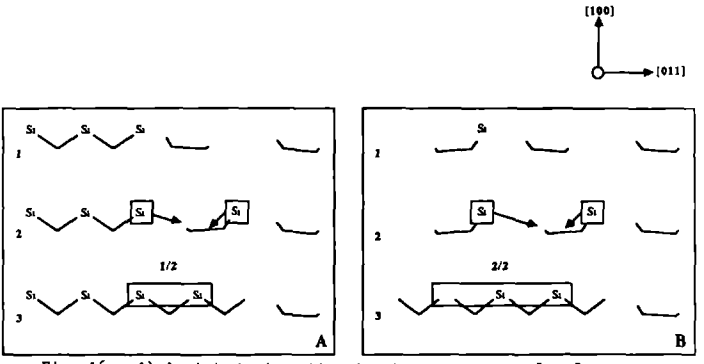

Fig. 16 A) Assisted adsorption in the growth of a [011] step two adsorbates break one dimer bond
B) Assisted adsorption in two dimensional nucleation two adsorbates break two dimer bonds

Two dimensional nucleation starts with the adsorption of a double-bonded silicon species at a β site. This costs one dimer bond, so energetically this process should be as likely as adsorption on an α site next to an occupied β site (e): the rate limiting step in propagation of a [0$\bar{1}$1] step via kink sites. So, at first sight, random nucleation should be competitive with step growth. To explain the observed step growth on Si(100) it must be assumed that adsorption on α and β sites is coherent. In fig. 16A it is sketched how this simultaneous breaking of a dimer bond is envisioned. A single-bonded silicon adsorbate is diffused to an (e) site (1). Since forming a double bond is difficult, because then a dimer bond has to be broken, it is favourable to wait until another single-bonded silicon adsorbate is diffused to the neighbouring α site (2). The adsorbate on the (e) site then moves to the other dangling bond of the α site to form a double bond. Simultaneously the other adsorbate adsorbs on the β site, since the dimer bond is weakened. So two silicon adsorbates assist each other in breaking one bond, thus dividing the reconstruction energy and lowering the activation energy considerably. In fig. 16B it is shown that the same process is not favourable for two dimensional nucleation: forming a double bond by the adsorbate at the α site is not only weakening the dimer bond at the right-hand side, but also at the left-hand side. Although in growth via kink sites as well as via

two dimensional nucleation - or adsorption along a smooth [0$\bar{1}$1] step - coherent attachment is possible, it is only favourable in the first case. Then only half of a dimer bond is broken per adsorbate, instead of one.

Though two dimensional nucleation is less probable then step growth, this does not mean that it will not occur. Fortunately if a nucleus is formed [0$\bar{1}$1] propagation is unlikely, only expansion in the [011] direction is probable. For outgrowth in the [0$\bar{1}$1] direction, adjacent nucleation is needed. Since nucleation is random, it is not likely that it will precisely occur adjacent to the double row of adsorbates. So a nucleus will not extend and can be incorporated easily in an impinging step. Only the dimerization can be out of phase; shifted 1 single row of atoms.

At higher supersaturations growth via steps no longer is preferred to two dimensional nucleation. Because of the large supply of growth species, the sticking probability (θ) no longer is dominated by the adsorption energy. At the point in the adsorption curves where $\Sigma\theta_{>Si,\beta_I}$ and $\Sigma\theta_{>Si,\beta_{II}}$ (figs. 7b and 9b), representing the breaking of a half, respectively one dimer bond, are both approaching unity, two dimensional nucleation is so easy that the surface roughens kinetically.

5.4. Outgrowth of macroscopic hillocks

Dislocations are also a source of kink sites, the importance depending on the growth rate, the applied misorientation and the crystalline perfection. According to the "Rough Heart" model, at the outcrop of a dislocation locally the reconstruction is removed [26]. This perfectly explains the initiation of a growth hillock. However, further outgrowth to macroscopic dimensions is up to now, not accounted for. The stress field, breaking up the dimers, is not extending that far, so it must be discussed how the stable [0$\bar{1}$1] step can propagate. In other words how the propagating growth hillock can produce its own kink sites.

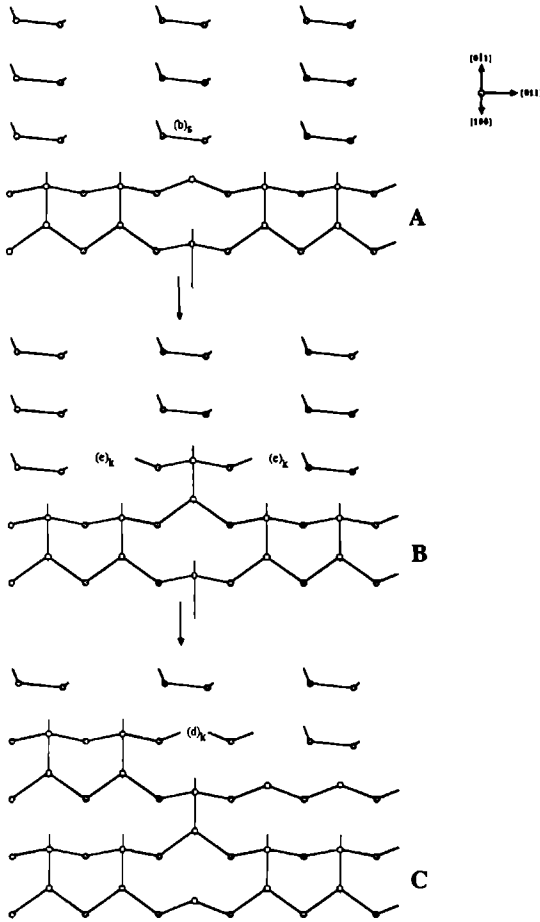

Fig. 17 A discontinuity in the dimerization as a nucleation site on a step.
A) A non-dimerized silicon adsorbate, causing easy adsorption on a β site at a step position; $(b)_s$
B) An out of phase silicon dimer as a source of kink sites, $(e)_k$
C) A kink site, $(d)_k$, as the start of a new dimer

Two dimensional nucleation adjacent to the step could be one possibility, however as the probability is not very large, at low supersaturations, this cannot explain the well developed growth hillocks often observed on (100) faces [31]. Attachment of growth species onto a

smooth [0$\bar{1}$1] step could be accounted for however, if a small interaction perpendicular to the step is assumed. An obvious cause for this interaction perpendicular to the surface dimers is the dimerization in the adsorbed layer. Normally only a two by two ordering is expected, however if a local disturbance in the dimerization of the adsorbates is present, a long order interaction is introduced. As can be seen in fig. 17A, for a smooth step a "dislocation" in the reconstruction allows easy adsorption on a β site. Instead of the difficult breaking of one bond, it is now a (b) site: if Si is attached to the already adsorbed growth unit, it can form a new dimer bond, while the surface dimer is broken. Then kink sites, $(e)_k$, are formed (fig. 17B), allowing further growth along the smooth step. The difficult step in the attachment to the dislocation is got round by the regular dimer chain, as the (d) site becomes a kink site; fig. 17C. After completion of the complete step, via (a) and (b) sites, situation A is regained. So a disturbance in the reconstruction of the adsorbed layer can be a continuous source of kink sites.

Such a discontinuity in the dimerization can be caused by the stress field around the dislocation; the reconstruction is not starting everywhere simultaneously. Another source of kink sites could be a different reconstruction mode, e.g. (2x2) instead of (2x1). A square hillock is formed, when the [011] and [0$\bar{1}$1] steps limiting the growth of successive layers are propagating equally fast. This will happen when the density of "kink sites" is equal for both steps. When the density becomes very high, or the difference in propability for growth via kinks or via the step low, as at high supersaturations, the four steps limiting the growth hillock roughen. Then the shape will be determined also by the diffusion field.

6. Discussion

6.1. Adsorption

It has been shown that adsorption and crystal growth are influenced enormously by the possibility of a bare (100) surface to reconstruct. An essential feature of surface reconstruction is the strongly reduced coverage of double-bonded silicon species. For adsorption on β sites it is obvious that for all adsorbates the breaking of a dimer bond must be accounted for, reducing considerably the gain in adsorption energy. For hydrogen attached to α sites, experimental evidence is available, indicating that the reconstruction is not removed [8]. Should this also apply for double-bonded silicon adsorbates, then the resulting surface coverage of the α sites would be comparable with the coverage of a broken bond surface. This is in contradiction with crystal growth experiments, which reflect a low coverage with growth units and oppose direct condensation of silicon. So silicon on α sites must influence strongly the stability of the dimer bond, when double-bonded. Experimental data are unavailable to what extent the adjacent dimers are weakened. In this paper the maximal influence is assumed, following the observation that double-bonded oxygen in N_2O preferably attaches to β sites [22]. Thus adsorption of >O on an α site obviously costs more than one dimer bond.

Should attachment of double-bonded silicon species on α sites in fact only cause the breaking of one adjacent dimer bond, the essence of the results would not change. The main difference would be that for the α_{III}-curves the energy correction is halved to 30 kcal/mol. As can be deduced from fig. 7a, this difference is negligible at low supersaturations, since the α_{II}- and α_{III}-curves already coincide, when 20 respectively 60 kcal/mol is used as the dimer correction. For high supersaturations, fig. 9a, the influence is larger resulting in a higher silicon coverage at the high temperatures, where α_{III} becomes important (fig. 10).

It should be realized, that the coverage strongly depends on the standard gain in adsorption energy. As the exact energy needed to break a dimer bond is not known - the reported values vary from 26 to

39 kcal/mol dimer [15,16] - the coverage evidently is influenced drastically by the choice made for the reconstruction energy. In fig. 18a, for low temperatures, the coverage with double-bonded silicon is shown for different stabilities of the dimers. It can be seen that with a change of only 10 kcal/mol the curve shifts 300 K. For $\Delta G^{o}_{reconstr}$ = 20 kcal/mol the silicon coverage is rather high until 800 K; if the correction is 40 kcal/mol, already at 400 K the coverage with growth units is negligible. As can be seen in fig. 18b, the effect is also considerable on the total coverage. Hydrogen is not able to attach properly to β sites and cannot compensate the absence of silicon. This results in a coverage of only the α sites for the "40"-curve. For small dimerization energies silicon is able to compete effectively with hydrogen at α sites, at low temperatures. At temperatures higher than 1200 K, basicly the coverage of the surface is to a large extent independent of the reconstruction energy.

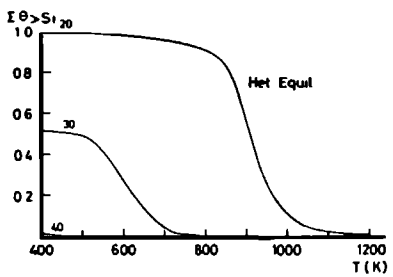

Fig. 18a Real total silicon coverage of a reconstructed (100) surface, in equilibrium with a "heterogeneous" gas phase at 1 atm total pressure, as a function of temperature for a reconstruction energy of 20, 30 and 40 kcal/mol dimer.

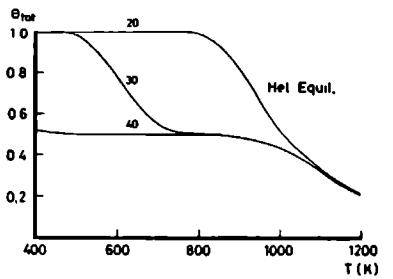

Fig. 18b Real total coverage of a reconstructed (100) surface, in equilibrium with a "heterogeneous" gas phase at 1 atm total pressure, as a function of temperature for a reconstruction energy of 20, 30 and 40 kcal/mol dimer.

It is this high-temperature region, at low supersaturations, which is interesting for monocrystalline step growth. As the discussion of the crystal growth model is only qualitative, regarding step growth and two dimensional nucleation, for the basic principles, it is not relevant what the exact value for the reconstruction energy is. It is thought

however that the choice of 30 kcal/mol gives a reasonable impression of the ratio of double- versus single-bonded silicon adsorbates. This value is choosen on the low side in order not to overestimate the influence of surface reconstruction.

At low temperatures the differences are rather large. Increasing the dimerization energy results in a surface coverage changing from SiH_2, adsorbed at all sites, to HH, selectively attached to α sites. To distinguish between the two situations should be possible with LEED, as only in the latter situation the reconstruction is preserved. However it is rather difficult to apply relevant partial pressures of the adsorbates to the surface. Gaining insight by studying the growth is hampered by the large influence of incorporation kinetics at low temperatures. Whether the surface is covered with silicon or hydrogen (apart from the influence of SiO_2) the quality of the crystal growth will be poor, either due to two dimensional nucleation or to blocking of the step propagation by hydrogen.

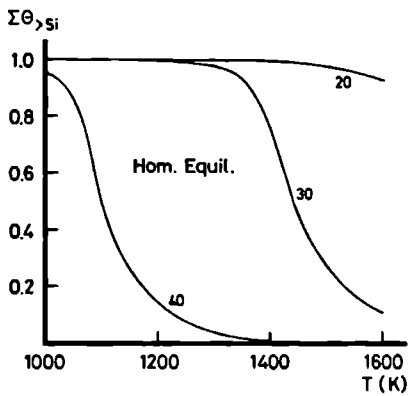

Fig. 19 Real total silicon coverage of a reconstructed (100) surface, in equilibrium with a "homogeneous" mixture of 1% SiH_4 in H_2 at 1 atm total pressure, as a function of temperature for a reconstruction energy of 20, 30 and 40 kcal/mol dimer.

At high supersaturations also a strong dependence on the dimerization energy can be observed; fig. 19. The temperature region, where the

influence is large, is in the epitaxial regime. So firm conclusions on the influence of supersaturation on two dimensional nucleation cannot be made. Nevertheless it can be stated that the concentration of double-bonded silicon is anyway considerably larger than for a (111) surface.

In this paper it is not pretended that the exact coverage is presented for all temperatures and partial pressures of the radicals in the gas phase. The intention is only to get insight in the interaction between gas phase and crystal surface, in order to gain knowledge on the structure of a Si(100) surface. Essential is the different affinity of α and β sites for single- and double-bonded species and the influence of adsorption on the stability of the neighbouring sites, resulting in one-dimensional related crystal growth and adsorption. The model, as reflected in eqs. (6) and (7), is not exact and use is made of the fact that the equilibrium coverage is calculated. However care is taken, to preserve the different nature of single- and double-bonded species regarding the breaking of dimer bonds and to apply the physically most realistic energy correction. In the model only limiting environments for the adsorbates are taken into account. This means that in the situations intermediate between a bare and a fully covered surface some uncertainty exists. Comparing figs. 18a,b and 19 with the calculated coverages as depicted in figs. 8 and 10 it can be noticed that where an intermediate situation exists on the surface, the dependence on the reconstruction energy is also large. The latter effect being much more pronounced, so a more detailed model would make little sense. For $\Delta\mu = 0$ at high temperatures the calculations are rather accurate with a well-defined α_{III},β_{II}-coverage. For high supersaturations, at low temperatures, the surface is certainly fully covered with double-bonded silicon species.

6.2. Crystal growth

Step growth on a reconstructed (100) surface is governed by the breaking of surface dimers and the formation of new dimers in the adsorbed layer in the perpendicular direction. In this paper two new aspects are introduced. The simultaneous incorporation of two

adsorbates to explain the easy propagation of a step in the [011] direction and the formation of a dimer bond in the adsorbed layer to explain the propagation of a [0$\bar{1}$1] step. For both processes no experimental evidence is available, however to explain the observed growth hillocks and step growth it is essential that they are introduced. Else two dimensional nucleation would be more pronounced.

To explain growth, the adsorption layer must be stabilized by additional bonds, first dimerization, then coverage with new adsorbates. As can be seen in the adsorption curve (fig. 8), full coverage with SiH_2 or Si is impossible at low supersaturations. However when a dimer bond is formed, silicon is attached with three bonds to the surface, similar to a (111) toplayer. Then the tendency to desorb, given by the adsorption curves for the broken bond model (fig. 3a), as net no dimer bond is broken, is low. Only at very high temperatures the coverage can be smaller dan unity, evaporation of adsorbed silicon becomes possible and the surface becomes rough, despite the formed dimers. Only by increasing the supersaturation the crystal surface can remain smooth, without too many vacancies.

The model is based on a regular (2x1) reconstructed surface. As it is likely that (2x1) areas coexist with for example (2x2) or (4x2) reconstructed areas it is significant to consider these deviations from regularity. In all cases the dimerization is still in the [011] direction. If the small interactions, which now exist in the [01$\bar{1}$] direction, are neglected, adsorption is still one-dimensional and is equal for all the different buckling modes of the dimers. As the dimerization of the succeeding layer is perpendicular, after breaking of the dimers the reconstuction pattern is not restored in the subsequent layers. The only influence a distortion can have is on the roughness of the growth. As shown in fig. 17 an irregularity in the (2x1) pattern gives a small interaction, if simultaneously with the incorporation a new dimer is formed, increasing the roughness of a [0$\bar{1}$1] step. On the other hand the perpendicular [011] step is more smooth if other dimerization modes are allowed. As can be seen in the bottom of fig. 14, the upper (e) site now can dimerize with its neighbour. Now attachment is dependent on the presence of a neighbour, though only on a

non-dimerized one. This equalizing of the steps will only occur if Si is attached, since this allows simultaneous formation a dimer bond; thus, predominantly at high temperatures and low pressures: then Si is favoured above SiH_2.

7. Conclusion

With the assumption that a (100) surface is reconstructed during crystal growth, it can be explained why step growth is experimentally observed. An extra interaction is present in the direction of the dimer bonds, which makes it preferable for growth units to attach adjacent to each other in that direction, resulting in a stepped-like surface. As the dimerization of the adsorbates, which becomes the surface of the next layer, is rotated 90°, this eventually results in growth of (100) as if it were a flat face.

Basicly for the step growth is the low surface coverage with double-bonded silicon species. Only at low temperatures and high supersaturations full coverage is attained. The α sites favour hydrogen, so at low supersaturation (and temperature), hydrogen and silicon are alternately adsorbed; hydrogen is attached to the dangling bonds and silicon at the dimer bond site. At temperatures higher than 800 K double-bonded silicon is also repelled from these sites; the energy loss because of the broken bond, becomes too large compared with the energy gain. Thus at high temperatures and low supersaturation the surface has a low hydrogen coverage and the reconstruction is hardly removed.

In step growth silicon adsorbed on the remaining dangling bonds accounts for the diffusion of growth units to the step. Two of them are able to break simultaneously one dimer bond at a step site, favouring step growth above two dimensional nucleation. So, dimerization of the crystal surface as well as in the adsorbed layer, is of primary importance in the crystal growth process. The start of two dimensional nucleation is caused by divalent silicon species, who preferably remove the dimer bond. As their presence is not negligible, even at low supersaturations, on a (100) surface two dimensional nucleation already will be likely, under conditions where on a (111) surface still smooth step growth will be observed.

Acknowledgements

The present investigations have been carried out under the auspices of the Netherlands Foundation for Chemical Research (SON) with financial support from the Netherlands Organization for the advancement of pure Research (ZWO). I am indebted to Professor L.J. Giling for the many fruitful discussions. I would like to thank Mr. W.P.J.H. Jacobs for performing calculations and Drs. J. v. Suchtelen for critically reading the manuscript.

Appendix A Adsorption constants for an unreconstructed (100) surface

Application of the broken bond model leads for a Si(100) surface to double-bonded silicon adsorbates, one bond is only formed by H and SiH_3. These single-bonded species can be assumed to be adsorbed similarly as on Si(111). In this appendix only the data specific for double-bonded silicon species are presented. The method of calculation as well as the adsorption constants of H and SiH_3 have already been discussed [5].

A1. Enthalpy

The standard enthalpy at a temperature T can be written as the sum of the enthalpy at 298 K and a temperature term. The bond strength, $\Delta H^{\circ}_{ad}(298)$, is 108 kcal/mol: the sublimation enthalpy of a silicon crystal [19]. As can be deduced from table 1 for most adsorbates the temperature contribution is marginal, viz. ~ -1 kcal/mol. This term is taken into account only to obtain more detailed information about the nature of the growth species. Significant is the difference in enthalpy between Si and SiH_2, the most important growth species. The 6 kcal/mol difference, which is due to low lying electronic states and the loss of rotation of SiH_2, has a great influence on the relative importance for adsorption, favouring SiH_2.

A2. Entropy

For double-bonded adsorbates the entropy loss can be written down as:

$$(A.1) \quad \Delta S^{\circ}_{ad} = S^{\circ}(vib + elec)_{ads} - S^{\circ}(elec)_{*} - S^{\circ}(transl + rot + elec)_{g}$$

The main difference with a (111) surface is the entropy gain of the adsorbed molecule. Because of the double bond, rotation is no longer possible and the frequency of the vibration is higher. Instead of 1 stretch and 2 bending modes, 2 stretch-bending and 1 bending will be present on (100); figs. 20a-d. The latter is a motion perpendicular to the plane of the Si-Si-Si bonds, while the former is a vibration in the direction of one of the bonds and almost perpendicular to the other. ν_{bend} has been calculated assuming that the bond strength is twice that of a single Si-Si bond; viz. 108 kcal/mol. The stretch-bending mode is a coupled motion. It can be argued that the motion connected with the strongest bonding, which is the stretching, will dominate. In the present results the stretch-bending is approximated to be a stretch vibration with the normal Si-Si bond length and strength.

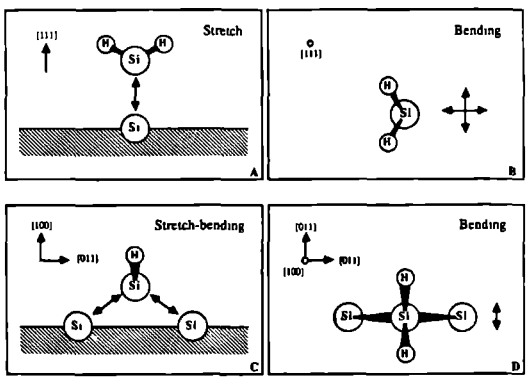

Fig. 20 a) Stretch of SiH_2 on a (111) surface
b) Top-view on a (111) surface; the two bending modes of SiH_2
c) The two stretch-bend modes of SiH_2 on (100)
d) Top-view on a (100) surface; the bending of SiH_2

Since the internal vibrations of the adsorbed molecule and crystal are assumed to be unaffected by the formed bonds, the only difference

left is the electronic contribution to the entropy. A vacant site now consists of two dangling bonds, with a corresponding entropy content of 2.8 cal/mol·K. The adsorbed molecules are considered to have the same electronic levels as the analogon with two more H, e.g. Si^* is resembling $SiH_2(g)$. The electronic contribution for Si_2 and Si_3 is assumed to be zero.

In table 1 the entropy loss, calculated according to the above given scheme, is presented. For Si, Si_2 and Si_3 the difference with (111) is -6 cal/mol·K. This is caused by the higher vibrational frequency - the bonding to the crystal surface is stronger - and a smaller electronic contribution: an additional saturated bond is formed. Compared with (111), for SiH and SiH_2 the adsorbate loses S_{rot}, which gives an extra loss of 7 cal/mol·K, leading to a total difference of -13 cal/mol·K.

REFERENCES

[1] J. Bloem and L.J. Giling, in: Current Topics in Materials Science Vol. 1 ch. 4, Ed. E. Kaldis, (North-Holland, Amsterdam, 1978)

[2] J. Bloem and L.J. Giling, in: VLSI Electronics: Microstructure Science Vol. 12 ch. 3, Ed. H.R. Huff, (Academic Press, 1985)

[3] W. Mönch, Surface Sci. 86 (1979) 672

[4] B.Z. Ol'shanetskii, A.V. Rzhanov and F.L. Édel'man, Sov. Phys. Semicond. 7 (1974) 1538

[5] L.J. Giling, H.H.C. de Moor, W.P.J.H. Jacobs and A.A. Saaman, to be published in J. Crystal Growth

[6] R. Cadoret and F. Hottier, J. Crystal Growth 61 (1983) 259

[7] A.A. Chernov and M.P. Rusaikin, J. Crystal Growth 52 (1981) 185

[8] T. Sakurai and H.D. Hagstrum, Phys. Rev. B14 (1976) 1593

[9] F. Hottier and R. Cadoret, J. Crystal Growth 61 (1983) 245

[10] L.J. Giling and W.J.P. van Enckevort, Surface Sci. 161 (1985) 567

[11] F. Langlais, F. Hottier and R. Cadoret, J. Crystal Growth 56 (1982) 659

[12] W.A.P. Claassen, J. Bloem, W.G.J.N. Valkenburg and C.H.J. van den Brekel, J. Crystal Growth 57 (1982) 259

[13] L.J. Giling, Mat. Chem. Phys. 9 (1983) 117

[14] D.J. Chadi, Phys. Rev. Letters 43 (1979) 43

[15] M.T. Yin and M.L. Cohen, Phys. Rev. B24 (1981) 2303

[16] W.S. Verwoerd, Surface Sci. 99 (1980) 581

[17] F.F. Abraham and I.P. Batra, Surface Sci. Lett. 163 (1985) L752

[18] J.E. Mayer and M.A. Mayer "Statistical Mechanics" p. 255 (Wiley, New York, 1961)
[19] JANAF Thermochemical Tables 2nd ed., NSRDS-NBS 37
(Natl. Bur. Std. US, Washington, DC. 1971)
[20] W.S. Verwoerd, Surface Sci. 108 (1981) 153
[21] F. Stucki, J.A. Schaefer, J.R. Andersen, G.J. Lapeyre and W. Goepel,
Solid State Commun. 47 (1983) 795
[22] E.G. Keim, thesis, Technical University Twente, The Netherlands (1986)
[23] P.I. Cohen, P.R. Pukite, J.M. Van Hove and C.S. Lent,
J. Vacuum. Sci. Technol. A4 (1986) 1251
[24] G.W. Cullen and J.F. Corboy, J. Crystal Growth 70 (1984) 230
[25] T.J. Donahue and R. Reif, J. Appl. Phys. 57 (1985) 2757
[26] L.J. Giling and B. Dam, J. Crystal Growth 67 (1984) 400
[27] W.J.P. van Enckevort and L.J. Giling, J. Crystal Growth 45 (1978) 90
[28] D.L. Rode, J. Crystal Growth 27 (1974) 313
[29] A.A. Chernov and M.P. Rusaikin, J. Crystal Growth 45 (1978) 73
[30] I. Noorbatcha, L.M. Raff and D.L. Thompson, J. Chem. Phys. 81 (1984) 3715
[31] J. Bloem, Y.S. Oei, H.H.C. de Moor, J.H.L. Hanssen and L.J. Giling,
J. Electrochem. Soc. 132 (1985) 1973

PART 2

THERMODYNAMICS IN CRYSTAL GROWTH OF SILICON

CHAPTER 4

EPITAXIAL GROWTH OF SILICON BY CVD IN A HOT-WALL FURNACE

THE Si-Cl-H SYSTEM

Reprinted from JOURNAL OF THE ELECTROCHEMICAL SOCIETY
Vol 132 No 8 August 1985
Printed in U S A

Epitaxial Growth of Silicon by CVD in a Hot-Wall Furnace

J. Bloem,* Y. S. Oei, H. H. C. de Moor, J. H. L. Hanssen, and L. J Giling

Faculty of Science, R.I.M. Department of Solid State III, Catholic University, Toernooiveld, 6525 ED Nijmegen, The Netherlands

ABSTRACT

A theoretical and experimental study has been performed for the feasibility of epitaxial growth in a furnace In this study, it is proven that growth in a hot-wall furnace in principle is possible — without deposition of silicon on the quartz ware of the cell — when the growth is carried out at near equilibrium conditions For supersaturations larger than 10%, deposition also occurs on the quartz of the wafer boat or cell A constant supersaturation, i e , a constant growth rate at all slices along the reactor tube can be achieved by imposing a temperature gradient over the cell The best results are obtained for growth with $SiHCl_3$, low Cl/H ratio, and high temperatures Growth rates amount to 0.1-0 3 μm/min for these conditions

The epitaxial growth of silicon has become an inherent part of the silicon device technology since in 1960 the first transistor with epitaxial base was described (1) Recently, silicon solar cells with epitaxial layers on metallurgical-grade silicon substrates showed the feasibility of chemical vapor deposition in this rapidly growing technology (2) The growth of device quality epitaxial material is performed in cold-wall reactors operating at atmospheric pressure and at temperatures well above 1000°C In this temperature range, the surface reactions leading to growth are relatively rapid and the growth rate is determined by the supply of reactant via gas phase diffusion The concept of the stagnant boundary layer has been successfully applied to describe and to monitor the growth rate and the growth rate uniformity in production-type reactors (3)

A rather low packing density of substrates can be used in the epitaxial cold-wall reactors and the numbers produced per batch are restricted to, say, 20 slices of 4 in diam The epitaxial growth, therefore, is among the most expensive steps in the silicon device technology, and reactors with a high packing density of substrates in a resistance-heated hot-wall diffusion-type furnace should be very welcome

The hot-wall reactor came into use when polycrystalline silicon had to be grown in thin layers on existing device structures acting as gate material in the self-aligned MOS technique It appeared that poly-Si could be deposited on slices stacked in a diffusion furnace to give an extremely uniform polycrystalline silicon layer over the whole batch (4)

This method only works at the low temperatures where poly-Si is grown and where the efficiency of the growth reaction is so low that depletion effects are of minor importance Growth also occurs on the hot quartz walls and substrate holders The method is therefore restricted to the deposition of thin polycrystalline layers at relatively low temperatures

Studies to grow monocrystalline silicon in a hot-wall furnace have been performed since 1960 Deal (5), Lombos and Somogyi (6), and Nishizawa (7) showed the main problems to be the strong depletion and the rapid deposition on the quartz ware of the reactor Ban (8) introduced a mechanically complex system in which a great number of slices can be processed simultaneously and rotating nozzles are used to direct the gas flow Recently, Langlais *et al* (9) gave an analysis of the thermodynamics of silicon deposition in a hot wall reactor Depletion effects were not studied specifically, but a growth at reduced pressure is recommended Indeed, Ogirima and Takahashi (10) showed that SiH_2Cl_2 plus H_2 at a total pressure of 2 torr could give a reasonable growth rate distribution in a LPCVD reactor around 1000°C, with a special nozzle to introduce the reactant A similar observation has been published by Duchemin *et al* (11) In all the work cited above, high supersaturations were needed to come to an acceptable growth rate Deposition of silicon on the hot tube wall and depletion in the direction of the gas stream does restrict the usefulness of the method Another approach to the epitaxial growth of silicon has been pursued for a number of years in our laboratory (12) Details of the underlying concepts and of some results will be given in the following sections

Equilibrium calculations—Thermodynamic calculations of the Si-Cl-H system have been performed with increasing accuracy Steinmaier (13) was the first to calculate the silicon growth rate as a function of the gas phase

*Electrochemical Society Active Member

composition Lever (14), Hunt and Sirtl (15, 16), van der Putte *et al* (17), and Langlais *et al* (9) showed the potentials of the computer calculations

Experimental evidence has been obtained by Sedgwick (18), Ban (19), and Duchemin (20) showing that equilibrium between the gas phase and solid silicon is rapidly established at temperatures well above 1000°C, leading to gas-phase concentrations of $SiCl_4$, SiH_2Cl_2, and HCl close to the ones calculated from thermodynamic data

In the present study, interest is focused on near-equilibrium situations in which only a small supersaturation is available, the equilibrium calculations, therefore, are even more interesting than in the cases discussed before where large supersaturations are involved

Using literature data together with an iterative computer program based on minimalization of the Gibbs energy, the equilibrium composition of several Si-H-Cl gas mixtures in contact with solid silicon was calculated This was performed for several Cl/H ratios, temperatures, and total pressures Figure 1 gives an example of the equilibrium composition as a function of temperature of a gas mixture for Cl/H = 0 162 and p_{tot} = 1 bar The total amount of silicon which is present in the gas phase can be deduced for each p, T, and H/Cl ratio by taking the sum total of all the partial pressures of gaseous compounds containing silicon This total sum is equal to the solubility L of silicon in the gas phase for the given conditions of p, T, and H/Cl under the condition of complete equilibrium between solid and gas

$$\Sigma p_{Si} = L = \sum_j x_j p_j (Si_x H_y Cl_z)_j \qquad (x \neq 0) \qquad [1]$$

The relative supersaturation percentage for an input pressure p_i follows from

$$\gamma = \frac{p_i - L}{L} 100 \qquad [2]$$

The difference in chemical potential ($\Delta\mu$) between input and equilibrium mixtures is given by

$$\Delta\mu = kT \ln p_i/p_{eq} \qquad [3]$$

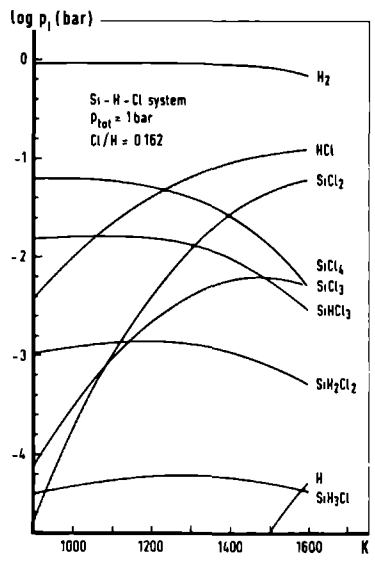

Fig 1 Calculated values of gas phase species in equilibrium with solid silicon as a function of temperature for Cl/H = 0 162 at 1 bar total pressure

For small supersaturations and with $p_i = p_{eq} + \Delta p$, we can put

$$\ln\left(1 + \frac{\Delta p}{p_{eq}}\right) \approx \frac{\Delta p}{p_{eq}}$$

so that

$$\frac{\Delta\mu}{kT} = \ln(1 + \Delta p/p_{eq}) \cong \frac{\Delta p}{p_{eq}} \qquad [4]$$

In this way, the relative supersaturation γ and $\Delta\mu/kT$ are equal for small supersaturations

In cases where the chemical reactions in the gas phase give rise to volume changes (nonequal number of reactants and reaction products), it is advisable to use a relative solubility L_{rel} given by the ratio of the number of moles of silicon in the gas phase and the total number of reacting atoms

$$L_{rel} = \frac{n_{Si}}{n_{tot}} = \frac{\Sigma p_{Si}}{\Sigma p_{Si} + \Sigma p_{Cl} + \Sigma p_H} \qquad [5]$$

where Σp_{Cl} and Σp_H are defined in the same way as Σp_{Si} in Eq [1]

In Fig 1, it is seen that at the lower temperatures $SiCl_4$ is the main gas phase component in equilibrium with solid silicon, at the higher temperatures the $SiCl_4$ content decreases, and $SiCl_2$ becomes the most important gaseous silicon compound This situation leads to a minimum in the silicon solubility (L) as a function of temperature for a specific Cl/H ratio Figures 2 and 3 give examples for different Cl/H ratios and total pressures For lower values of Cl/H, the absolute value of L decreases and the minimum shifts to higher temperatures For reduced pressures (or a replacement of H_2 by an inert gas), the minimum shifts to lower temperatures For input partial pressures of $SiCl_4$, $SiHCl_3$, or SiH_2Cl_2, the appropriate Cl/H curve can be selected and growth is expected for input values greater than the value of L, for $p_i < L$ etching of solid silicon will occur

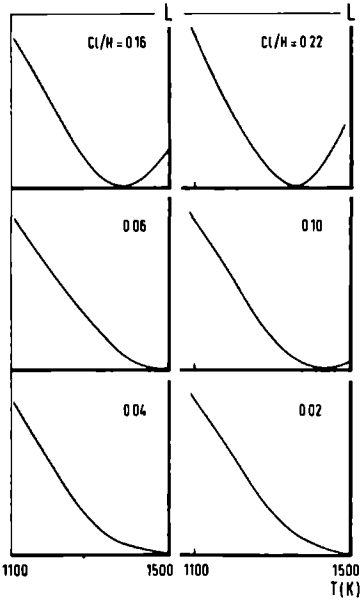

Fig 2 The silicon solubility L, constructed from calculations as given in Fig 1 for different values of Cl/H ratio at atmospheric total pressure The minimum in L shifts to lower temperatures for increasing chlorine content The preferred epitaxial temperature is around 1350 K

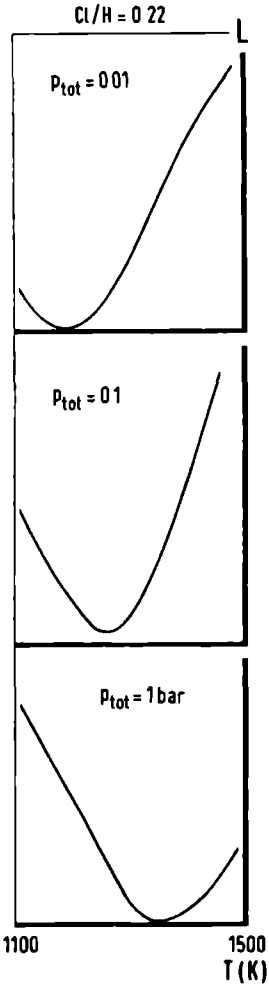

Fig 3 The silicon solubility L as a function of temperature at a constant Cl/H ratio at various total pressures in the Si Cl-H system Replacement of hydrogen by an inert gas as helium has the same thermodynamic consequences

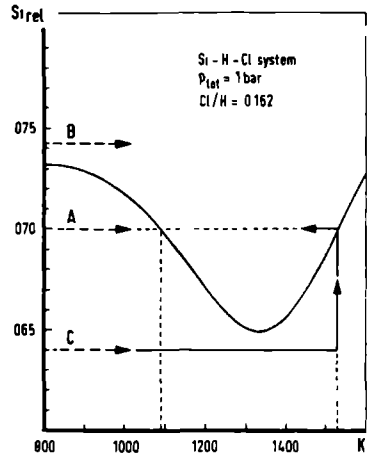

Fig 4 The silicon solubility as a function of temperature in relation to various input conditions Input mixtures with a Si/Cl ratio higher than the equilibrium value (L) give rise to growth at all temperatures (B) Lower input concentrations of silicon (A and C) lead to etching or growth dependent on temperature (see text)

In Fig 4, three experimental situations are depicted Point A corresponds to an experiment where the input of $SiCl_4$, $SiHCl_3$ or SiH_2Cl_2, and HCl in H_2 is such that for T = 1000 K the input mixture contains less silicon than the corresponding equilibrium value So once this mixture comes into contact with the solid silicon crystals, the system will strive toward an equilibrium situation and the crystals will be etched This applies for every situation where the combination of input concentration and temperature is lying below the solubility curves Growth will occur when the input values exceed the solubility line For mixture A, this is achieved at T larger than 1100 K So for input concentration A below 1100 K, etching will take place, above 1100 K, the crystal will grow Starting with an input composition at B directly will give growth because the silicon content exceeds the solubility of silicon To prevent deposition of silicon in colder parts of the reactor, conditions have to be chosen such that deposition does not start below a specified temperature (situation A) It has also to be realized that an input mixture of say $SiHCl_3$ in H_2 can have the required Si/Cl and Cl/H ratio, the gas phase species however, still have to be adjusted to the equilibrium concentrations of $SiCl_4$, SiH_2Cl, $SiCl_2$, etc This process may take some time

For a real growth experiment in a hot wall reactor, a supersaturation has to be introduced in order to come to growth The small supersaturations envisaged in the present experiments then will lead to a rapid reduction in growth rate in the direction of the gas stream This depletion can be overcome in two ways First, it is possible to introduce additional reactant via an inlet tube with carefully designed holes, in this way the Si/H or Cl/H ratio can be altered as a function of position in the reactor Second, the temperature in the tube can be changed In the latter case, we work in a temperature gradient and the solubility curve can be followed until the minimum in the solubility is reached This idea is followed in the present study All along the temperature gradient the gas phase is brought out of equilibrium and comes to equilibrium again by the deposition of silicon on the substrates

The growth of silicon under a small supersaturation as can be realized by the gradual change of temperature described above has the additional advantage that growth of silicon on silicon is readily possible, growth of silicon on a foreign substrate, however, meets with nucleation difficulties and needs a higher supersaturation (21) This bears the possibility that growth on tube walls and quartz boats can be prevented and also gives the possibility of selective growth in windows of oxide layers present on a large number of silicon substrates in the reactor

Growth rate —For growth at a constant temperature, the growth rate (G) can be calculated for a constant flow rate V liter/min an initial silicon partial pressure p_i bar, and a solubility L of silicon in the gas phase in bar at the temperature T from

$$G = \frac{(p_i - L)VM}{RTA\rho} 10^4 \ \mu\text{m/min} \qquad [6]$$

where R is the gas constant (82 06 cm³ bar/K mol) M is

the molecular weight of silicon (28 086g), ρ is the density of silicon (2 3 g/cm^3), and A is the silicon substrate surface area (cm^2)

The flow V depends on temperature and total pressure (p_{tot}) present in the reactor cell

$$V = \frac{V_n T p_n}{T_n p_{tot}} \qquad [7]$$

where V_n is the gas flow at normal p and T (p_n = 1 bar, T_n = 298 K) For growth on a greater number of slices, each wafer has to be in contact with a gas phase with the same supersaturation This can be realized as discussed before in a temperature gradient in which the gas phase is constantly brought out of equilibrium In that case the equation for the growth rate becomes

$$G = \left(-\frac{dL}{dT}\right)_T \left(\frac{dT}{dx}\right)_x \frac{lV_n M}{RT_n A(x)\rho} \frac{p_i}{p_{tot}} 10^7 \ \mu\text{m/min} \qquad [8]$$

where $(dL/dT)_T$ is the gradient of the solubility curve at temperature T for the Cl/H ratio and total pressure in question, $(dT/dx)_x$, the gradient of the temperature at position X, l the distance between two slices, and $A(x)$ the substrate surface area at position X Growth has to be expected for a positive product $(-dL/dT)(dT/dx)$, i e , at the low temperature side of the minimum of the solubility curve ($dL/dT < 0$) a positive temperature gradient must be applied, whereas a temperature drop in the direction of the flow ($dT/dx < 0$) is needed when one works at the high temperature side of this minimum, where (dL/dT) is positive (Fig 2-4)

For constant growth rate all along the reactor tube, it is sufficient that the product $(dL/dT)(dT/dx)\ l$ is constant In practice, a constant value of dT/dx combined with a constant wafer spacing is preferred In this case, constant growth rate requires a linear change in the solubility curve This optimal thermodynamic working point directly will follow from the solubility curves by calculating dL/dT for each T No real constant value for dL/dT is present, however, a more or less flat region — where the deviations are smaller than 10% — is present around each inflection point in the L *vs* T plot, allowing crystal growth in a temperature region with a width of about 100-200 K around 1200 K for each Cl/H ratio

In principle, it is possible to work at the high temperature side of the minimum in L *vs* T A disadvantage will be that the gas mixture has to enter from the hottest side of the furnace During the heating up from room temperature, the gas will pass a temperature region where, already, a state of supersaturation will be obtained and spontaneous nucleation in the gas phase may occur This problem can be solved by following route C as indicated in Fig 4, where in principle the gas mixture at high T is prepared *in situ* from an unsaturated silicon mixture in contact with a solid silicon source

This disadvantage does not exist for growing in a positive temperature gradient, i.e , at the low temperature side of the solubility curve Low temperatures are preferred in hot-wall reactors, especially when lower total pressures are of advantage, in order to prevent damage of the tube and attack of the quartz ware

Equipment and procedures —Basically, the system is a normal CVD system equipped with a furnace instead of a RF generator A schematic presentation including the gas mixing system is depicted in Fig 5

The complete system is home-built and consists of a four-zone furnace with a total heated length of 135 cm The inner diameter of the reactor tube was 45 mm, with a total length of 260 cm, including the necessary load-lock provision With four independent controllers, any desired temperature profile can easily be adjusted

Mass flow controllers and mass flowmeters controlled the flow of the hydrogen carrier gas, the dichlorosilane, or trichlorosilane and additional HCl For the present experiments, the silicon samples [one side polished, low resistivity, Sb doped, (100) orientation, with a diameter of 5

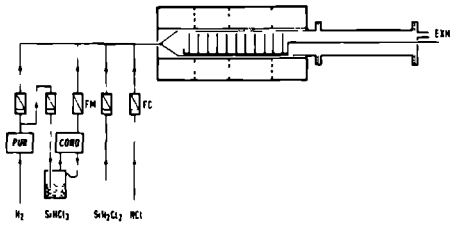

Fig 5 The apparatus used in the growth experiments consists of a four-zone furnace in which is a long quartz tube such that the load can be flushed at room temperature before introduction into the furnace All gases can be directed to the vent when needed (not shown in the figure) The slices can be positioned parallel to or perpendicular to the gas stream, the experimental results being comparable

cm], were cut into two parts and placed parallel to the long axis of the furnace This has the advantage of giving a small disturbance on the flow characteristics, it has the disadvantage that because of the high heat conductivity of the silicon, the upstream part of the crystal is somewhat higher and the downstream part is somewhat lower in temperature than would correspond with its position in the furnace (for positive T gradient in the flow direction)

In additional experiments it has been shown that the slices can be placed parallel to or perpendicular to the main gas stream without significant differences in growth rate and crystallographic quality

The moisture and oxygen content of the H_2 carrier gas was always below 1 ppm The total flow (NTP) was always 3 5 liter/min, giving a gas velocity of about 15 cm/s at the growth temperature

The sample holder loaded with up to 20 slices is introduced into the cold part of the quartz tube, purged with N_2 and H_2, then slowly moved into the hot furnace Just before the start of the growth experiments, an *in situ* HCl etch was performed with 0 5% HCl for 5 min The etch rate of silicon by HCl is rather independent of temperature between 900° and 1200°C and amounts to 0 02 μm/min (21) for the given HCl content

Results

Experiments were performed with $SiHCl_3$ as well as with SiH_2Cl_2 as silicon sources $SiHCl_3$ was taken to study (i) the effect of the input concentration on the growth rate (this gives indication about the practical usable concentration for growth and gives information indicating whether the equilibrium situation is achieved) and (ii) the influence of the temperature gradient on the growth rate

With SiH_2Cl_2 it is possible to check whether a similar growth will be observed for a given Si/H and Cl/H ratio as obtained with $SiHCl_3$ This directly gives proof that equilibrium situations are attained in both situations

$SiHCl_3/HCl/H_2$ mixtures —In order to obtain homogeneous epitaxial layers with good crystalline qualities at reasonable growth rates, a number of initial requirements have to be fulfilled when growth is to be performed in an oven

1 For optimal crystalline quality, the temperature range should be as high as possible (> 1200 K)

2 The adsorption of, e g , chlorine should be as low as possible, which is favored by high temperatures and low chlorine content

3 The solubility of silicon preferably should change linearly with T in order to achieve constant growth rates in the temperature gradient of the furnace

4 The slope of the solubility curve should be as steep as possible to obtain high growth rates and high yields

5 Deposition on furnace wall and quartz boats has to be prevented

From the solubility curves as presented in Fig 2 and 3, it can be seen that the requirements can best be met for Cl/H = 0 06 and p = 1 bar. For this ratio, a reasonable

value for dL/dT is obtained at high temperatures In addition, the chlorine content of the gas mixture is relatively low, which favors a small coverage of the surface with chlorine A temperature region around 1200 K should be preferred to guarantee constant growth rates Since it can be expected that the crystalline perfection for $T < 1200$ K is not optimal, the temperature region above $T = 1220$ K was chosen, accepting beforehand that the growth rate theoretically should decrease at higher temperatures (smaller absolute values of dL/dT) For an equilibrium mixture ($\gamma = 0$) at the entrance of the furnace, it is expected that the growth rate starts at zero, as soon as the mixture comes out of equilibrium because of the temperature gradient, a constant growth rate should result With the gradients used, every centimeter in the furnace gives a change in equilibrium concentration corresponding to $\gamma = 0.1\%$ Several growth experiments have been performed, some results are presented in Fig 6 and 7 For Cl/H = 0 0604, various mixtures with a silicon content above and below the equilibrium value at the temperature at the entrance of the furnace (1220 K) were used From the figures, it is apparent that etching occurs over the temperature range where the γ of the first wafer is negative (Fig 6, $\gamma = -5.0$) Etching turns into growth almost at the point which theoretically was calculated In this respect, the experiment is in agreement with theory For low initial supersaturations, no growth is observed on the first slices, whereas the growth rate increases on the following slices Above $x = 70$ cm, the growth rate drops drastically because of the decrease in $(dL/dT)_T$ In Fig 6, every value of x represents a specific temperature, replotting Fig 6 as log G *vs* $1/T$ (Fig 7, $\gamma \sim 10\%$, $dT/dx = 2$ K/cm) shows that only above 1000°C a constant plateau is reached Even with a value of γ independent of x, the growth rate is limited by slow surface reactions at the lower temperatures Higher initial supersaturations increase the growth rate at lower temperatures as long as the gas mixture is not yet in equilibrium For $\gamma = 6.4$ and 4 8%, no silicon deposit was observed on the quartz ware of the reactor cell or on the wafer boat. For $\gamma \sim 10\%$, a slight deposit on the wafer boat in between the first four slices was observed For higher initial supersaturations, the first part of the boat up to the fourth slice was covered with silicon, beyond this fourth slice, only the rim of the boat was slightly covered

By comparing the equivalent experiments at different dT/dx, the highest growth rate is observed for the highest temperature gradient (Fig. 8) A general trend observed in all experiments is that for a given dT/dx all growth curves converge to the same growth rate 40-50 cm from the entrance This may be an indication that equilibrium has been attained from that place

The surface morphology of the grown layer strongly depends on the growth temperature and on the Cl/H ratio

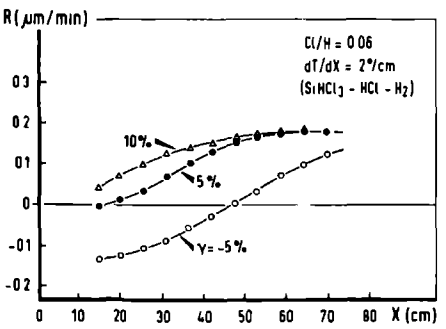

Fig 6 The silicon growth rate as a function of position in the furnace for Cl/H = 0 06, a temperature gradient of 2 K/cm between 1220 and 1340 K in the $SiHCl_3$-HCl-H system for different initial supersaturations

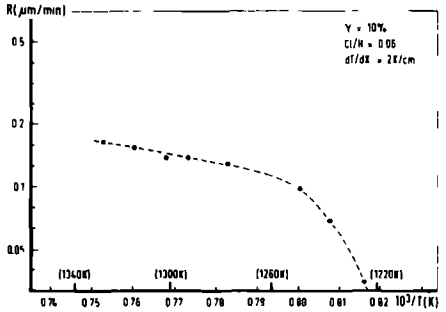

Fig 7 The silicon growth rate in the furnace system plotted as a function of reciprocal temperature for Cl/H = 0 06 in a mixture of $SiHCl_3$, HCl and H , a temperature gradient of 2 K/cm and an initial supersaturation of 10% The curve shows the same character as in a cold-wall system at much lower chlorine content

At low temperatures, the surface contains many growth hillocks, at temperatures between 1050° and 1080°C, the number of large growth pyramids is reduced, but many small bunches which have grown out almost isotropically are observed, whereas at high temperatures ($T > 1080$°C), the surface is almost free of defects (Fig 9) For the surface morphology, the temperature is more important than the degree of supersaturation It must be remembered that, although the initial supersaturations may change, a constant Cl/H ratio is always present, so that most probably the same chlorine surface coverage is also present for experiments at the same temperature For the highest growth rates (high temperature gradient, high γ initial) and low temperatures, locally polycrystalline growth could be observed on the first slices in the wafer boat. Except for these cases, all epilayers were monocrystalline It has to be stressed that selective growth is nearly perfect for small supersaturations, below $\gamma = 10\%$ Growth on silicon is possible then without deposition on the quartz tube or boat

SiH_2Cl_2, HCl H_2 mixtures—The experiments with SiH_2Cl_2 were performed to check the validity of the principle For the same Cl/H ratio, temperature gradient, and initial supersaturation, one would except the same growth curves as obtained in the equivalent $SiHCl_3$ experiment Figure 10 gives the result for such a series of experiments, which have to be compared with those collected in Fig 6 Apart from a higher growth rate, the

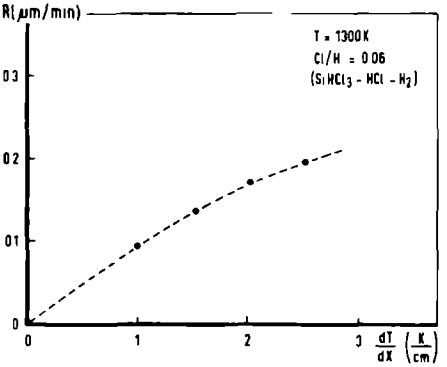

Fig 8 The silicon growth rate as a function of the temperature gradient in the furnace, measured at 1300 K, for Cl/H = 0 06 in the $SiHCl_3$-HCl-H_2 system

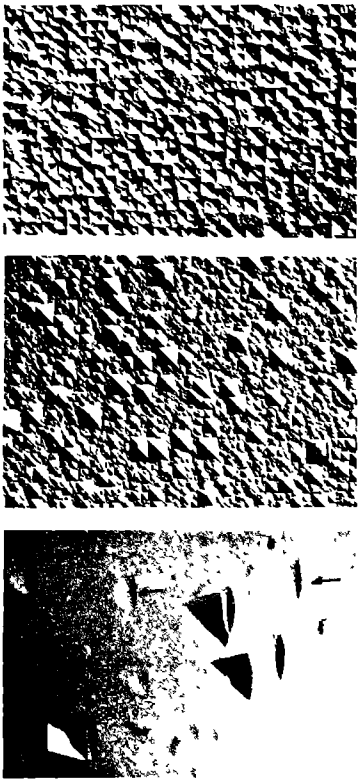

Fig 9 Surface structures obtained at different temperatures for Cl/H = 0 06 and a layer thickness of about 20 μm At the higher temperatures, smooth surfaces are obtained, sometimes with characteristic "half moon terraces" and full-size hillocks Top, 1000°C, middle, 1050°C, bottom, 1080 C The half moon terraces are indicated with an arrow Magnification 100× before reproduction

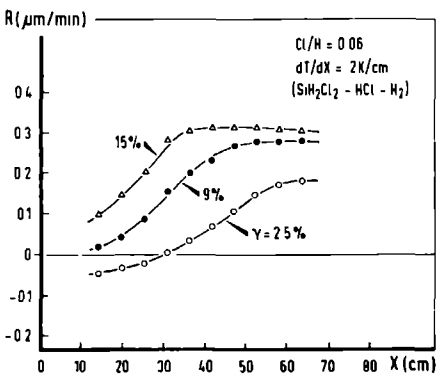

Fig 10 Silicon growth rates as a function of position in the furnace for Cl/H = 0 06 and dT/dx = 2 K/cm in the SiH_2Cl_2-HCl-H_2 system at different initial supersaturations

growth curves are very similar, including a complete absence of silicon growth on the boat On the other hand, the surface morphology for SiH_2Cl_2-grown layers is not as good as for $SiHCl_3$-grown layers under identical conditions The epilayer is monocrystalline, but many small hillocks are present at these temperatures and growth rates, where the $SiHCl_3$ grown layers are nearly defect free This unexpected feature will be discussed below

Experiments were also performed at higher Cl/H ratios, using mixtures of SiH_2Cl_2-HCl and H Equilibrium concentrations were calculated for Cl/H = 0 16 and 0 35 The latter case already represents a concentrated mixture of 17% SiH_2Cl_2 and 26% HCl in hydrogen In all cases, the temperature gradient in the furnace gave rise to silicon growth as expected, indicating the quality of the thermodynamic data The growth rates, in the order of 0 1-0 2 μm/min, are plotted in Fig 11, the relatively high growth rate at lower temperatures is obvious for the more concentrated systems The quality of the grown layers was poor compared to growth at Cl/H = 0 06, even polycrystalline growth was observed at the lower temperature end of the furnace Again, silicon deposit on quartz ware was observed for supersaturations exceeding 10%

Discussion

It has been demonstrated, *e g* , by Sirtl *et al* (22), Arizumi (23), and Claassen (24), and mathematically founded by Bollen *et al* (25) that by using the mechanism of selective nucleation, growth of silicon is possible on surfaces with low nucleation barriers, *i e* , on silicon itself, whereas no growth will occur on foreign surfaces The present work demonstrates that this principle can be extended to all SiO surfaces within a furnace system, thus, epitaxial growth of silicon is made possible in a hot-wall reactor Contamination of walls and boats can be prevented provided a low supersaturation can be maintained in the entire system The experiments have to be guided by a thorough knowledge of the thermodynamics of the system This point is illustrated in experiments with high Cl/H ratios, *e g* , Cl/H = 0 16 with 7 9% SiH_2Cl_2 and 14% HCl, and Cl/H = 0 3482 with 17 1% SiH_2Cl_2 and 26 4% HCl. Experiments with these mixtures demonstrate the reliability of the thermodynamic data on the Si Cl H system as selective growth sets in at $\gamma \approx 0$ and is restricted to a narrow range of initial supersaturations up to 10% In the following the etch and growth behavior and the crystallographic quality of the layers will be sketched in order to come to some conclusions on the feasibility of the system

Etch and growth behavior —As pointed out before, an equilibrium mixture entering the furnace will ideally

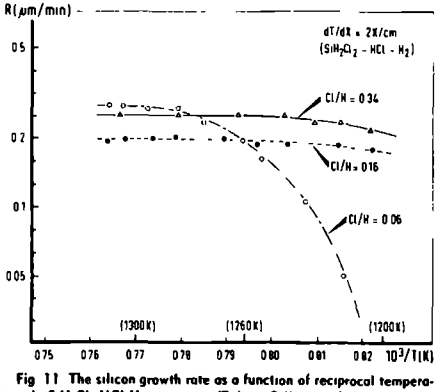

Fig 11 The silicon growth rate as a function of reciprocal temperature in SiH_2Cl_2-HCl-H_2 system at dT/dx = 2 K/cm and three Cl/H ratios The surface reactions appear to be much faster in the more concentrated mixtures (higher Cl/H ratio)

show no growth or etching In the temperature gradient imposed on the system, a supersaturation is then building up of the order of 0 1% per degree Figure 6 shows that with a gradient of 2 K/cm, about 40-50 cm are needed to bring the gas phase into equilibrium This can be interpreted as a supersaturation of 10% being needed to come to continuous growth, this being improbably high, still, it is found that a steeper temperature gradient leads to a somewhat shorter pre-equilibrium zone

Another possibility, however, points to the time needed to come to complete equilibrium For the chosen gas velocity of about 15 cm/s, the results given in Fig 6 point to a preliminary stage of about 3s This view is further illustrated in the series of experiments with SiH_2Cl_2 in which the temperature gradient is kept constant, the Cl/H ratio, however, is changed from 0 06 to 0 16 and 0 35 Very clearly, the time needed to come to constant growth is much shorter at the higher Cl/H ratios

This behavior can be explained from the known characteristics of the SiH_4Cl_2, $SiHCl_3$, and $SiCl_4$ systems (26, 27), in which two easy gas phase reactions are present

$$SiH_4Cl_2 \leftrightarrow SiCl_2 + H_2 \qquad [10]$$

$$SiHCl_3 \leftrightarrow SiCl_2 + HCl \qquad [11]$$

The $SiCl_4$ concentration, however, can only be brought to the required equilibrium level via a surface reaction

$$SiCl_2 + 2Cl^* \rightarrow SiCl_4 + 2^* \qquad [12]$$

where Cl^* stands for an adsorbed chlorine atom on a reactive silicon site (*) given by

$$HCl + * \rightarrow Cl^* + 1/2\ H_2 \qquad [13]$$

There is a slow reverse reaction

$$SiCl_4 + 2^* \rightarrow SiCl_2 + 2Cl^* \qquad [14]$$

This reaction is the cause of surface controlled kinetics already at 1100°C for $SiCl_4$ as the initial reactant (27) In the SiH_2Cl_2 HCl input mixture, therefore, $SiCl_2$, $SiHCl_3$, and SiH_2Cl_2 can be present in near equilibrium concentrations via the rapid gas phase reactions [10] and [11] The formation of $SiCl_4$, however, lags behind As long as $SiCl_4$ is missing, an excess of HCl is present It is known (21) that HCl etching proceeds at a constant rate rather independent of temperature down to about 900°C (dependent only on the purity, i.e , oxygen content, of the gas) At 900°C, 1% HCl gives an etch rate of 0 1 μm/min, 1 5% HCl already 0 25 μm/min In this way, the excess HCl can counteract the growth in situations where the complete equilibrium has not yet been established Changes in $SiCl_4$ concentration occur via reactions [12] and [14], a decrease in $SiCl_4$ content will take place slowly, rather independent of HCl content (27) The reverse reaction, formation of $SiCl_4$, will be faster for higher HCl contents From Eq [12], the rate of formation of $SiCl_4$ and thus the rate of "equilibrization" can be given as

$$R_{SiCl_4} = K\, p_{SiCl_2}\, [Cl^*]^2 = K'\, p_{SiCl_2}\, p_{HCl^2/H_2} = K''\, p_{SiH_2Cl_2}\, p_{HCl^2/H_2^2} \qquad [15]$$

When we now compare the situation for Cl/H 0 06, 0 16, and 0 35, the rate of $SiCl_4$ formation is calculated to increase from 1 16 105 This may explain the short introduction time as a kinetic factor needed to conform the mixture to a quasi-equilibrium one The temperature dependence of the growth rate in the SiH_2Cl_2/HCl system has been given in Fig 11 The diffusion-limited region of crystal growth is extended to much lower temperatures, presumably because of the enhanced surface reaction rate discussed before It has been postulated that for a diffusion-limited growth the surface quality will be superior to growth in a surface-limited region This supposition is not confirmed here, this point will be discussed in the next section It can be further mentioned that, in the region of constant growth, the growth rates found are not too far from, but always lower than, the calculated values and constant over the diameter of the substrates ± 40%

According to Eq [8], we expect a typical growth rate of 0 41 μm/min, to be compared with the measured rates of 0 1-0 3 μm/min The calculated growth rate could apply to polycrystalline growth (9), for monocrystalline growth also, the density and velocity of atomic steps on the surface will play a part

Crystallographic quality —Growth and etching in the Si-Cl-H system leads to smooth and perfect surfaces only at higher temperatures and relatively low etch and growth rates For the growth of silicon, Burmeister (28) and Revesz *et al* (29) showed hillock formation and faceting to occur as a function of growth rate and temperature A comparable change from monocrystalline to polycrystalline growth habit was observed by Bloem (30) Van der Putte *et al* performed an extensive study on the silicon surface structure after etching with gaseous HCl (31)

Figure 12 combines these experimental results, indicating regions in which good quality epitaxial layers can be grown as well as regions with bunched or even polycrystalline growth, all on good quality substrates in the Si-Cl H system at atmospheric pressure Trapping of impurities or growth units has to be considered as the main reason for the occurrence of growth defects The experiments in the near equilibrium growth in a furnace are reasonably in line with the data in Fig 12, some additional influence of higher Cl ratios seems to be present At Cl/H = 0 16 and 0 35, a diffusion controlled growth regime appears to be present even at low temperatures The layer quality, however, is by no means superior to layer growth at the same temperature and growth rate in the Cl/H = 0 06 system This can be caused by the increased adsorption of chlorine containing species Another point can be important too, i e , the quality of the HCl gas used in the experiments The water content of the HCl may be adequate for normal CVD use, in the concentrated mixtures (26% HCl at Cl/H = 0 35) a small impurity content already counts heavily

At 1000°C the formation of solid SiO_2 is possible for a water content exceeding 1 ppm More than 4 ppm in the HCl cylinder thus already may be sufficient to deteriorate the crystalline quality because of blocking of moving steps on the growing surface

Good quality epitaxial growth at still lower temperatures than given in Fig 12 are possible under UHV condi-

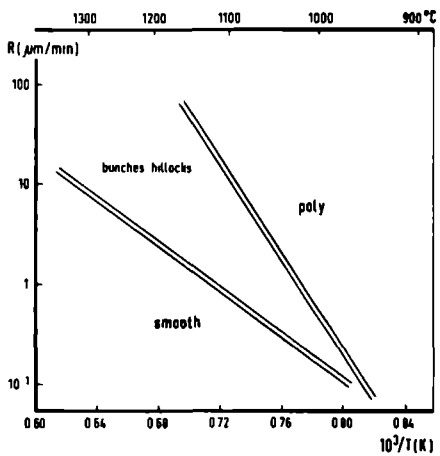

Fig 12 The experimental growth morphology in the Si-Cl-H system at atmospheric pressure as it depends on growth rate and growth temperature Trapping of defects and impurities plays an important part in the determination of the resulting structure, low growth rates and high growth temperatures are favorable there

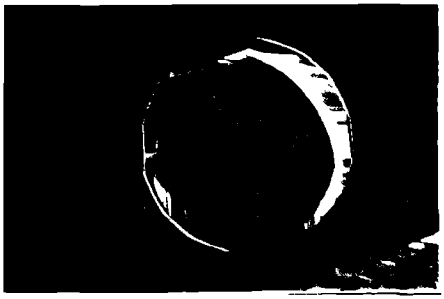

Fig 13 Example of selective growth of silicon inside a window etched into an oxide layer on top of a silicon wafer

tions (molecular beam epitaxy), where disturbing effects of undesired impurities are minimized In this respect, the conclusion comes forward that impurities have a stronger effect on the layer quality than the trapping of silicon containing growth units as such At the lower temperatures the surface is heavily textured, going to higher growth temperatures, the (100) surface becomes smooth with isolated growth hillocks (Fig 9) Each hillock has a dislocation in its center, often hollow cores are observed Sometimes, however, a typical flat top is present Tsukamoto and van der Hoek (34) found the same type of defect, called half-moon terraces, on garnets and explained them as growth hillocks that have become inactive and obtained a flat top On further growth they develop into the half moon terraces

The hillocks have a mean deviation of 2 56° from (100), with a variation from 0 5 to 3 On the edges of growth regions facets form on prolonged growth (Fig 13) mostly (111) faces are exposed and some (113) and (115) facets are also found A closer study of the faceting is underway A further point in favor of the furnace system is the absence of steep temperature gradients that can be the origin of stress and slip in the substrates (35)

Feasibility of the system —In CVD intended for growth of silicon on metallurgical silicon substrates for the production of solar cells the crystalline quality obtained in the present setup can be quite satisfactory when the specifications for surface planarity can be relaxed an increased surface area could even have some advantage

Another attractive feature is the batch wise selective deposition of silicon in windows opened in SiO layers on silicon substrates in this application, thin layers are envisaged

For other silicon device processes, the CVD in a furnace can be achieved satisfactorily only well above 1000°C The furnace process will gain when the surface quality at the low temperature side can be improved Working at lower oxygen impurity levels is one approach

Introduction of $SiCl_4$ in the main gas stream reduces the amount of HCl needed and will help in bringing down the impurity content

The growth rates obtained are in the order of 0 1-0 3 μm/min in order to obtain thick layers (< 10 μm), this rate is too low Therefore the selective deposition of silicon in oxide windows appears to be the most attractive proposition for practical use of the near equilibrium system in the furnace

Conclusion

Chemical vapor deposition in a hot-wall reactor is possible without deposition of silicon on the quartz ware of the cell or the wafer boat In terms of crystalline quality the best results are obtained for growth with $SiHCl_3$, low Cl/H ratio, and high temperatures

An important conclusion is the discovery of fast surface reactions at high Cl/H ratios, such that a gas phase diffusion-controlled growth rate extends down to nearly 900°C in the furnace system In order to profit in the sense of improved layer quality, the water content has to be reduced to very low levels

In general it can be stated that quite a number of questions are still present, but in principle a new and interesting method to produce epitaxial silicon has become available

Acknowledgments

The authors like to thank Mr H v d Linden and Mr J van Oyen for skillful technical assistance and Mr C Dominguez for his contributions during his stay in Nijmegen This work was partly supported by the Commission of the European Communities via Contract no ESC R 045 NL

Manuscript submitted Aug 6, 1984, revised manuscript received March 20, 1985

Catholic University assisted in meeting the publication costs of this article

REFERENCES

1 H C Theuerer J J Kleinack H H Roar, and H Christensen *Proc IRE* **48**, 1642 (1960)
2 R V Daiello P H Robinson and H Kressel, *Appl Phys Lett* **28**, 231 (1976)
3 F C Eversteyn and H J Peek, *Philips Res Rep* **25**, 472 (1970)
4 R S Rosler *Solid State Technol* **20**, 63 (1977)
5 B E Deal, *This Journal* **109**, 514 (1962)
6 B A Lombos and T R Somogyi *ibid*, **111**, 1097 (1964)
7 J I Nishizawa, *J Cryst Growth* **56**, 273 (1982)
8 V S Ban *ibid* **45**, 97 (1978)
9 F Langlais, F Hottier and R Cadoret, *ibid*, **56**, 659 (1982)
10 M Ogirima H Saida, M Suzuki and M Maki, *This Journal* **124**, 903 (1977)
11 J P Duchemin M Bonnet and F Koelsch, *ibid*, **125**, 637 (1978)
12 J Bloem Y S Oei, J H L Hanssen and L J Giling, in '3rd European Conference on Photo Voltaic Solar Energy ' p 574 Cannes 1980, Reidel Publishers, Dordrecht Holland
13 W Steinmaier *Philips Res Rep* **18**, 75 (1963)
14 JANAF Thermochemical Tables 2nd ed NSRDS-NBS 37, National Bureau of Standards, Washington DC (1971)
15 L P Hunt and E Sirtl *This Journal*, **119**, 1741 (1972)
16 L P Hunt and E Sirtl *ibid* **120**, 806 (1973)
17 P van der Putte L J Giling and J Bloem *J Cryst Growth* **31**, 299 (1975)
18 T O Sedgwick J E Smith R Ghez, and M E Cowher *ibid* **31**, 264 (1975)
19 V S Ban and S L Gilbert *ibid* **31**, 284 (1975)
20 J P Duchemin, Thesis University of Caen, France (1976)
21 J Bloem and W A P Claassen, *J Cryst Growth*, **49**, 435 (1980)
22 E Sirtl and H Seiter in "Semiconductor Silicon" R R Haberecht and E L Kern Editors p 189 The Electrochemical Society Softbound Proceedings Series New York NY (1969)
23 T Arizumi, in 'Current Topics in Material Science," Vol I E Kaldis Editor Chap 5 North Holland, Amsterdam (1978)
24 W A P Claassen and J Bloem, *This Journal* **127**, 1836 (1980)
25 L J M Bollen C H J van den Brekel, and J Kuiken, *J Cryst Growth*, **51**, 581 (1981)
26 W A P Claassen and J Bloem *ibid* **50**, 807 (1980)
27 J Bloem W A P Claassen, and W G J N Valkenburg *ibid* **57**, 177 (1982)
28 J Burmeister, *ibid* **11**, 131 (1971)
29 A G Revesz and R J Evans, *Trans Metall Soc AIME*, **230**, 58 (1964)
30 J Bloem *J Cryst Growth*, **18**, 70 (1973)
31 P van der Putte, L J Giling and J Bloem *ibid*, **41**, 133 (1977), **43**, 659 (1978) **47**, 437 (1979)
32 W W Webb *J Appl Phys*, **33**, 1961 (1962)
33 L J Giling *Mat Chem Phys* **9**, 117 (1983)
34 K Tsukamoto and B van der Hoek, *J Cryst Growth*, **57**, 131 (1982)
35 J Bloem and A H Goemans, *J Appl Phys*, **43**, 1281 (1972)

CHAPTER 5

NEAR EQUILIBRIUM GROWTH OF SILICON BY CVD

THE Si-I-H SYSTEM

Journal of Crystal Growth 65 (1983) 406–410
North-Holland, Amsterdam

NEAR EQUILIBRIUM GROWTH OF SILICON BY CVD
II. The Si–I–H system

J.H.L. HANSSEN, A.A. SAAMAN, H H C. DE MOOR, L.J GILING and J BLOEM

Research Institute of Materials, Department of Solid State Physics, University of Nijmegen, Toernooiveld, 6525 ED Nijmegen, The Netherlands

The epitaxial growth of silicon in the electronics industry tends to develop into two directions (1) growth at lower temperatures in order to obtain sharper p/n junctions, and (2) growth at lower costs for large scale applications in the field of MOS devices Both objectives have created efforts into alternative ways and means of epitaxial growth, including the reconsideration of methods that have been postulated long before and never have reached maturity The chemical vapour transport of silicon in the Si–I system is one example A thermodynamic analysis is given of the system, various results reported in literature can be explained satisfactorily Methods are given in order to obtain a high packing density of substrates in a near equilibrium hot wall reactor Experimental results are shown, supporting the analysis given A low growth rate of silicon is possible on a number of substrates in a system where growth of silicon on quartz walls and boats is prevented

1. Introduction

In the discussion of near equilibrium growth in the Si–Cl–H system [1] it has been shown that in principle epitaxial growth of silicon on silicon can be executed in a hot wall reactor, such that no deposit of silicon on the quartz walls takes place. Because of the near equilibrium nature of the process, the supersaturation in the gas phase remains small, leading to growth rates in the order of 0.1 μm/min The number of wafers treated per batch can be relatively large, provided the hot wall furnace can be given a temperature gradient such that the system is brought out of equilibrium continuously; deposition of silicon then restores the gas phase equilibrium with the silicon substrates

In the semiconductor field the Ge–I system has been explored by Marinace [3] and the Si–I system has been described in relation to a close spaced technique [4,5] It has also been shown that in a temperature gradient transport is possible in both directions depending on temperature and pressure [6] Braun and Kosak [7] showed the possibility of monocrystalline growth of silicon at temperatures as low as 750°C in the Si–I system In the quartz ampoules used in the Si–I system, a marked segregation because of gravity is observed, especially the heavy iodides (SiI_4, SiI_2) show this phenomenon.

The present study is aimed at a thermodynamic analysis to indicate possible regions where chemical vapour transport, close spaced growth and near equilibrium growth in a temperature gradient can be performed with a possibility of success This study is of importance as the existing equipment for the epitaxial growth of silicon works with high supersaturations in a regime where gas phase diffusion of species determines the growth rate This growth mode prevents a high stacking density of substrates in the reactor and keeps the equipment large and expensive

The possibilities of near equilibrium growth, avoiding high supersaturations, have to be studied in order to see whether another type of reactor could be attractive In this respect the iodine system is of importance because of the reported low-temperature growth capabilities [7] A closer look at the Si–I–H system is therefore desirable.

2. Equilibrium calculations

Thermodynamic data have been collected for a great number of gaseous compounds expected to

0022-0248/83/$03.00

be important in the Si–I–H system, e g Si(g), Si_2(g), Si_3(g), SiI(g), SiI_2(g), SiI_3(g), SiI_4(g), SiH_3I(g), , I_2(g), I(g) [8–10] For every compound the equilibrium constant K_p is calculated for the formation of the compound from the elements in their standard state at the temperature under consideration The total pressure, the temperature and the I/H ratio are then used as input of a computer program to minimize the free energy of the system in an iterative procedure resulting in the partial pressures of all species in equilibrium with solid silicon [1,11]

Results are given also in terms of the solubility (L) of silicon in the gas phase, being a summation of the partial pressures of all silicon containing gas phase components in which the partial pressures of a component is multiplied by the number of silicon atoms in the molecule of that compound

$$L = x_i \sum \left(p_{Si(x)H(y)I(z_i)} \right)$$

In the Si–I–H system we thus have

$$L = p_{Si} + 2p_{Si_2} + 3p_{Si_3} + p_{SiI} + p_{SiI_2} +$$

Fig 1 gives the gas phase composition for $P_{tot} = 1$ atm and I/H = 0 06 At low temperature SiI_4 appears to be the most abundant silicon containing species and for $T > 1100$ K it is seen that SiI_2 takes over The resulting solubility curve is shown in fig 2 It will be appreciated that differences in solubility can give rise to transport of silicon in a temperature gradient, growth occurring at the temperature where L is lowest and etching of silicon taking place at the site with the highest equilibrium value of L

Fig 3 gives some solubility curves for different I/H ratios at $P_{tot} = 1$ atm and at temperatures between 1100 and 1480 K It is apparent that for

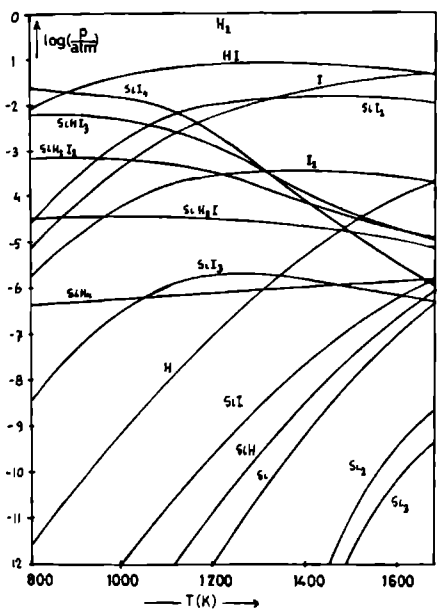

Fig 1 Calculated gas phase composition in the Si–I–H system as a function of temperature I/H = 0 06 $P_{tot} = 1$ atm

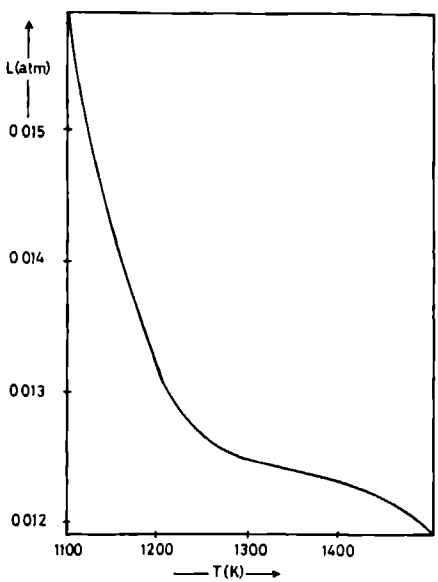

Fig 2 The solubility of silicon (L) deduced from fig 1 L is the sum of all the concentrations of silicon containing species

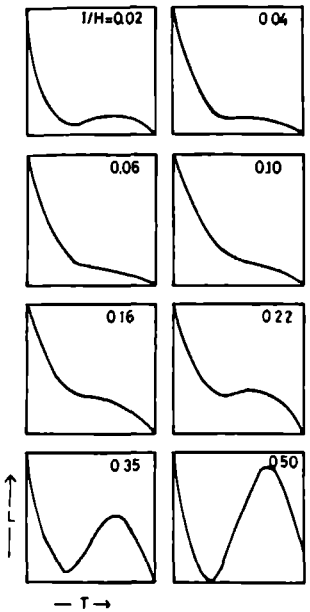

Fig. 3 The calculated silicon gas phase solubility L for different values of I/H between 1100 and 1480 K, $P_{tot} = 1$ atm.

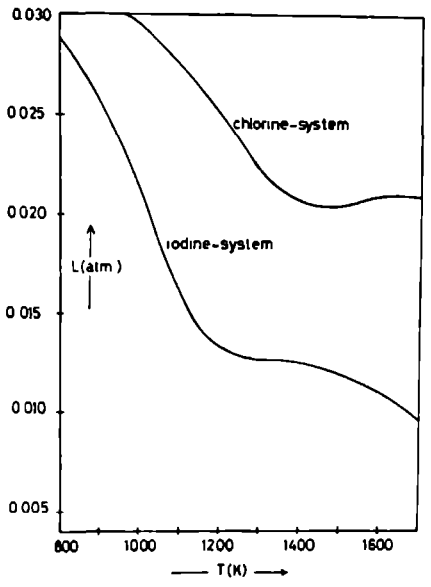

Fig. 4 Comparison of the Si–Cl–H and Si–I–H systems, calculated at $X/H = 0.06$ and $P_{tot} = 1$ atm

$I/H = 0.02$, local minima and maxima develop in the L versus T curves. This is the more so in the Si–I system without hydrogen. Using these types of curve, it is possible to explain the experimental results reported in the literature [4,5,7]. Direction of transport as well as the magnitude of the driving force are reasonably explained.

In a near equilibrium system, growth is executed in a temperature gradient. In order to obtain a nearly constant growth rate between evenly spaced silicon slices, a linear decrease in solubility L with changing temperature is favoured [1]. In fig. 4, calculated solubility curves for a total pressure of 1 atm and $X/H = 0.06$ are given for X = Cl and X = I. Near equilibrium growth appears to be possible between 1200 and 1400 K in the Cl system when an equilibrium mixture enters the reactor at the low temperature side and loses silicon going to the higher temperatures. At 1 atm and $I/H = 0.06$ the iodide system appears less attractive in this respect. At some higher X/H ratio the situation becomes different and fig. 5 shows a comparison between the chloride and iodide systems at $X/H = 0.22$ and three different total pressures. It is seen that the iodide system at reduced total pressures shows a long range of temperatures where a near equilibrium growth experiment could be performed.

3. Equipment and experimental results

A four-zone furnace of 100 cm total zone length has been assembled in which a 55 mm quartz tube is inserted. The tube is long enough to enable flushing of the load at room temperature. Then the boat with the slices is brought into the temperature

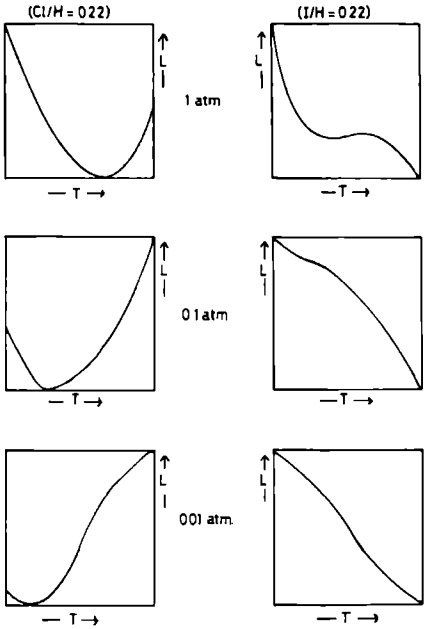

Fig 5 As fig 3, for X/H = 0 22 and three different total pressures T = 1100–1480 K

gradient Mass flow meters are used to monitor the following gases H_2, He, HCl, HI and SiH_4, I_2 can be delivered by means of a thermostated I_2 evaporator.

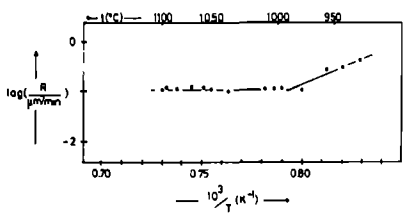

Fig 6 Experimental growth rate versus temperature in the furnace in a near equilibrium situation, plotted as log R versus $1/T$, dT/dx = 2 K/cm and I/H = 0 06

Mixtures of H_2 and He can be used to simulate the thermodynamic situation at lower total pressures. In the Si–I system, He is also used as a carrier gas. An internal silicon source is needed to bring the incoming gas into equilibrium, the first slices of the load are used for this purpose. In the initial experiments the slices were halves of 2 inch wafers positioned every 5 cm along the boat. During the experiments a white deposit of SiI_4 appears at the outlet of the quartz tube outside the furnace system. Reaction of SiH_4 with HI already takes place at temperatures around 100°C, indicating that equilibrium conditions will be reached easily at higher temperatures

Some results are given in fig. 6 where log R is plotted versus $1/T$ The temperatures quoted are equivalent to the position in the furnace in which a linear temperature gradient of 2 K/cm was maintained The gas enters at the low temperature side. There is no drastic reduction in growth rate at lower T as was found in the Si–Cl–H system [1] The higher growth rate at lower T comes from a steeper L versus T curve below 1330 K (see fig. 2). Up to 1100°C a nearly constant growth rate is achieved These results confirm the thermodynamic expectations, as the growth rate can be predicted from the solubility curves. Furthermore there is no silicon deposit on quartz walls or boats and selective growth in oxide windows is perfectly possible with some facet formation along the edges. Moreover, it is obvious that the growth rate is orientation dependent. Slightly misoriented (111) wafers as normally used in (111) epitaxial growth show a growth rate nearly a factor of 2 higher than that of (100) slices. This indicates that the growth is not only controlled by the supply of reactant, but that surface reactions play an important role, as can be expected in the near equilibrium system with its small supersaturations.

The grown layers are monocrystalline, the density of growth hillocks on the surface increases with decreasing growth temperatures Only above 1050°C were perfectly flat surfaces obtained. In line with other observations [12,13], the hillocks originate at defects and impurities present at the interface The purity, especially of HI and I_2, is not yet sufficient to guarantee perfect growth at the lower temperatures.

4. Feasibility of the system

The thermodynamic analysis has shown that chemical transport of silicon in a temperature gradient offers good opportunities in the Si–I–H system. Transport of silicon from high to low temperatures as well as inverted transport directions are possible depending on the conditions. Extended regions are found where a nearly linear variation of silicon solubility as a function of temperature is present, enabling growth of silicon in a near equilibrium configuration without growth on quartz parts. Also for close spaced growth optimum conditions can be identified. Especially growth at the high temperature side of close spaced wafers seems attractive, as possible oxides are transported to the colder parts of the system [14].

The heavy iodides (SiI_2 and SiI_4) segregate because of the gravity field; this causes local differences in growth rate. A horizontal position of the slices is therefore of advantage in this respect.

5. Conclusions

Both in the Si–Cl–H system possibilities are present for near equilibrium growth in a temperature gradient. The iodide system in principle offers the best possibilities for low temperature epitaxial growth. The Si–Br–H system is so close to the chloride system that specific advantages only will be very small.

References

[1] J Bloem, Y S Oei, H H C de Moor, J H L Hanssen and L J Giling, J Crystal Growth 65 (1983) 399
[2] H Schäfer, in Chemical Transport Reactions (Academic Press, New York 1964)
[3] J C Marinace, IBM J Res Develop 4 (1960) 248
[4] J E May, J Electrochem Soc 112 (1965) 710
[5] E A Taft, J Electrochem Soc 118 (1971) 1535
[6] H Schäfer and W Morcher, Z Anorg. Allg Chem 290 (1957) 279
[7] P D Braun and W Kosak, J Crystal Growth 45 (1978) 118
[8] JANAF Thermochemical Tables (NSRDS-NBS, 1971), for example
[9] L.P Hunt and E. Sirtl, J Electrochem. Soc 119 (1972) 1741
[10] L P Hunt and E. Sirtl, J Electrochem Soc 120 (1973) 806
[11] P van der Putte, L J Giling and J Bloem, J Crystal Growth 31 (1975) 299
[12] A G Revesz and R J Evans, Trans Met Soc AIME 230 (1964) 1981
[13] J.J Baliga, J Electrochem Soc 129 (1982) 1078
[14] J Bloem and J W.A Scholte, J Electrochem Soc 112 (1965) 1211

PART 3

THERMODYNAMICS AND KINETICS IN DOPING AND ETCHING OF GaAs

CHAPTER 6

SUBSURFACE TRAPPING DURING GROWTH AND DOPING OF III-V COMPOUNDS BY CVD

Abstract

When growth is faster than the exchange velocity of atoms adsorbed on the surface with the atoms in the subsurface layers, subsurface trapping will occur. This is demonstrated using as an example the incorporation of sulfur in GaAs by CVD: at low growth rates the subsystem of sulfur is in complete equilibrium, whereas at growth rates larger than the diffusion rate of S in GaAs the incorporation is kinetically controled. This reflects itself in a slope ½ or a slope 1 of the plot of carrier concentration versus dopant input concentration. A quantitative agreement with the slope, under equilibrium as well as trapping conditions, can be attained after evaluation of n_i, K_{ion} and $D_{S\text{-}GaAs}$. Although subsurface trapping has been shown to be active for the dopant elements, it can be generalized to all species present in the system, including vacancies, interstitials and antisite defects. It is shown that subsurface trapping is a rather general phenomenon during growth and doping of III-V compounds. Whether CVD, MOCVD, MBE or LPE is applied, always the possibility of trapping must be considered, especially for growth at lower temperatures, as is normal for MBE.

1. Introduction

During chemical vapour deposition always kinetic steps are present accompanied by rapidly adjusted equilibria. A priori it is difficult to predict which step is rate determining. Only careful examination of the growth process, viz. of the growth parameters, can give precise information to what extent a certain step is rate limiting. For the elemental semiconductor silicon a fair knowledge exists about the exact kinetic steps during growth and dopant incorporation [1]. For the binary semiconductors this information is still in an early stage of development and no clear picture exists where in the sequence of steps equilibrium is present and where not. In literature a number of excellent experiments have been reported however, which can serve as a reference framework for theoretical models as has been done for instance in the computer modeling of the Ga-As-Cl-H system, with and without sulfur doping [2,3]. From the viewpoint of completeness, computer modeling is the wisest thing to do, but it has the disadvantage of being non-transparant to the unexperienced in this field. It gives no clear direct picture where in the sequence of equilibria a kinetic barrier is found and what its physical background is. And because there is no distinct reason why a simple basic chemical approach should not lead to the same result - with the additional advantage of giving transparancy in the analysis and also indicating immediately where and why the kinetic step is present - such a simple analysis should be preferred in discussions of reaction mechanisms.

To discuss the kinetics of dopant incorporation in III-V compounds, the doping of GaAs with sulfur is studied. The method which is followed in this paper at first assumes that the growth rate is so low that all steps, leading to the dopant incorporation, can come into equilibrium with each other. From this situation a critical appraisal is given which step might break down when the growth rate is raised. It will be shown that a kinetic step which is often overlooked in doping is subsurface trapping. An excess of incorporated dopant atoms is not able to diffuse out of the crystal, since the growing interface is propagating with a higher velocity. This mechanism was already proposed by Webb to explain point defect trapping [4] and was more mathematically

worked out by Chernov [5,6] who already pointed out the difference between doping under intrinsic and extrinsic conditions. As done earlier in a preliminary paper [7], we will treat this subject more from a chemical point of view using the incorporation of S in GaAs as an example. It will be concluded that subsurface trapping can be generally observed for the incorporation of dopants as well as for the intrinsic point defects in the growth of III-V compounds.

2. The incorporation of sulfur in GaAs: experimental information

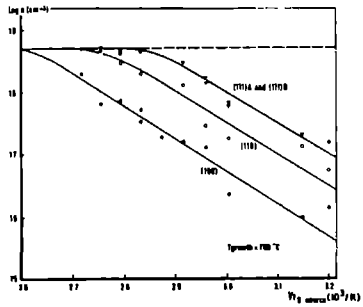

Fig.1
log n (300K) versus $\frac{1}{T}$ of an elemental S-source used during the CVD of GaAs. Experimental data from Gentner [8].

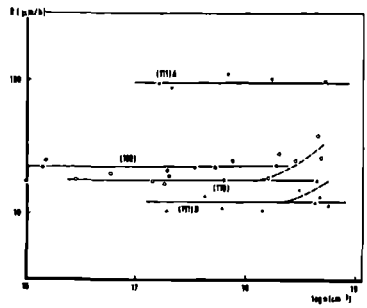

Fig.2
Experimentally observed growth rates for the four orientations of fig. 1 versus dopant concentration (Gentner [8]).

Doping of GaAs with S has been studied by Gentner [8], Veuhoff et al. [9] and Heyen et al. [10], all using the Ga-As-Cl-H system. The results as obtained by Gentner are given in figs. 1 and 2. In fig. 1 the carrier concentration is plotted as a function of the temperature of the elemental sulfur source, in fig. 2 the growth rate versus the carrier concentration. Since the vapour pressure of elemental sulfur is known [11], the data of fig. 1 can also be plotted as carrier concentration versus the input partial pressure of sulfur, or even better the pressure of H_2S; fig. 3. This can be done because in the H_2 atmosphere used in this CVD process all the incoming sulfur quantitatively is converted into H_2S at the growth temperature, as can be shown by calculating the

equilibrium situation (table 1). From fig. 3 it can be seen that a slope 1 is obtained for this incorporation process. The experiment was performed at all 4 orientations simultaneously. Striking is the equal amount of S which is incorporated for 111(A) and (111)B, despite a difference in growth rate of a factor of 10 (fig. 2). For (110) and (100), the quantity of sulfur which is built in is significantly less compared to the (111) orientations. It must be noted that all growth rates are higher than 10 μm/h. All orientations saturate at a level of about 3×10^{18} cm^{-3}.

Table 1

Composition of the gas phase at 1025 K, at 1 atm total pressure, for an input of 10^{-7} mol S and 1 mol H_2

	log P_i (atm)
H_2	-0.0
H	-8.4
H_2S	-7.0
HS	-12.0
S	-16.9
H_2S_2	-17.3
S_2	-18.1
S_3	-28.1

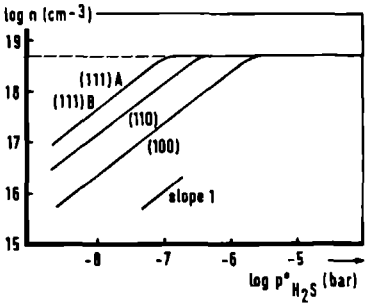

Fig.3 The same data as given in fig. 1 transfered into partial pressures of H_2S.

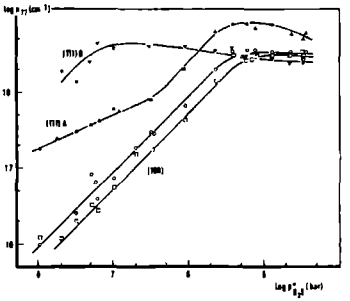

Fig.4 log n (77K) versus input pressure of H_2S used as dopant source during the CVD of GaAs (data from Veuhoff et al. [9]).

Similar results were obtained by Veuhoff et al. [9] who used H_2S as the dopant source. From fig. 4 it is clear that now the log-log plot of n versus P_{H_2S} is more complicated: a slope 1 is obtained for the (100) orientation, a slope ½ for (111)Ga, whereas the (111)As orientation already saturates for small values of P_{H_2S}. The growth rates were 12 μm/h for (100) and (111)As, but 5 μm/h for the (111)Ga orientation. Heyen et al. [10] also found a slope 1 but no growth rate was reported.

3. Equilibrium considerations

In the process of growth and doping by chemical vapour deposition one can distinguish a number of chemical systems. Those of the growth units, i.e. the gallium and the arsenic subsystems (which are coupled at the surface by the formation of GaAs) and the subsystem of the dopant element, which can be regarded as independent of the others. Here we will concentrate on the chemistry of the dopant element. In fig. 5 schematically the total equilibrium is sketched for the dopant compound H_2S. Basicly the process consists of equilibria in the gas phase, adsorption on the crystal surface, incorporation of sulfur at an arsenic site and ionization in the bulk of the crystal. We will at first assume that the growth rate is so low that the total subsystem of S can achieve equilibrium. In the second approach we will then discuss the case that the growth rate is so high that the equilibrium in the S-subsystem has to break down.

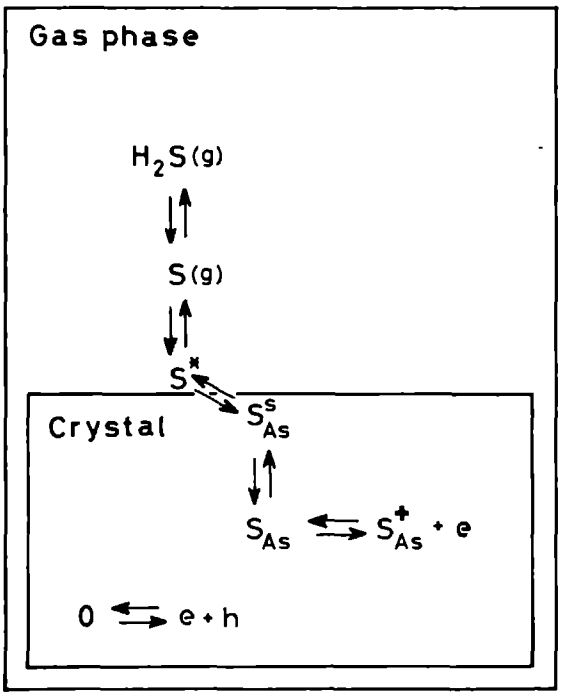

Fig.5 Equilibria for the dopant system in gas phase and in the solid for zero growth rate.

3.1. Complete equilibrium in the S-subsystem

It is important to notice that the incorporation of dopants in this case is determined by the partial pressure of the monatomic dopant species in the gas phase [12,13]. Therefore, for the case of complete equilibrium in the sulfur system, one can write down the following equations for the dopant atom S which is generated from the H_2S input gas in the following way:

(1) $H_2S(g) \rightleftarrows S(g) + H_2(g)$ with $K_1 = \dfrac{P_S\, P_{H_2}}{P_{H_2S}}$

(2) $S(g) + * \rightleftarrows S^*$ $K_2 = K_{ads} = \dfrac{[S^*]}{P_S\,[*]}$

(3) $S^* + V_{As}^S \rightleftarrows S_{As}^S + *$ $K_3 = K_{inc} = \dfrac{[S_{As}^S]\,[*]}{[S^*]\,[V_{As}^S]}$

(4) $S_{As}^S + V_{As} \rightleftarrows S_{As} + V_{As}^S$ $K_4 = K_{diff} = \dfrac{[S_{As}]\,[V_{As}^S]}{[S_{As}^S]\,[V_{As}]}$

(5) $S_{As} \rightleftarrows S_{As}^+ + e^-$ $K_5 = K_{ion} = \dfrac{[S_{As}^+]\,n}{[S_{As}]}$

Here * is a free surface, step or kink site, S^* is an adsorbed S atom, S_{As}^S an S atom at an arsenic site in the surface; V_{As}^S and V_{As} are arsenic vacancies in the surface and in the crystal, respectively.
The total amount of sulfur incorporated in the GaAs crystal is given by:

(6) $[S_{inc}] = [S_{As}] + [S_{As}^+]$

A few remarks have to be made on the above given scheme. First, one can imagine that the surface can act catalytically on the H_2S decomposition.

$$H_2S^* \rightleftarrows S^* + H_2$$

This of course may happen, but it is only of interest whenever kinetics play a role. If equilibrium is established - as is assumed in this section - the above mentioned process is irrelevant, it will only enhance the equilibration.

A second remark has to be made about the adsorption and incorporation process. In principle all sulfur species which are present in the gas phase can adsorb (chemically or physically) on the crystal surface, but in equilibrium only monatomic sulfur will be incorporated effectively. The others are too large to be accomodated within the lattice and will be segregated into the gas phase because of this instability. It must be reminded that because of a high adsorption energy, monatomic S will be enriched on the surface as compared with the gas phase. In this way an appreciable concentration of S* can be present at the surface.

A third remark concerns the incorporation process itself. This can take place at the step, but also directly at the surface when an adsorbed S atom tumbles into a surface vacancy. In both cases there is equilibrium between the gas phase and the bulk of the crystal. The reaction given in eq. (3) is valid for both situations, only the character of the vacancy will change.

A last assumption is that sulfur incorporated in the surface, S^{s}_{As}, which is electronegative with respect to Ga and As, will not ionize. The physical argumentation for this assumption is that S-atoms in the surface layer - which have only two or three gallium neighbours - are not subject to the same potential field as the tetrahedrally bonded S-atoms inside the bulk. So there is no reason at all for them to follow the same ionization behaviour. In the language of energy bands it can be said that the S-atoms in the surface layer are filling the empty surface states which are positioned below the Fermi level.

The reaction scheme (1)-(5) as given above, now can be worked out for further analyses. First consider the ionization process in the solid. Important is whether the electron concentration n is determined by an intrinsic process as for instance:

(7) $\qquad 0 \rightleftarrows e^- + h^+ \qquad\qquad$ with $K_1 = n_1 p_1 = n_i^2$

or by the extrinsic process (eq. (5)):

$$S_{As} \rightleftarrows S_{As}^{+} + e^{-} \qquad \text{with} \quad K_{ion} = \frac{[S_{As}^{+}]\, n}{[S_{As}]}$$

The generation of intrinsic charge carriers of course is not limited to a process as given by eq. (7). Significant contributions can come from the ionization of intrinsic point defects, such as arsenic vacancies or interstitials. The number of carriers may even be determined by background doping arising from e.g. C_{As} or Si_{Ga}. The point is that at given growth conditions the electron concentration is fixed and independent of the addition of sulfur. As long as the electron concentration caused by these defects is smaller than the value of K_{ion} the following discussion is valid.

Table 2
Values for K_{ion}, n_i, N_c, N_v and Eg for three temperatures.

T(K)	K_{ion}	n_i	N_c	N_v	Eg(eV)
77	1.15×10^{16}	- 0	5.7×10^{16}	1.2×10^{18}	1.51
300	1.66×10^{17}	2.2×10^{6}	4.2×10^{17}	9.5×10^{18}	1.42
1000	2.70×10^{18}	3.6×10^{16}	5.8×10^{18}	5.8×10^{19}	1.07

The value of K_{ion} determines how much S is ionized during the growth conditions. In table 2 for three temperatures values are given for the ionization constant K_{ion}, the intrinsic electron concentration n_i, the density of states of the conduction and valence band N_c and N_v and the bandgap Eg of GaAs. The intrinsic electron concentration was calculated using $n_i = \sqrt{N_c N_v}\, \exp(-Eg/2kT)$. The ionization constant was calculated according to $K_{ion} = \frac{1}{2} N_c \exp(-E_D/kT)$ with E_D = 6 meV for S in GaAs. This relation may only be used if classical or non-Fermi-Dirac statistics is valid, which is reasonably true up to $n = 2.7\times10^{18}$ cm^{-3}, because at this value the Fermi level still is 66 meV below the conduction band, at the growth temperature, as can be calculated. For higher electron concentrations the ionization constant K_{ion} becomes a function of n and must be calculated using the correct Fermi statistics. The n_i, N_c and Eg values are from [14,15], taking into account the contributions of higher lying conduction bands.

For dopant incorporation the following three regions can be distinguished:

1. the intrinsic region with $n = n_i$,
2. the extrinsic region when $n_i < n < K_{ion}$,
3. the extrinsic region with $n > K_{ion}$.

The concentration of sulfur which is built in the lattice now will be calculated for these three regimes.

3.1.1. Intrinsic region: $n = n_i$

In this case $[S^+_{As}] < n_i$ and the ionization of sulfur (eq. (5)) can be written as:

$$[S^+_{As}] = K_{ion} \frac{[S_{As}]}{n_i} \tag{8}$$

The essence is that n_i is constant and not dependent on the dopant concentration. From table 2 it follows that $(K_{ion}/n_i) \simeq 75$, so nearly all sulfur is ionized: $[S^+_{As}] = [S_{inc}]$. Using eqs. (1)-(4), $[S_{As}]$ can be substituted by $[S^s_{As}]$, $[S^*]$, P_S and P_{H_2S}, finally ending with:

$$[S_{inc}] = \frac{K_{ion}}{n_i} K_{diff} K_{inc} K_{ads} K_1 \frac{[V_{As}]}{P_{H_2}} P^{\circ}_{H_2S} \tag{9}$$

where in addition P_{H_2S} is replaced by $P^{\circ}_{H_2S}$, as H_2S dominates the gas phase (table 1). As $[V_{As}]$ is determined by the Schottky equilibrium, which is constant at given T and P_{As}, and as $P_{H_2} = 1$ bar, we can conclude that in the intrinsic region a linear relation exists between the dopant concentration in the crystal $[S_{inc}]$ and the input pressure of H_2S for constant growth conditions.

3.1.2. Extrinsic region: $n_i < n < K_{ion}$

In this part of the extrinsic region the dopant concentration is so high that $n \gg n_i$, so almost all electrons are donated by S and consequently:

$$[S^+_{As}] = n \tag{10}$$

Eq. (5) for this case becomes:

$$(11) \qquad [S^+_{As}] = \{K_{ion}\,[S_{As}]\}^{1/2}$$

In this part of the extrinsic region, still all incorporated sulfur is ionized, so after substitution of $[S_{As}]$ in eqs. (1)-(4), we arrive at:

$$(12) \qquad [S_{inc}] = \left\{(K_{ion}\,K_{diff}\,K_{inc}\,K_{ads}\,K_1)\,\frac{[V_{As}]}{P_{H_2}}\,P^{\circ}_{H_2S}\right\}^{1/2}$$

which gives rise to a slope ½ in the log-log plot of $[S_{inc}]$ versus $P^{\circ}_{H_2S}$.

3.1.3. Extrinsic region: with $n > K_{ion}$ and $n = [S^+_{As}]$

From $\quad S_{As} \rightleftarrows S^+_{As} + e^-$ and $\quad K_{ion} = \dfrac{[S^+_{As}]^2}{[S_{As}]}$

follows that the neutral S_{As} must dominate when n i.e. $[S^+_{As}]$ becomes larger than K_{ion}. In that case $[S_{inc}] = [S_{As}]$, which will ultimately result in a slope 1 in the plot of $[S_{inc}]$ versus $P^{\circ}_{H_2S}$.

Finally at a certain value of $[S_{inc}]$ the solid will be saturated by S_{As} and the curve will level off. It must be noted that this atomic saturation level experimentally is higher than the level where electrical saturation at room temperature (or 77K) occurs [9].

The total equilibrium behaviour, as deduced for these three regions, is combined in fig. 6. The measurements of the electron concentration, as presented by Gentner and Veuhoff et al., have a one to one correlation with $[S_{inc}]$, as all sulfur will ionize at the low temperatures, which were used for the determination of n, and also because n is above the intrinsic concentration. Therefore the total equilibrium curve for the three regions as depicted in fig. 6, can be compared directly with the experimental curves, given in figs. 3 and 4.

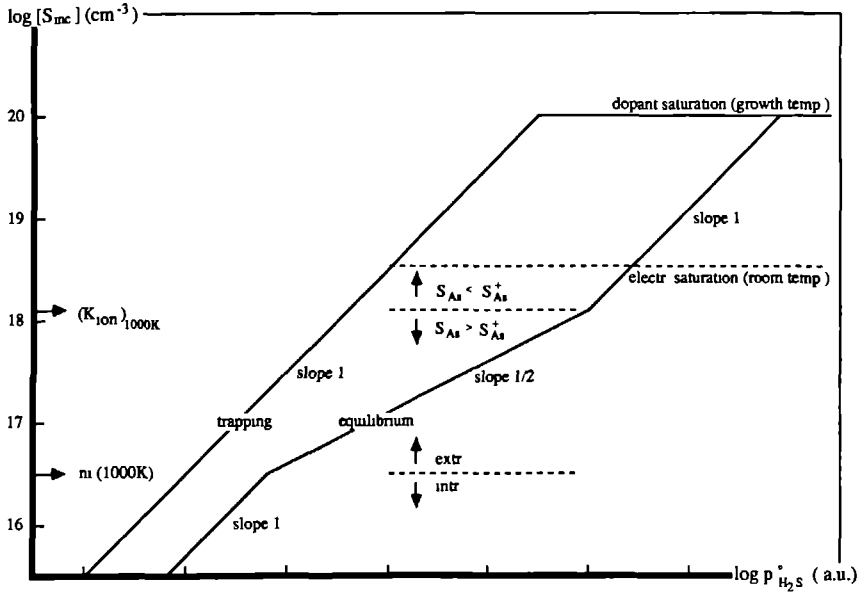

Fig.6 Theoretically predicted curves for the incorporation of dopants in GaAs for low and high growth rate conditions (equilibrium curve and trapping curve respectively). The position of the trapping curve is orientation dependent. The saturation level at $n = 10^{20}$ has arbitrarily been chosen.

3.2. Trapping of the dopant atoms during growth

The predicted equilibrium behaviour with the characteristic slope ½, for $n_i < [S_{inc}] < K_{ion}$, in general is not observed in the experiments of Gentner and Veuhoff (figs. 3 and 4).

A possible influence of chemistry in the gasphase, for instance a predominant occurence of S_2 or S_4, cannot explain why the observed slope is 1 instead of ½, because such a dimer formation only would weaken the slope into 1/4 (for S_2) or even 1/8 (for S_4), (see also [12] in this respect). Other models which explain the linear behaviour by surface band bending or the ionization of intrinsic defects are also not completely satisfactory. These models will be given more attention in the discussion section.

So another explanation has to be looked for, which to our opinion can be found by considering the kinetics of the process. This means that in the scheme as given in fig. 5 a rate limiting step must be present. The equilibria in the gas phase and the ionization equilibrium in the solid are not thought to be slower than the growth rate, they normally have reaction rates which far exceed the rate of growth. An argument to support this view is that the incorporation of dopant is not inversely proportional to the growth rate as it should be if one of the gas phase reactions leading to monatomic S, or the supply of sulfur via the gas phase, were rate determining. However a very likely candidate is the exchange of dopant atoms between surface and subsurface layers in the crystal, which process is determined by the rate of diffusion in the solid. This equilibrium is given by eq. (4):

$$S^{s}_{As} + V_{As} \rightleftarrows S_{As} + V^{s}_{As}$$

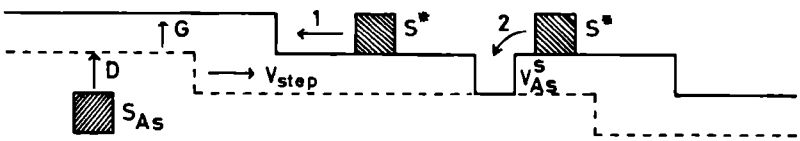

Fig.7 Incorporation of adsorbed sulfur atoms, S^{*}, via a step (1) or directly (2) in an arsenic surface vacancy, V^{s}_{As}, versus the outdiffusion of sulfur from the subsurface, S_{As}, to the surface.

When the growth rate is larger than this diffusion rate, incorporated dopant atoms cannot diffuse out of the grown layers to the surface and this particular part of the total equilibrium breaks down. This has been depicted in fig. 7 where, incorporation via the step (1) and surface (2) is sketched. Normally, in equilibrium, in the first subsurface layers a higher concentration of dopant atoms is present than in the bulk of the crystal, due to the difference in the standard chemical potential; see fig. 8. As the crystal is growing, a given layer is effectively propagating towards the bulk, with an accompanying decrease of the equilibrium dopant concentration. So to obtain equilibrium incorporation a transport of dopant out of the just grown

layers to the crystal surface must occur [4]. When the growth rate G is larger than the velocity as determined by diffusion of the incorporated sulfur atoms in the subsurface, the dopant cannot be segregated anymore at the crystal surface and will be effectively trapped. So subsurface trapping is related with the growth rate measured normal to the surface. This in contrast to the phenomenon of step trapping where the lateral velocity of the steps determines the trapping. It must also be remarked here that the diffusivity in the first few atomic layers can be higher than in the bulk, especially because of a difference in vacancy concentrations.

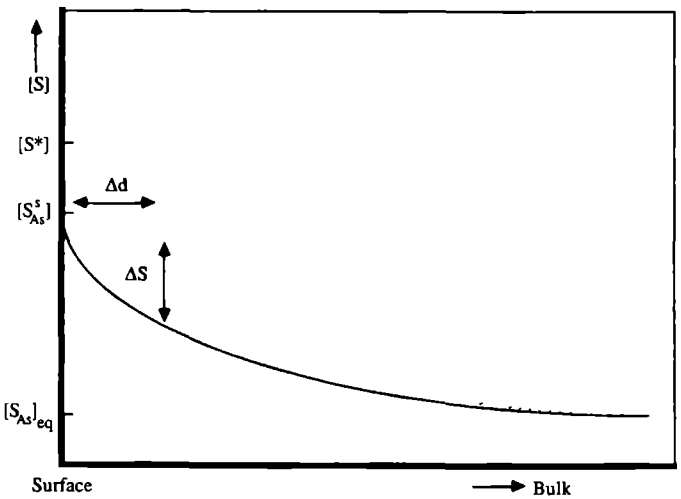

Fig.8 Equilibrium sulfur concentration as a function of the distance from the surface. The dashed line refers to the situation after growth of an additional layer of thickness Δd. The excess concentration of sulfur, ΔS, which tends to be built in has to diffuse out of the subsurface. The maximum excess concentration in case of subsurface trapping is $[S^S_{As}] - [S_{As}]_{eq}$. This occurs for $G > \frac{D}{x}$ ($x \approx 4Å$). In the case of step trapping an excess of $[S^*] - [S_{As}]_{eq}$ can be built in.

It is important to notice that the phenomenon of subsurface trapping applies for the incorporation of dopant directly via the surface or via the steps. Equilibrium may even be present up to and including these incorporation processes (eq. (3)), the rate limiting step is introduced after this process (eq. (4)). For step trapping to occur the growth

rate and also the lateral velocity of the steps has become so high that the adsorption - desorption equilibrium at the step breaks down (eq. (2+3)). In this process up to the whole surface concentration of S^* can be built in. Thus the subsequent transport of dopants back to the surface must be substantial. However step trapping can only be observed in the final result if the diffusion in the subsurface also is slow compared to the normal growth rate, so that the segregation of the excess incorporated dopants is hindered. Finally it must be noted that subsurface trapping can be observed for crystallographic rough growth as well as for growth via steps, in the latter case the lateral velocity of the steps is indifferent up to the limit where step trapping occurs.

In case of subsurface trapping the total dopant concentration in the solid consequently is determined by the concentration of trapped dopant atoms, which, using eqs. (1)-(3), is given by:

$$(13) \qquad [S_{inc}] = [S^s_{As}] = K_{inc}\, K_{ads}\, K_1\, \frac{[V^s_{As}]}{P_{H_2}}\, P^{\circ}_{H_2S}$$

It should be noticed that K_{inc} as well as K_{ads} are dependent on orientation, K_{inc} is also a function of the amount of adsorbed S incorporated via the steps and surface. It is assumed that V^s_{As} is independent of the sulfur input and constant, since the Schottky equilibrium at the surface is determined by P_{As} and P_{Ga}. In this way a linear relation is obtained between $[S_{inc}]$ and the input pressure of H_2S for all regions of the electron concentration.

In fig. 6 both theoretically predicted curves, the s-shaped equilibrium form and the kinetic trapping curve, are depicted. Indicated are the intrinsic and the extrinsic regions and the region where neutral S dominates. Both curves level off at a saturation value. The statement is that always a slope 1 will be observed if the growth rate is larger than the diffusion rate of the dopant atoms in the bulk.

This can be quantified as follows. The basic and fastest step in the transport of incorporated dopant atoms is its jump to a neighbouring arsenic site. If this step takes, on the average, more time than growing a new layer, a sulfur atom will recede more and more into the bulk. The time to make a jump to a neighbouring arsenic site is given

by $t = x^2/D$, with $x = 4$ A. In this time the growing interface, with growth rate G, must propagate more than 4 A to trap the dopant, leading to:

$$(14) \qquad G > \frac{D}{x}$$

A similar expression has been derived by Webb for point defect trapping [4] and by Chernov [5,6]

This statement can be applied to the diffusion of S in GaAs. According to Goldstein, Frieser and Young and Pearson the diffusion coefficient of S at 750°C is 1×10^{-14} cm^2/sec [16-18]. This results in trapping of sulfur if:

$$G > \frac{10^{-14}}{4 \times 10^{-8}} \text{ cm/sec} = 0.15 \text{ µm/min} = 9 \text{ µm/h}$$

By comparing the experimental results (figs. 3,4) with this trapping condition a striking correspondence is observed. A slope 1 is observed for all experiments where the growth rate is 10 µm/h or larger; all the experiments of Gentner and (100) and (111)B of Veuhoff. For a growth rate of 5 µm/h, as used for the (111)A orientation of Veuhoff, a slope ½ is found which at higher concentrations, for $[S_{inc}] > K_{ion}(1000\ K)$, changes in a slope 1, just as predicted for low growth rates.

4. Orientational dependence of the incorporation

Under trapping conditions the (111)A and (111)B surfaces build in equal amounts of S, whereas (110) and (100) incorporate significantly less amount of sulfur (figs. 1,4), although all are in contact with the same gas atmosphere. The explanation for this phenomenon primarily is based on the presence of equilibrium in the gasphase including adsorption, especially for the arsenic and sulfur subsystem. This assumption is justified by the well-known fact that in the chloride system the desorption of chlorine via reaction with hydrogen at the steps is rate limiting [19]. Consequently all other preceding processes are faster, can achieve equilibrium and the growth rate is orientation dependent (fig. 2).

In this gaseous equilibrium situation each crystal orientation is exposed to the same vapour composition, with respect to P_{Ga}, P_{As} and P_S. Both As and S have to compete for the same free surface site which is an arsenic site. As the end situation for each incorporated S-atom is the same, viz. four bonds with the GaAs lattice, and as also the begin situation is identical (gas phase composition), the only orientational dependence can be introduced during the adsorption at the surface or subsequent incorporation. In this respect it can be envisaged that surface relaxation and reconstruction, which are orientation dependent, energetically will have different effects on the incorporation of arsenic and sulfur.

Both incorporation processes are given by:

$$As(g) + V^S_{As} \rightleftarrows As^S_{As} \qquad K_{tot}(As) = K_{ads}\, K_{inc}(As)$$
$$S(g) + V^S_{As} \rightleftarrows S^S_{As} \qquad K_{tot}(S) = K_{ads}\, K_{inc}(S)$$

where the incorporation includes adsorption at a surface site followed by reaction with a surface vacancy of arsenic. The final incorporation step into the lattice, i.e. covering of these subsurface positions with one atomic layer, is determined by the growth process itself. As the dopant is trapped, all the sulfur present in the subsurface will be buried and built in into the lattice.

Comparing the sulfur uptake of (111)Ga and (111)As, it is not to be expected a priori that the adsorption sites and surface vacancies are equal for (111)Ga and (111)As. In this respect, it must be noticed that for growth in the chloride system, predictions about the surface structure of (111)Ga are complicated by the fact that either the surface is covered by chlorine, or is arsenic enriched, due to the greater stability of arsenic stabilized structures. So a detailed atomistic picture is difficult to give here.

The fact that equal amounts of S are incorporated for the (111)Ga and (111)As face, however points to the fact that the ratios of the total equilibrium constants for the incorporation of S and As are equal for both faces:

$$(15) \qquad \left[\frac{K_{tot}(S)}{K_{tot}(As)}\right]_{(111)Ga} = \left[\frac{K_{tot}(S)}{K_{tot}(As)}\right]_{(111)As}$$

which means that energetically the total bonding situation for the incorporation of S and As, at least for their ratio, must have been the same for both (111)As and (111)Ga, which is in accordance with the absence of surface relaxation for these orientations.

On a (100) surface quite a special bonding situation exists. Here the dangling bonds of the arsenic atoms will form a dimer bond, i.e. the well-known (2x4)As reconstruction. If an arsenic atom is incorporated within a surface vacancy it is able to form a dimer bond with one of the adjacent arsenic surface atoms. This results in an additional energy gain of ca 30 kcal/mol dimer [20]. Sulfur atoms however have an extra electron and cannot form such a favourable bond when incorporated. So arsenic may be preferentially incorporated in a surface vacancy, explaining why here less sulfur is built in as compared with the (111) surfaces, despite the same P_{As}/P_S in the gas phase. In other words the adsorption energy for S has to be diminished with the energy for surface reconstruction, diminishing the sulfur concentration, as the dimers are broken upon adsorption.

On the (110) surface the surface vacancies resemble those in (111), because also here three bonds are dangling. An important difference with (111) however, is the very stable relaxation of the (110) surface which gives a stabilization of 12 kcal/mol [21]. Analogous to (100) the incorporation of sulfur reduces the energy gain of the relaxation. However for (110) no new bond is formed, the surface atoms are only subjected to a Jahn-Teller distortion, which causes them to relax to a more stable position with an accompanying charge separation. Sulfur has already an extra electron, so the latter effect will be hindered. Therefore it can be expected that arsenic is favoured compared to sulfur, but less pronounced than on (100).

This discussion stresses the importance of surface relaxation and surface reconstruction for the incorporation process. Here the difference in chemical nature between lattice atoms (As) and dopant atoms (S) will come out. Whenever a surface is stabilized by the

lattice atom, its incorporation is favoured over the dopant atom. The observed tendency for GaAs is at least qualitatively in accordance with this concept:

sulfur incorporation	$[S]_{(111)A} = [S]_{(111)B} > [S]_{(110)} > [S]_{(100)}$
surface stabilization	$(111)A \simeq (111)B < (110) < (100)$
	~0 kcal/mol < 12 kcal/mol < 30 kcal/mol dimer

5. Generalization

The principle of equilibrium and trapping can be applied more generally to other dopants and materials and to other growth methods.

Most convincing for the above given model are the experiments performed by Nelson and Westbrook on Zn and Cd doped InP [22]. They indeed observed the predicted slopes ½ and 1 and could explain them by correlating the growth rates with the simultaneously measured diffusion coefficients, by means of SIMS profiling, using the condition $D < Gx$.

Jacobs [23] observed a slope 1 for the incorporation of Te in GaP during CVD. Also here the growth rate is high (18 µm/h) and much larger than the diffusion rate of Te in GaP at 850°C, the temperature where the growth was performed. So also here the adsorbed dopant atoms are trapped during the growth giving a slope 1 in the log-log plot of $[Te_{inc}]$ versus dopant input.

Wood and Joyce [24] doped GaAs with Sn during MBE growth experiments and obtained a slope 1 at T = 720 to 820 K for growth rates between 0.3 to 1.5 µm/h, which indeed is much larger than can be calculated for a complete equilibrium in the dopant system. Trapping typically can be expected for all MBE growth experiments due to the lower growth temperatures.

Also in LPE growth experiments frequently a slope 1 is observed. Casey et al. [25] for instance published results on the LPE growth of GaAs doped with Te. Growth rates typically are 1 µm/h or larger, and this explains why for the incorporation process a slope 1 is observed as the equilibrium between bulk and surface atoms of Te is broken when

G > 0.9 μm/h at the growth temperature of 1000 K [26].

The only other example known to the authors which represents an equilibrium incorporation process for dopant atoms is the incorporation of Zn in GaP by Trumbore et al. [27]. Here the growth process took 5 weeks which indeed might easily explain why equilibrium was achieved.

It is evident that even the growth itself can be subject to trapping phenomena, as shown by Webb [4]. Only very low growth rates can avoid that the intrinsic defects V_{Ga}, V_{As}, Ga_i, As_i, Ga_{As} and As_{Ga} are trapped during the growth of GaAs. From the diffusion data of Chiang and Pearson [28] it can be calculated that at 1000 K V_{As} is trapped if G > 0.05 μm/h and if G > 3.5 μm/h at 1100K. On the other hand from the same data it is clear that V_{Ga} is rather mobile, it will only be trapped at 1000 K for G > 50 μm/h. This in contrast to the antisite defects which are almost immobile [15,29] and will be trapped under nearly all growth conditions.

When GaAs is grown by MOCVD under a high partial pressure of arsenic, the surface layer will be rich in As which, at the typical growth temperature of 1000 K, will easily diffuse into the lattice creating a supersaturation of As_i. Bublik et al. [30] have shown that the creation of point defects on the arsenic sublattice is much more likely than on the gallium sublattice. When the crystal is cooled this amount may be trapped and induce intrinsic microprecipitates of As_i. For such a high surface concentration of As also the probability of the antisite defect As_{Ga} is rather large. This defect will be trapped and may give rise to electrical compensation effects. However the surface will remain smooth during these circumstances. For low P_{As} conditions the surface becomes rich in Ga. This gives a gallium rich surface layer which, by the gallium equilibrium, will ultimately result in gallium droplets. This leads to a rough surface for growth at 1000 K [31]. The trapped V_{As} or Ga_i are rather immobile and will affect the Schottky equilibrium in the bulk. Nevertheless it is to be expected that a smooth surface can be obtained under low P_{As}, when the growth temperature is raised to 1100 K or higher, because then both V_{Ga} and V_{As} can come into equilibrium.

6. Discussion

The evidence presented in this paper, especially the data of Nelson and Westbrook, strongly points to subsurface trapping as a likely phenomenon during the growth of III/V compounds. This should be compared to the band bending model as discussed by Zschauer and Vogel [32] and used by Casey et al. [25]. In this model the concentration of electrons at the surface is constant and independent of the concentration of dopant in the bulk. It will be clear that this model indeed can explain the linear dopant behaviour because of the high value of n_i, independent of the amount of incorporated sulfur. However the model has difficulties in explaining the experimentally observed equilibrium incorporation process where $n = [S^+]$, leading to a slope ½. Merten and Hatcher [33] tried to explain why at very high dopant concentrations the observed linear behaviour weakened to a slope < 1 and extended the band bending model of Zschauer and Vogel. For this they assumed that the diffusion of dopant through the space charge layer to the surface was a limiting factor. In their paper they already point out the inportance of the rate of diffusion with respect to the growth rate. Hurle [34] assumes that at the growth temperature a high concentration of electrons is present which are donated by an equally high concentration of ionized arsenic vacancies. Such a high and constant electron concentration indeed could explain a slope 1 for the incorporation of other dopants, but not that such an incorporation is orientation dependent as observed. It also fails to explain the observed slope ½ at low growth rates and, equally important, that a slope 1 also is observed under arsenic rich growth conditions where the concentration of arsenic vacancies is bound to be very low.

The high concentration of V_{As} as assumed by Hurle is based on a high value for the dimensionless entropy factor (viz. 442) in his expression of the ionization constant, which value has been obtained by curve fitting. However the physical meaning of such a high value is questionable in view of the value 6×10^{-5} which should apply in this case, as can be calculated from the statical equation for the ionization constant which is given by $K_{ion} = \frac{1}{2}N_c \exp(-E_D/kT)$.

In view of these arguments we do not support Hurle's model, but rather believe that trapping can explain the incorporation process.

A problem still to be discussed is the incorporation of neutral S_{As} at high temperatures which at room temperature are not electrical active. Neutron activation analysis clearly has shown that S has been built into the lattice up to high concentrations $\sim 10^{20}$ cm^{-3} with a slope 1 [9]. This is still consistent with both equilibrium and trapping models. A straightforward explanation however has to be given for the observed saturation at room temperature of the electrical activity when the sample has been cooled down to room temperature. It can be expected that for the measurements at low temperatures, the dopant level will have disappeared into the conduction band, which will happen for dopant concentrations above and around 10^{17}, so all incorporated S atoms should have provided one electron to the conduction band. The reason that this is not observed for $[S] > 3 \times 10^{18}$, may be due to sulfur precipitation at these high values of $[S_{inc}]$ which make them electrically inactive. Another explanation may be that the sulfur donors are completely compensated by arsenic interstitials which can act as acceptors. The As_i can be produced by the incorporation process itself as given by the following overall reaction:

$$S(g) \rightleftarrows S_{As} + As_i$$

Above a certain concentration of sulfur the As_i concentration will be dominated by this effect and donor-acceptor pairs are created, giving complete compensation, whenever As_i has a deep level. In S-rich material for $n > 2 \times 10^{18}$ cm^{-3} indeed microprecipitates are observed, which by TEM analysis appear to consist of faulted interstitial arsenic loops [35]. This may also explain the observed electrical saturation.

The often observed slopes higher than one, basically can be explained by step trapping of dimers or polymers of dopants. Subsequent subsurface trapping prevent the unstable dopant species to be segregated at the crystal surface. This situation can only occur when these dopant molecules dominate as adsorbates and dissociate inside the lattice.

7. Conclusions

The above given analysis has shown that a consistently followed chemical approach can be useful when the correct physical data are applied. Using this framework all the reported doping phenomena can be explained in a logical way without the need for any assumptions. The essential feature of the model is that in III-V compounds diffusion coefficients are low with the consequence that the exchange between atoms at the surface with those in the subsurface layers easily can be broken down when the crystal is grown too fast.

This phenomenon of trapping can be avoided by using very small growth rates. This certainly is possible for growth by CVD, but more difficult for growth by MBE (due to the low growth temperatures) and also for LPE because here the growth rates are rather large at relatively low temperatures.

The consequences of trapping intrinsic defects in large amounts are not fully explored as yet. It may well be that better quality epitaxial layers can be grown by avoiding this trapping effect.

Acknowledgements

The investigations have been carried out under the auspices of the Netherlands Foundation for Chemical Research (SON) with financial support from the Netherlands Organization for the Advancement of Pure Research (ZWO). I would like to thank Professor L.J. Giling for the fruitful discussions and permitting me to use this study for my thesis.

REFERENCES

[1] J. Bloem and L.J. Giling, in: Current Topics in Materials Science vol I, ch. 4, Ed. E. Kaldis, (North-Holland, Amsterdam 1978)

[2] J. Korec, D. Grundmann and M. Heyen, J. Electrochem. Soc. 131 (1984) 1433

[3] J. Korec and M. Heyen, J. Crystal Growth 60 (1982) 297

[4] W.W. Webb, J. Appl. Phys. 33 (1962) 1961

[5] A.A. Chernov, "Growth of Crystals", vol 3, p. 35, Ed. A.V. Schubnikov and N.N. Sheftal', Consultants bureau New York (1962)

[6] A.A. Chernov, Modern Crystallography, III. Crystal Growth Springer Series in Solid State Sciences, vol. 36 (1984) p. 159

[7] L.J. Giling and H.H.C. de Moor, Proc. EuroCVD IV (1983), p. 184,
Ed. J. Bloem, G. Verspui and L.R. Wolff (Eindhoven, The Netherlands)
[8] J.L. Gentner, Thesis, Université de Clermont II (1981) and
J. de Physique 43 (1982) C5-267
[9] E. Veuhoff, M. Maier, K.-H. Bachem and P. Balk, J. Crystal Growth 53 (1981) 598
[10] M. Heyen, H. Bruch, K.-H. Bachem and P. Balk, J. Crystal Growth 42 (1977) 127
[11] K.C. Mills, Thermodynamic data for inorganic sulphides, selenides and
tellurides, (Butterworths, London, 1974)
[12] J. Bloem, L.J. Giling and M.W.M. Graef, J. Electrochem. Soc. 121 (1974) 1354
[13] H.T.J.M. Hintzen, J. Bloem and L.J. Giling, J. Electrochem. Soc. 131 (1984) 1900
[14] J.S. Blakemore, J. Appl. Phys. 53 (1982) 520
[15] M. Neuberger, Handbook of electronic materials vol 2
"III-V Semiconducting compounds" (JFJ/Plenum, New York, 1971)
[16] B. Goldstein, Phys. Rev. 121 (1961) 1305
[17] R.G. Frieser, J. Electrochem. Soc. 112 (1965) 697
[18] A.B.Y. Young and G.L. Pearson, J. Phys. Chem. Solids 31 (1970) 517
[19] R. Cadoret in: Current Topics in Materials Science Vol. 5, ch. 2
Ed. E. Kaldis, (North-Holland, Amsterdam, 1980)
[20] D.J. Chadi, C. Tanner and J. Ihm, Surface Sci. Lett. 120 (1982) L425
[21] R. Chang and W.A. Goddard III, Surface Sci. 144 (1984) 311
[22] A.W. Nelson and L.D. Westbrook, J. Crystal Growth 68 (1984) 102
[23] K. Jacobs, J. Crystal Growth 56 (1982) 362
[24] C.E.C. Wood and B.A. Joyce, J. Appl. Phys. 49 (1978) 4854
[25] H.C. Casey Jr., M.B. Panish and K.B. Wolfstirn,
J. Phys. Chem. Solids 32 (1971) 571
[26] R. Sankaran, J. Crystal Growth 50 (1980) 859
[27] F.A. Trumbore, H.G. White, M. Kowalchik, R.A. Logan and C.L. Luke,
J. Electrochem. Soc. 112 (1965) 782
[28] S.Y. Chiang and G.L. Pearson, J. Appl. Phys. 46 (1975) 2989
[29] D.L. Kendall in: Semiconductors and Semimetals vol 4 p. 198,
Eds. R.K. Willardson and A.C. Beer, (Academic Press, New York, 1968)
[30] V.T. Bublik, M.G. Mil'vidskii and V.B. Osvenski, Sov. Phys. J. 23 (1980) 1
[31] J. van de Ven, J.L. Weyher, H. Ikink and L.J. Giling,
J. Electrochem. Soc. to be published
[32] K.H. Zschauer and A. Vogel. Proc. 3rd Int. Symp. GaAs,
Inst. Phys Conf. Ser. (1971) p. 100
[33] U. Merten and A.P. Hatcher, J. Phys Chem. Solids 23 (1962) 533
[34] D.T.J. Hurle, J. Phys. Chem. Solids 40 (1979) 613
[35] G. Pennock and J.L. Weyher, private communication.

CHAPTER 7

STABILITY AND REACTIVITY OF GaAs

Abstract

To gain knowledge on the surface processes occurring during high temperature treatment of GaAs, its surface structure, the gas phase composition of GaAs in contact with N_2, H_2, H_2O and HCl, and the phase diagram of GaAs, with special emphasis on stoichiometry, is studied. Analysis of the structure of a (100) surface learns that the As-As dimerization is very stable, so that (100) is an F-face with growth and etching via steps. The gallium reconstruction is not stable, as the electron density is much lower. The stability of the steps on (111)Ga and (111)As differs considerably. As on (111)As, gallium determines the reactivity of the steps, the absence of Ga-Ga dimerization, makes them unstable; in contrast with the steps on (111)Ga, which are very stable. An equation is derived for the influence of the gas phase composition on the stoichiometry of GaAs. Based on V_{As} and As_i this states that the existence region is extended more to the As-rich side. Comparison with experimental data points to the fact that often kinetics will determine the stoichiometry. A P-T plot of the phase diagram learns that arsenic is eager to evaporate due to the stability of As_2. A study of the gas phase composition of GaAs shows that gallium hydrides can be of some importance in etching. Introduction of HCl or H_2O in the gas phase results in a preferential removal of gallium in the form of GaCl, GaOH and Ga_2O.

1. Introduction

Gallium arsenide is an interesting material to study, not only because it is increasingly important in opto-electronic applications, but also because of the fundamental aspects related with the binary character of the compound. It is known that small deviations from stoichiometry in the bulk of the material can have drastic effects on the electrical properties; off-stoichiometry in the surface layers rather influences the incorporation, or removal, of gallium and arsenic, or the building in of dopants.

A point which has had too little attention so far, is the relation between the stoichiometry of the crystal, during high-temperature processing, and the composition of the ambient gas phase. Two aspects should be considered in this respect: the reactivity of the gallium and the arsenic atoms towards species introduced in the gas phase, and the tendency of the crystal itself, to evaporate and build up an arsenic and gallium pressure. Because of this latter aspect, GaAs tends to become poor in arsenic at the high temperatures where gas phase etching or epitaxial growth is performed. This is a general feature of all III-V compounds and especially important, when crystals are heated to very high temperatures, or heated at low pressures [1-3]. Especially for InP this can cause deterioration of the surface quality of grown layers, but also for GaAs it is necessary to use an overpressure of the V compound in order to suppress the incongruent evaporation. It is not well understood to what extent this is really needed.

The reactivity of GaAs towards oxygen and chlorine is interesting to study in order to get a better understanding of the etching process with H_2O and HCl. These etchants are important in the transport of GaAs, as well as for in situ etching, used to clean the crystals prior to deposition [4]. In the latter systems it is important to have a detailed knowledge of the thermodynamics and kinetics of the etching process to obtain a good morphology and good electrical properties of the epilayer [5,6]. In this respect it is essential to maintain the stoichiometry in the surface layers and to avoid surface processes to become rate limiting, since then the etching becomes defect sensitive and orientation dependent.

This study intends to give a theoretical background for high-temperature gas phase etching and for the tendency of arsenic to evaporate in atmospheric CVD processes. Three aspects, which had up to now too little attention are discussed: the structure of the crystal surface at high temperatures, the gas phase composition in etching and evaporation, and the point defect equilibria in the solid.

2. Structure and properties of GaAs surfaces

2.1. Adsorption of H

Essential for a description of surface processes at high temperatures is, that the crystal surface can be considered to be bare. Etching and growth can proceed via diffusion of reactants to step and kink sites, where the chemical reaction can take place. The most notorious adsorbate in CVD systems is monatomic hydrogen. It is known to form strong chemical bonds with semiconductor surfaces and is usually present in rather high concentrations in the gas phase. Therefore the coverage of this species is discussed. For the Ga-As-H-O and Ga-As-H-Cl systems as discussed in section 3, the hydrogen coverage will dominate over the coverage with etchants. Their concentration on the crystal surface will be low, only at step and kink sites they can accumulate [7].

The H-coverage is calculated assuming Langmuir chemisorption following the model of Giling and de Moor [8]. As the bond strength of As-H closely resembles that of Ga-H, 65.2 respectively 64.4 kcal/mol (as can be derived from table 1), it is assumed that the coverage is equal for arsenic and gallium sites. In a first approximation the coverage of every crystallographic orientation can be set equal, as hydrogen forms only one bond on all surfaces. However it should be realized that, when relaxation or reconstruction is removed by the adsorption process, the coverage is reduced considerably [9]. Then the adsorption energy gain must be reduced with the reconstruction or relaxation energy. As polarization plays an important role on the surface of binary semiconductors, As being negatively and Ga positively charged, and Jahn-Teller distortions makes As more susceptible to adsorption, it could be that attachment to arsenic is favoured somewhat above reaction with gallium.

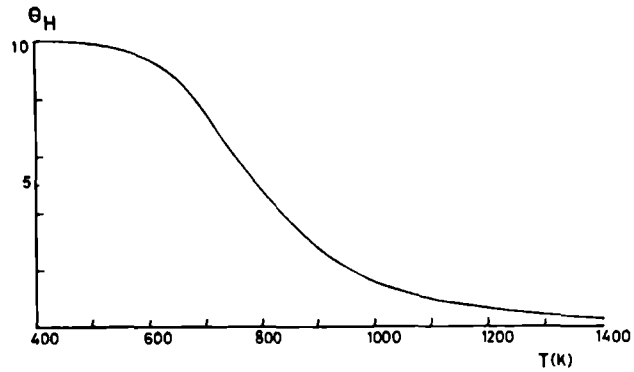

Fig. 1 Adsorption of H on an As- or Ga-site of a GaAs surface.
Gas phase 1 atm H_2 in equilibrium with H.
Bond strength H-As or H-Ga 65 kcal/mol, bond length 1.55 A.

In fig. 1 the hydrogen coverage is shown for a GaAs surface. It can be seen that at low temperatures the coverage with monatomic hydrogen is complete. At 600 K the coverage diminishes and becomes negligible above 1000 K, the temperature where monocrystalline growth and smooth etching can be observed. Comparing the H-coverage of GaAs with a Si(111) surface, which is extensively discussed [8], it can be seen that the curve is shifted ~300 K. It can be expected that surface diffusion is not hindered by adsorbed hydrogen above 900 K [12]. So the conclusion indeed is that, at high temperatures the surface is essentially bare, allowing monocrystalline step growth and smooth etching.

2.2. The structure of steps on {111} faces

The most important semiconductor surfaces are (111)A, (111)B, (100) and (110). For an understanding of the surface processes, the structure of each orientation is discussed. A special emphasis is laid on the consequences of the structure for step growth.

The binary character of GaAs is most prominent for the (111) face. The crystal surface is either terminated by gallium or by arsenic. The surface atoms have one protruding dangling orbital and three bonds inwards the crystal with As, respectively Ga; fig. 2A. As arsenic is

electronegative compared with gallium, this results in an electron deficient (111)Ga surface on one side and an electron rich (111)As surface on the opposite side of a crystal slice.

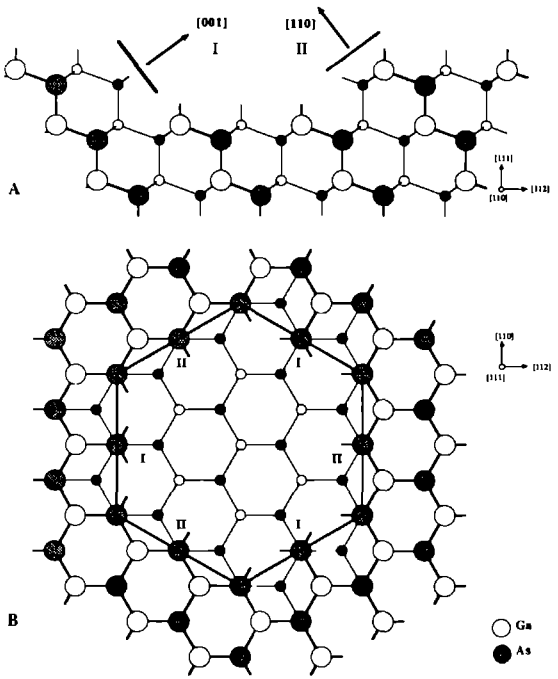

Fig. 2 A) Cross-section of a (111) surface.
A (111)Ga surface is shown on top, (111)As at the bottom.
At the left-hand side a $[\bar{1}\bar{1}2]$-step is depicted with a {100} character,
at the right-hand side a $[11\bar{2}]$-step with a {110} character, for (111)Ga.
B) Topview on a (111)Ga surface, showing the threefold symmetry
of the $\langle\bar{1}\bar{1}2\rangle$- (I) and $\langle11\bar{2}\rangle$-steps (II), making an angle of 60°.

In many experiments the polar character of the {111} faces is quite distinct. In room-temperature wet oxidation the (111)B face dissolves faster than (111)A, where primarily tetrahedrical etch pits develop at the outcrop of dislocations [10,11]; so towards chemical attack the Ga-face is more noble than the As-face. In thermal decomposition the evaporation rate is similar, but the morphology of the As- and Ga-faces is markedly different. On the latter surface triangular etch pits are

observed, the (111)B face is corroded in a noncrystallographic manner [3]. In analogy, for MOCVD growth, the morphology of (111)Ga is much better than of (111)As, for an identical gas phase input and growth rate. Under conditions where a (111)As surface shows irregular star-shaped defects, on (111)Ga tetrahedrical growth hillocks are present [12]. The orientational dependence of the growth rate in chlorine epitaxy learns that (111)Ga grows fastest and (111)As slowest, all other stable faces having a growth rate in between [13,14].

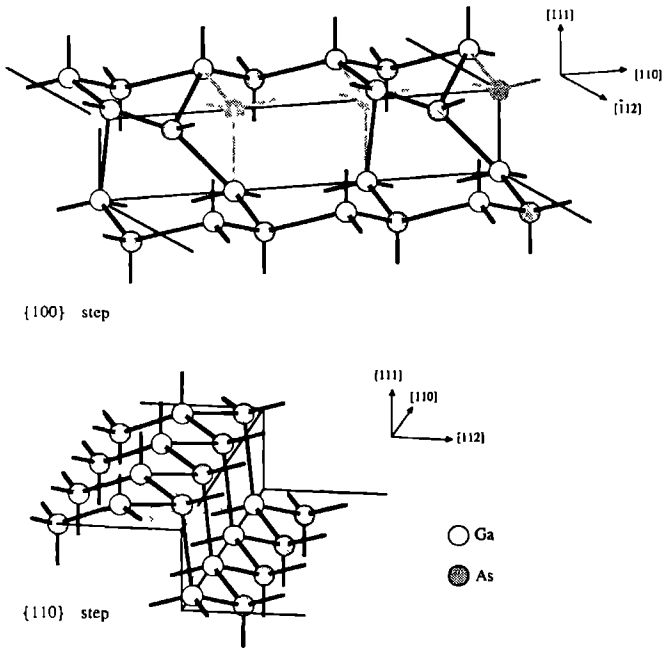

Fig. 3 Schematic view on the two types of steps present on (111)Ga.
For the {100}-type steps asymmetric dimerization is indicated, resulting in a negatively charged protruding As-atom and a withdrawn positive one.
The shaded atoms indicate the position of unreconstructed arsenic.
The {110}-type step shows step relaxation; arsenic is moved upwards and negatively charged, gallium has sunk into the surface and is positive.
The shaded atoms indicate the unrelaxed postions of the first two Ga and As.

In the latter two examples the importance of the structure of the steps on the growth process is acknowledged [12,15]. Though the affinity of the surface towards adsorption is important, the presence of steps is dominant in growth and etching, as {111} surfaces are F-faces for GaAs, a crystal with a zinc blende structure. In fig. 2A-B the two types of stable steps present on a (111)Ga surface are sketched. One type - $[\bar{1}\bar{1}2]$, $[\bar{1}2\bar{1}]$ and $[2\bar{1}\bar{1}]$ - indicated with I, has a {100} character; the other type (II) - $[11\bar{2}]$, $[1\bar{2}1]$ and $[\bar{2}11]$ - has the character of a {110} face [16]. In analogy with a {100} surface it is energetically favourable for the $[\bar{1}\bar{1}2]$ steps to reconstruct: the formation of dimer bonds; fig. 3 [17]. Only strong interactions with adsorbates are likely to prevent this dimerization. Because of this stabilization removal of the arsenic atoms is the rate limiting step in the etching via $[\bar{1}\bar{1}2]$-steps. The gallium atoms have also two bonds when their corresponding arsenic step atom is removed, but it is unlikely that they form a bond with the gallium atom in the lower lying layer. The triple-bonded gallium has little tendency to move upwards and the electron density of the bond, which could be formed, cannot be high because of the positive character of Ga.

The $[11\bar{2}]$-step has a {110} character, as it consists of <110> chains of Ga and As, so step reconstruction is impossible. Instead relaxation will occur; the gallium atoms move a little downwards, with respect to (110), and the arsenic upwards, with an accompanying transfer of electron density from Ga to As. Because of this Jahn-Teller distortion arsenic has become more susceptible to attack. The rate limiting step in the etching of a $[11\bar{2}]$ step is removal of either As or Ga, which costs three bonds. Then a kink site is formed and in two directions the step can be stripped by breaking two bonds. So when step reconstruction plays an important role, etch pits are bound by type (I) steps. Then the pit expands slowest in the $<11\bar{2}>$ directions [17].

Of course for the opposite (111)As face a similar step structure exists. The stability of the steps is strongly reduced however. As will be discussed in the paragraph on (100), gallium is not able to form as stable dimer bonds as arsenic, so step reconstruction will not be prominent for the $<11\bar{2}>$-steps. The possibility that instead, arsenic will form a bond with As in the lower lying layer is also unlikely, as

the triple-bonded arsenic can only move towards the arsenic step atom at the cost of considerable strain in the As-Ga bonds. For $\langle\bar{1}\bar{1}2\rangle$-steps the {110}-like relaxation is more effective with respect to the reactivity of As than for $\langle 11\bar{2}\rangle$-steps on (111)Ga. Arsenic sticks more out of the (111)As surface and the largely filled dangling orbitals are geometrically more susceptible to attack. Gallium on the other hand, is more hidden and less accessible for reactants.

So it is to be expected that on (111)As no distinct step pattern will be seen in contradiction to (111)Ga. The great stability of steps on the latter surface will inevitably lead to stable triangular etch pits for a wide range of temperatures and etch velocities. On (111)As the removal of arsenic from a step site is unlikely to be rate limiting and it is questionable, whether under conditions where arsenic is preferably removed from the crystal, etching via steps will be discernable. It could even be conceived that then arsenic is removed directly from the surface, explaining the rough morphology often observed [3,4].

Significant for adsorption on (111)Ga is the relaxation of the surface in the absence of interacting species. As calculated by Chadi [18] the (2x2)Ga relaxation stabilizes the surface 13 kcal/mol, an energy to be raised by the adsorption of e.g. Cl, as this removes the relaxation [19]. According to Chadi such a stable (2x2) structure is absent for (111)As. Thus relaxation relatively favours the adsorption on (111)As, making removal of arsenic directly out of the surface more likely than removal of gallium out of a (111)Ga surface. All the same, both {111} surfaces are F-faces with steps as reactive sites.

2.3. Surface reconstruction for (100) faces

The most important feature of a (100) face is the possibility of the surface atoms to form dimer bonds. This changes (100) from an S-face, in the broken bond model, to an F-face. Evidence for this surface reconstruction is presented in UHV studies, where various structures are observed ranging from gallium to arsenic rich [20]. Basicly all structures show dimerization, often in addition with vacancy formation (the surface is then poor in As, or Ga, compared with a completely

As- or Ga-terminated surface). Most easily prepared are the Ga-rich (4x2), often mistaken for c(8x2), and the As-rich (2x4) (c(2x8)) reconstructed structures [21]. The basic features for these two types of surfaces will be treated here. It should be realized that the exact structure is not elucidated yet; fortunately in CVD studies this is not felt as a shortcoming.

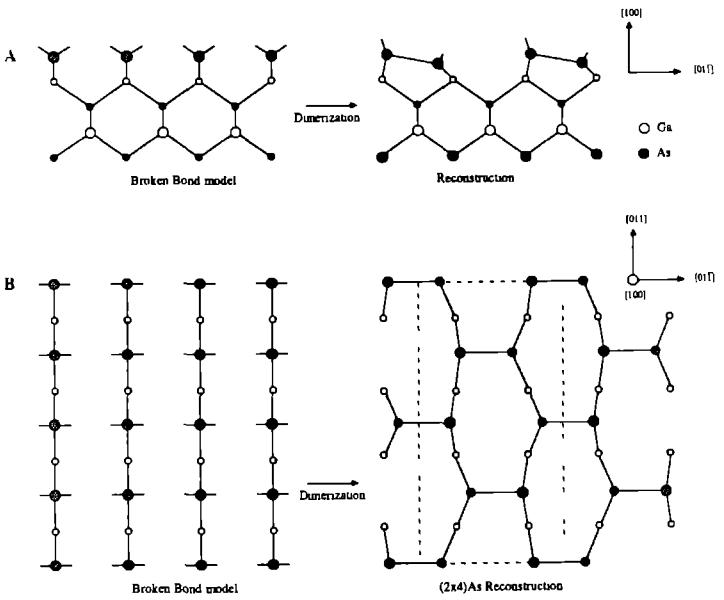

Fig. 4 A) Cross-section of an arsenic terminated broken bond and an As-dimerized (100) surface.
B) Topview of a broken bond and a (2x4) reconstructed As-stabilized (100) surface.
The dashed lines indicate the (2x4) unit mesh.

In fig. 4A the dimerization process is sketched, resulting, for (100)As, in the formation of surface bonds lying in the [01$\bar{1}$] direction and a Jahn-Teller distortion: a charge shift leading to negative As with a dangling bond pointing upwards and positive arsenic sunken into the surface. This reconstruction produces an energy gain of -30 kcal/mol dimer for the As-stabilized structures [22]. It can be shown that such a high reconstruction energy is not easily raised by

adsorbates, resulting in reconstructed GaAs surfaces in growth and etching experiments, at atmospheric pressures and high temperatures [9]. In fig. 4B the topview on a (100) surface is shown, assuming that the top layer of a (2x4) structure completely consists of arsenic. Due to the dimerization, which stabilizes the surface in the [01$\bar{1}$] direction, (100) has become an F-face as all the atoms in the surface layer are connected via strong bonds. Consequently random etching is unlikely at low undersaturations it preferably takes place at steps. After removal of the arsenic top layer a gallium surface is created, which is in principle identical to (100)As, apart from a 90° rotated reconstruction pattern. Whether a (2x4)As, a (4x2)Ga, or an intermediate structure is observed, depends on the relative stability of the arsenic and gallium surfaces. This is not only related to the reactants in the gas phase, but also to the intrinsic stability.

Although firm evidence is not available yet, it is thought that the gallium reconstruction is far less stable than the arsenic (2x4) structure. Experimentally it is observed in MBE that the existence region, the Ga/As ratio of the impinging flux for which (4x2)Ga is stable, is very narrow. For an increasing Ga-flux only an additional 5%, to the value where the (4x2) pattern is first observed, results in free gallium on the surface [21]. It is also observed that the arsenic content in the top layer is 30% for the gallium reconstruction, whereas it is 100% for the arsenic stabilized structure [20]. This means that, in contrast to the As-reconstruction, the gallium dimerization is not that stable to prevent formation of gallium vacancies. The reason for this unfavourable dimerization is the low electron density of gallium as compared to arsenic. In the a-polar limit, gallium contributes 3/4 electron to each Ga-As bond. So for a broken bond surface, two gallium atoms possess 3 electrons, whereas two As have 5 electrons. According to Chadi et al. [22] the surface bonds formed in reconstruction can accommodate 5 electrons in bonding orbitals, as long as 4 or more atoms are present per unit mesh. So in a (4x2)Ga structure only 3/5, or less, of the bonding capacity is used. As the gain in energy by forming new bonds and dipoles is partly counteracted by the distortion of the lattice in the surface and subsurface, the resulting reconstruction energy for gallium is at least halved compared with arsenic. This leads

to an easily removed Ga-dimerization upon adsorption [9].

So in CVD experiments it is expected that a (100) surface prefers to be arsenic rich, as the As-dimerization is energetically favoured to the Ga-reconstruction. The stabilization makes (100)GaAs an F-face, with steps as reactive steps, and arsenic, in principle, the most difficult species to remove.

2.4. Surface relaxation for (110)

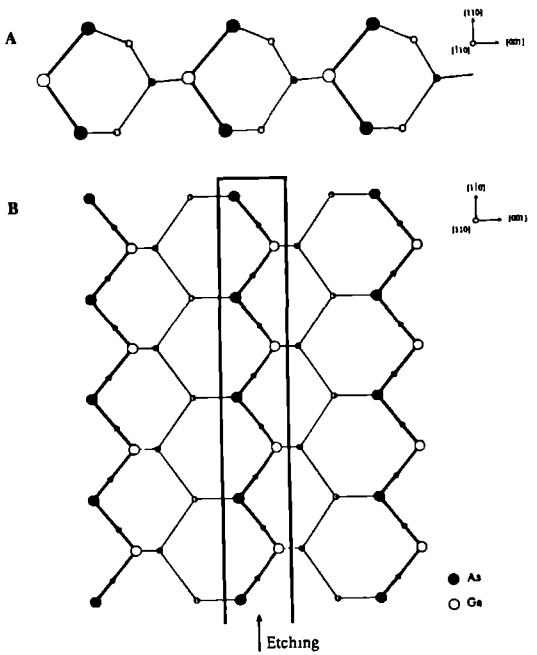

Fig. 5 A) Cross-section of a relaxed (110) surface.
B) Topview on a relaxed (110) surface.

The (110) face is the only stoichiometric surface which has been studied. As can be seen in fig. 5A the surface layer is relaxed. The Ga-As bond, which is lying in the (110) plane for a truncated surface, is rotated 27° towards [110], resulting in arsenic, which is raised and has become more negative, and gallium, more positive and sunken into the surface [23]. Arsenic is now more or less in its atomic configuration,

3 bonds with gallium making angles of ~90° and a filled s-orbital. Gallium is sp^2 hybridized with an empty p-orbital. Towards chemical attack the polar character of Ga and As is enhanced by the relaxation. On the other hand the energy gain, 13 kcal/mol [24], caused by the relaxation, stabilizes both gallium and arsenic, as this has to be raised by adsorbing species [25].

In a topview on the (110) surface the stepped (S) character of the face can be discerned clearly, in the (110) plane a PBC is running in the [1$\bar{1}$0] direction. The etching occurs row by row, once an arbitrary Ga- or As-atom is removed at the cost of three bonds, a whole bond chain (indicated in the rectangle) can be stripped by successive breaking of two bonds. As the surface relaxation only causes distortions within one row, they could etch, or grow independently, preserving the S-character. Yet the Coulomb interactions between the chains could give a stabilization in the [001] direction strong enough to couple the chains under conditions relevant for CVD, making (110) an F-face. So, the nature of (110) still is a matter of discussion.

3. Thermodynamics

Thermodynamic calculations are essential to obtain a first impression on the reactions of a GaAs crystal with its ambient gas phase [26-28]. The composition of the gas phase in contact with the crystal can be predicted, which in addition gives the possibility to calculate the adsorption of impurities and growth units on the crystal surface [8]. With a given composition of the gas input also the kind of chemical reactions that might occur on the crystal surface can be established. The difference between input and equilibrium composition leads to the amount of material to be etched or deposited and, which is the major point in this study, indicates whether gallium or arsenic is preferentially attacked by gaseous reagents.

The best correspondence between thermodynamic predictions and kinetic measurements is evidently found at low under- or supersaturations, as for example for the growth in the Ga-As-Cl-H or Si-Cl-H system at high temperatures [28,29]. At low temperatures, or for reactants far from

equilibrium, it can be expected that kinetic barriers result in a (steady-state) partial pressure deviating from the equilibrium value. However the calculations still have their value, since the order of magnitude of the partial pressures and the direction of a specific reaction is given.

In the subsequent discussion it should be reminded that the merits of a thermodynamic approach not only can be affected by kinetic hindrances, but also depend on the accuracy of the available thermochemical data. The determination of the enthalpy is always the limiting factor, as this has to be calculated from experimental partial pressures. Although these pressures strongly depend on the enthalpy, reducing the error, the accuracy is seriously limited by the difficulty to really attain equilibrium and by the interference of side reactions, making the determination of the partial pressure of a specific species ambiguous. Rare species are often experimentally unaccessible. In these cases the enthalpy has to be calculated from bond strengths, with a corresponding low accuracy, so that, because of the logarithmic relation, the error in the partial pressure can become orders of magnitude. On the other hand the entropy and heat capacity can be calculated rather accurately, using statistical thermodynamics, when the molecular structure is known and spectroscopic data are available of the species themselves, or analogues.

3.1. Ga-As system

A fundamental problem in the growth of III-V compounds is the incongruent sublimation of the V component at elevated temperatures. This makes it necessarily to apply an arsenic pressure over the crystals at all high temperature processing. This is quite critical, since defects in epitaxial layers are observed for too low as well as too high III/V ratios [30,31]. Also for optimum electrical and optical properties (near-)stoichiometric growth is preferred. A better understanding of the influence of the gas phase on the stoichiometry can be obtained by studying a P-T plot of the Ga-As phase diagram.

The basic reaction for GaAs in equilibrium with its vapour is given by:

(1) $GaAs(s) \rightleftarrows Ga + As \qquad K_1 = P_{Ga}P_{As}$

According to the phase rule, at constant T, for the gas phase in equilibrium with solid gallium arsenide, one degree of freedom is left: either the gallium or the arsenic pressure still can be chosen. Then the pressure of the other component and the total pressure is fixed. It should be realized that the total pressure is increased considerably by the possibility of As to polymerise to As_2, As_3 and As_4. It is especially this recombination to more stable species which promotes the arsenic evaporation at high temperatures. The choice of a certain arsenic pressure determines also the point defect equilibria in the solid. So the deviation from stoichiometry of the GaAs crystal is fixed implicitly by the arsenic pressure. At the limit of the existence region of GaAs a second condensed phase is formed. Then P_{Ga} and P_{As} evidently are fixed, so that the pressure of the III- or V-component can only be chosen between those related with the As- and Ga-liquidus. For the Ga-liquidus, which is most relevant in thermal decomposition, the gallium pressure is given by:

(2) $P_{Ga} = a(T)\ P^{\circ}_{Ga}$

As the liquid gallium contains arsenic when GaAs(s) is present, the evaporation is suppressed compared with the pure element (P°_{Ga}) and the activity (a) is lower than 1. Once the gallium pressure is known, the arsenic pressure can be calculated easily via eq. (1), as well as the related pressures of As_2, As_3 and As_4.

The difficulty in calculating the liquidus pressures is the value which should be taken for a(T). From a theoretical point of view it is most elegant to start from the free energy of mixing of the binary solution and solve the resulting equations, or simplifications thereof, like the regular or simple solution model [32-34]. When accurate pressure data are available it is also possible to fit experimental data (P_{Ga}) to thermodynamically derived values (P°_{Ga}) [35]. In this study the most simple model is used, the solution is assumed to be ideal, i.e. the mixing energy is zero. Thus the activity coefficient (γ) is always 1

and the activity (a) is equal to the concentration of gallium in the liquid solution. This leads to a total pressure of 0.9 atm for the Ga-liquidus closely near the melting temperature, in good agreement with the experimental value of 1.0 atm [36]. Application of a regular solution model with T_{melt}(GaAs) = 1511 K and an entropy of fusion of 16.64 cal/mol·K [33], would lead with our thermodynamical data set to 8.1 atm. Obviously this theoretical model fits poorly with the experimental observations.

Table 1

Thermodynamic data for the Ga-As-H system

	$\Delta H^\circ_{f,298}$ (kcal/mol)	S°_{298} (cal/mol K)		$C_p = a + bT + cT^{-2} + dT^2$ (cal/mol·K) a	b×10³	c×10⁻⁵	d×10⁶	Ref.
Ga(l)*	1.334	14.164	T < 700 K	5.829	0.547	0.742		[37]
			T >	6.35				
Ga	65.0	40.38		7.61	-1.85	-0.83		[26]
As(s)	0	8.534		5.504	1.373			[37]
As(l)**	5.452	13.106		6.95				[34]
As	72.12	41.611		4.968				[37]
As_2	45.54	57.19		8.891	0.036	-0.483		[37]
As_3	62.481	74.121		14.841	0.048	-0.662		[37]
As_4	36.725	78.232		19.696	0.283	-1.68	-0.125	[34]
GaAs(s)	-19.5	15.35		10.8	1.45			[37]
GaAs	83.0	61.702		8.935	-0.105			[37-39]
H	52.103	27.392		4.968				[40]
H_2	0	31.207	T < 800 K	7.653	-1.738	-0.323	1.356	[40]
			T >	5.568	1.538	2.27	-0.114	
GaH	52.7	46.72		5.74	3.61	0.24	-1.2	[41,42]
GaH_2	39.2	53.5		6.86	7.55	-0.07	-2.4	[42]
GaH_3	25.8	52.1		6.69	13.6	-1.0	-4.3	[42]
Ga_2H_6	30.1	66.0		16.61	30.6	-6.6	-9.8	[42]
AsH	59.0	48.0		5.5	3.2	0.5	-1.0	[42]
AsH_2	40.4	44.4		5.81	8.2	0.31	-2.4	[42]
AsH_3	15.88	53.25		10.07	5.42	-2.20		[41,26]

* $\Delta H_{melt,Ga}$ (302.9 K) = 1335 cal/mol

** $\Delta H_{melt,As}$ (1090 K) = 5842 cal/mol

All species gaseous unless designated, (l): liquid, (s): solid

Evaluation of the thermodynamic data available for the Ga-As system learns that particularly the equilibrium between As_2 and As_4 has been subject to many discussions. Unless great care is taken in Knudsen cell mass spectrometry, building up of arsenic in the ionization chamber, leads to too high As_4/As_2 ratios [35]. Our data result in a low ratio consistent with the recent analysis of Tmar et. al [34]. In table 1 the complete data set is presented for the Ga-As system. As far as possible the collected data of Barin and Knacke are used to obtain a consistent set. New compared with most studies is the introduction of As_3 and the gaseous molecule GaAs.

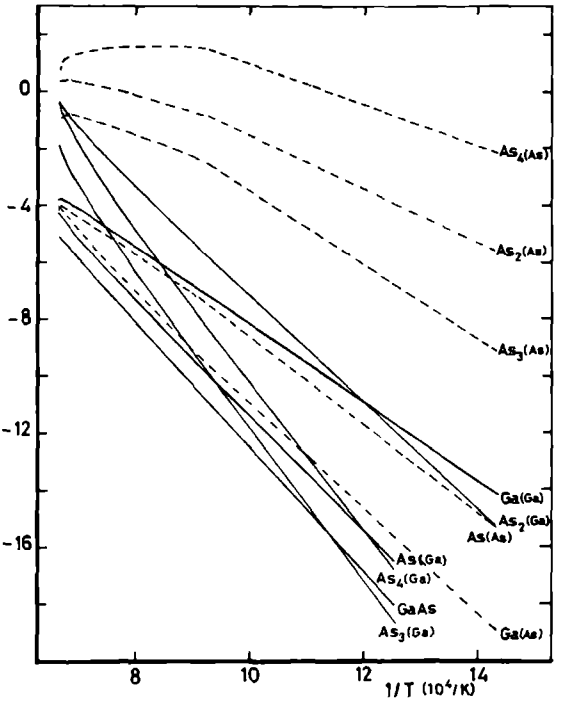

Fig. 6 Partial pressures of gaseous arsenic and gallium species in equilibrium with solid GaAs along the binary liquidi, as a function of 1/T.
——— GaAs-Ga liquidus - - - - GaAs-As liquidus

In fig. 6 the partial pressures of the arsenic and gallium species are shown as obtained using the thermodynamic data of table 1 and $\gamma = 1$.

The composition of the Ga- and As-solutions is taken from Tmar et al [34]. Until 1250 K the gallium, respectively arsenic, pressure deviates less than 10% from the value in equilibrium with the pure element. At high temperatures the gas phase is composed mainly of arsenic, for gallium rich as well as poor conditions. The gallium pressure however is at all temperatures comparable with that of monatomic arsenic, indicating that As itself is not eager to leave GaAs. At the melting point, 1513 K [34], the pressure is calculated to rise from 0.9 to 7.0 atm. This is an artefact, introduced by the method of calculating the activity coefficient. If two condensed phases are present, here GaAs(l) and GaAs(s), the pressure of the gas phase is fixed at a given temperature. So the ideal solution model is not completely adequate for a detailed analysis at temperatures very close to the melting point; then it is best to use experimental determined data, for example those of Rakov et al. [36]. At low temperatures the activity of the solutions approaches unity and good agreement with experimental data should be obtained, independent of the solution model. As_3 is clearly present for the arsenic liquidus at high temperatures, however it can be neglected if only the total (arsenic) pressure is of interest. The evaporation of GaAs in molecular form is, for thermodynamical reasons, not of much influence on the total sublimation process.

3.2. Stoichiometry in GaAs related to the gas phase composition

If perfect growth or etching is aimed at, it is a necessity to calculate also the pressures related with the stoichiometric composition of the solid. Unfortunately this situation is experimentally not as easy accessible as the Ga- or even the As-liquidus. All experiments reported so far are ambiguous due to kinetic factors and impurities, such as Si and C, influencing the native defect distribution. As especially unintentional doping is irreproducible, only a theoretical evaluation is meaningful yet.

It is assumed in this paper that the major native point defects are arsenic vacancies (V_{As}) and interstitials (As_i). This is in accordance with Morozov et al. [43] and to a large extent with Hurle [44]. However

we do not agree with his conclusion that the vacancies are completely ionized; his entropy factor (442) in the ionization constant is too high [45]. So for $[V_{As}] = [As_i]$ a GaAs crystal has a stoichiometric composition. The relation between the arsenic pressure in the gas phase and the creation of interstitials or vacancies can be written down as:

$$(3) \qquad As_{As} + As_1 \rightleftarrows As_2 + V_{As} + V_i \qquad K_{stoich} = \frac{a_{V_i}[V_{As}]P_{As_2}}{a_{As_{As}}[As_1]}$$

For low point defect concentrations the activity of arsenic on an arsenic site (As_{As}) and the activity of interstitial sites (V_i) is unity, so that the arsenic pressure, for the stoichiometric composition, is given by:

$$(4) \qquad P_{As_2} = K_{stoich}$$

Table 2
Thermodynamics of point defect equilibria in GaAs

	ΔH kcal/mol	ΔS kcal/mol·K
$0 \rightleftarrows V_{As} + V_{Ga}$	83	18.1
$As_{As} + V_i \rightleftarrows V_{As} + As_i$	71	18.1
$As_2 \rightleftarrows 2As_{As} + 2V_{Ga}$	21	-31.0

The data to calculate the equilibrium constant of eq. (3) are given by Morozov et al. [43] and depicted in table 2. A small correction is applied for the different enthalpy used for As_2, to obtain consistency with the data from table 1. Using these data it can be derived that for reaction (3):

$$\Delta H_3 = 74 \text{ kcal/mol} \qquad \Delta S_3 = 49.1 \text{ cal/mol·K}$$

In fig. 7 the resulting As_2 pressure, $P_{As_2}(V_{As}\text{-}As_1)$, is plotted. It can be seen that the arsenic pressure needed to suppress the formation of arsenic vacancies is only low and that on the basis of this result incorporation of interstitial arsenic is easy. In other words the

existence region is more extended towards the As-rich side. Comparing this result with Hurle [44] a great discrepancy can be noticed. Assuming the same point defects to be dominant, he concluded that especially at low temperatures GaAs can exist mainly as an arsenic poor compound. Yet Hurle did not apply a fully theoretical approach. He estimated the stability of As_1 using annealing data from Nishizawa et al. [46]. Also for other experiments of Nishizawa et al. [47] (LPE), as well as for MOCVD [48], it is found that much higher arsenic pressures, as can be deduced from our results, were necessary to obtain stoichiometric growth.

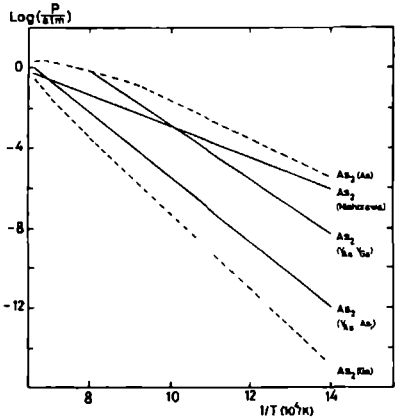

Fig. 7 Theoretical and experimental P_{As_2} corresponding with stoichiometric GaAs.
——— stoichiometry
Nishizawa [47]
V_{As}-As_1 only Frenkel disorder
V_{As}-V_{Ga} only Schottky disorder
- - - - liquidi

A closer look at Nishizawa's results learns that the As_2 pressure he actually had to apply to obtain stoichiometric growth (converting his P_{tot} to P_{As_2} with our thermodynamic data) is given by:

$$P_{As_2}(atm) = 8.7\times10^{4}\exp\{-18\times10^{3}/T\}$$

The activation energy found by Nishizawa was 36 kcal/mol, to compare with our theoretical value of 74 kcal/mol. Though the inaccuracy in the theoretical data is great, this cannot account for such a large discrepancy. The data of As_2 are rather accurate and the stability of

arsenic vacancies is certainly not underestimated. The formation enthalpy of V_{As} applied here is 46 kcal/mol, whereas Van Vechten reported 60 kcal/mol [49], a value corrected by Hurle [44] to 52 kcal/mol. That the formation enthalpy of interstitial arsenic also cannot explain the data of Nishizawa (and Hurle) can be seen in fig. 7. There it is shown that not only the stability difference between V_{As} and As_i results in much lower theoretical stoichiometric As_2 pressures than experimentally found, but also the Schottky equilibrium between V_{As} and V_{Ga}, gives that result at low temperatures. As the thermodynamical data for V_{Ga} are well established [43,44,49], it must be concluded that Nishizawa's relation is certainly not representing an intrinsic point defect equilibrium, when extrapolated to temperatures lower than 1000 K. Also for higher temperatures our theoretical relation gives a better description of stoichiometry. Suppose that all the same Nishizawa's curve does represent equal concentrations of V_{As} and As_i. Then the theoretical model to calculate ΔH and ΔS of arsenic interstitials [43] must be discarded, as the difference is much greater than the error limit. But more important, it implies that vacancy formation is dominating over Frenkel disorder below 1000 K. As this is in contrast to modern point defect theory [43,44,50], it is most likely that as well in LPE as in MOCVD kinetic factors are dominant in determining the V/III ratio in the grown layer.

Nishizawa applied, in LPE experiments, an arsenic pressure to a gallium liquid in which a crystal was growing. Evidently this cannot represent equilibrium; then only Ga-rich GaAs would be grown. So to achieve stoichiometric growth the gallium solution must be supersaturated considerably with arsenic. It is known from gas phase epitaxy that diffusion limited processes are quite common. As in liquids the diffusion coefficients are 3 to 5 orders of magnitude lower, large concentration gradients are likely to exist when the solution is not stirred. This can lead to an arsenic pressure, which is decades higher, than the equilibrium value.

In MOCVD it is known that the stoichiometry is not determined by the absolute applied arsine pressure, but merely the III/V ratio [48,51]. As arsenic is present in excess and consequently converted only partially into GaAs, this is in contradiction with the hypothesis that

the excess is all needed to suppress the evaporation of arsenic. If the III/V ratio in the surface layer would be thermodynamically determined, it should be expected that a constant excess pressure of arsenic is needed for stoichiometric growth. Clearly kinetics plays a role, an excess arsenic is needed to obtain an arsenic rich surface layer, as this only leads to proper epitaxial growth. A gallium rich surface layer easily leads to the formation of a liquid-like metal layer and loss of the epitaxial feeling [52]. Thus it may be concluded that the electrical properties of an epilayer, which are optimal at a certain III/V ratio, are not only depending on the deviation from stoichiometry, but are certainly also related with Si, C and group II elements introduced by the growth sources [48,51]. So the transition from p- to n-type material does not reflect only a stoichiometric composition but also a balancing of unintentional dopants.

The theoretically derived stoichiometric As_2-curve, as presented in fig. 7 ($P_{As_2}(V_{As}\text{-}As_i)$, is in good agreement with current theory, which stresses the importance of Frenkel disorder on the arsenic sublattice. Though the accuracy is not very high, the slope has an error of approximately 10 kcal/mol, it is thought to give a good impression of the main point defect equilibrium. As the stoichiometric arsenic pressure is expected to cross the As-liquidus only very close near the melting point, a new value for the enthalpy would also imply a new one for the entropy. On the basis of LPE and MOCVD growth it can be concluded that the experimental pressure needed to obtain optimal morphology and electrical properties is far above the theoretical pressure. This is due to kinetic reasons, which can in principle be studied theoretically and to, unpredictable, unintentional doping. So in the subsequent analysis it should be remembered that, with respect to stoichiometry, a discrepancy between theory and experiment is likely to be found.

3.3. Stability of GaAs

In order to study the tendency of gallium and arsenic to leave the crystal when it is heated up, it is useful to plot the total arsenic ($\Sigma x P_{As_x}$) and the gallium pressure related with the Ga- and As-liquidus; fig. 8. In this figure also the pressures related with the stoichiometric composition are indicated, as this shows what the total arsenic and gallium input, in e.g. a CVD reactor, should be theoretically, to maintain a perfect crystal. Thermodynamically it is most relevant to define the total arsenic pressure as:

(5) $$\Sigma x P_{As_x} = P_{As} + 2P_{As_2} + 3P_{As_3} + 4P_{As_4}$$

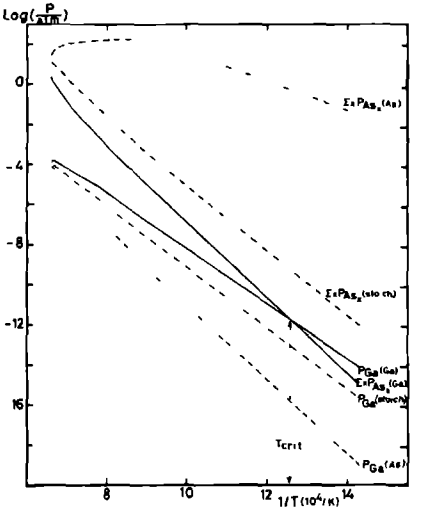

Fig. 8 Total arsenic, $\Sigma x P_{As_x}$, and gallium pressure in equilibrium with solid GaAs along the binary liquidi and with stoichiometric GaAs as a function of 1/T.
——— liquidi - - - - stoichiometry

At low temperatures the arsenic pressure above stoichiometric GaAs is mainly built up of As_2, above 1300 K As_4 takes over. For the Ga-liquidus As_2 prevails until close to the melting point, then the total arsenic pressure becomes so high that As_4 also has to be considered and it becomes the dominating species for the As-liquidus.

When a stoichiometric crystal is heated the gallium pressure, the crystal tries to built up, is lower than $\Sigma x P_{As_x}$(stoich) for all temperatures. So arsenic has a much stronger tendency to evaporate than gallium and the crystal will loose more As than Ga and arsenic vacancies will be formed. This results in a reduced tendency of arsenic to leave the crystal and an increased equilibrium pressure for gallium. Suppose that all the arsenic and gallium, which is released from the crystal, is removed from the gas phase instantaneously, then the evaporation flux will remain proportional to the equilibrium pressure. Below a certain temperature, T_{crit}, it is possible for GaAs to establish a steady-state situation with congruent sublimation, as equal pressures of gallium and arsenic are possible within the existence region. For higher temperatures the gallium liquidus is reached before the arsenic pressure is as low as the gallium pressure. Then the arsenic flux remains constant and larger than the gallium flux, so that the amount of liquid gallium is increased, until the GaAs has disappeared.

In fig. 8 it can be seen that T_{crit} = 794 K. Compared with Thurmond [53], who calculated 933 ± 100 K, Arthur [35], who determined 910 K, and Foxon et al. [2], who reported 898 K, our value is remarkably low. This is due to the greater stability of As_2: the As_2-curve crosses at lower temperatures the Ga-line. As discussed before, this is in better agreement with the latest opinion about the stability of As_2 versus As_4.

3.4. Stability of GaAs in N_2 and H_2

Up to now GaAs was studied as a two-phase system, which for example is applicable to UHV experiments, or to annealing of a crystal in a sealed evacuated ampoule. To study the stability of GaAs in CVD systems, it is useful to introduce hydrogen or nitrogen in the calculations as this is commonly used as carrier gas.

In an inert gas, with respect to GaAs, such as N_2, a crystal will built up a gallium and an arsenic pressure just as described in fig. 6 and 8. The only consequence of the introduction of an extra element is, according to the Gibbs phase rule, that an extra degree of freedom is obtained. As CVD is usually performed at a constant pressure of 1 atm this parameter is fixed. The composition of the gas phase in

equilibrium with an evaporating GaAs crystal in a nitrogen atmosphere is the same as were the N_2 absent, as long as the arsenic pressure ($P_{As_2} + P_{As_4}$) in the P-T plot of the phase diagram is lower than 1 atm. At temperatures where the arsenic pressure is higher than 1 atm no equilibrium with solid GaAs can be achieved and the crystal will evaporate completely.

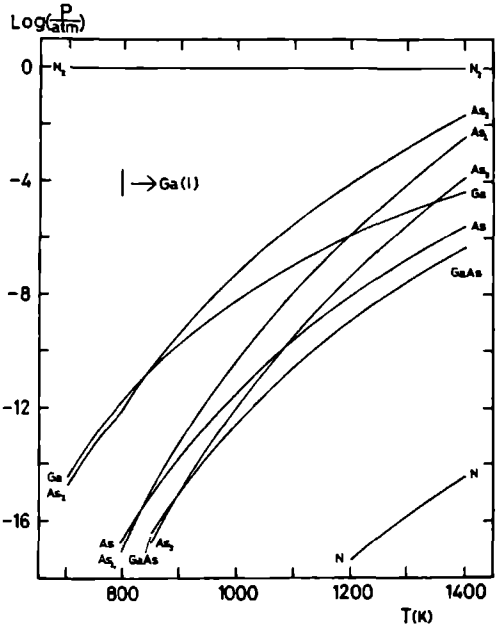

Fig. 9a Gas phase composition of GaAs in equilibrium with a nitrogen atmosphere at 1 atm total pressure as a function of temperature.
The presence of GaN has been discarded for kinetic reasons.
Above 794 K liquid gallium is present.

In fig. 9a the gas phase composition of GaAs(s) in a N_2 atmosphere is depicted. In principle at low temperatures, until 920 K, GaN(s) will be formed. This reaction is not considered to occur as nitrogen is very inert in the form of N_2. Congruent evaporation of GaAs is possible up to 794 K, as already indicated in the P-T plot of the phase diagram. Comparison with fig. 7 learns that at lower temperatures, the As_2 pressure is lower than for stoichiometric GaAs, so GaAs is, in fig. 9a, always gallium rich. At higher temperatures the Ga-evaporation cannot

keep up with that of As_2 and consequently the excess is collected as droplets on the crystal surface.

In hydrogen it must be taken into account that arsenic as well as gallium hydrides are significant at low temperatures. The existence of arsine is well known, as it is often used as the source of arsenic in epitaxial growth. It is less realized that hydrogen can react also with gallium. As already mentioned in the description of adsorption on GaAs, the bond strength is similar for AsH and GaH (see also [54]). As the entropy of the gallium and arsenic hydrides is also expected to be comparable, the stability with respect to the monatomic elemental gas phase species will be similar. For stoichiometric GaAs the gallium pressure is, especially at low temperatures, considerably larger than P_{As} (fig. 10), so the reactivity of hydrogen towards gallium is then larger than towards arsenic.

In table 1 also the thermodynamic data for the hydrides are given. Up to now, Tirtowidjojo and Pollard are the only ones reporting on the Ga-As-H system [42]. Experimentally little is known about the Ga-As-H system, apart from AsH_3, so the reliability of the available thermodynamic data is not well-established yet. Although confidence is put in the adopted data, two comments should be made. It is thought that the formation enthalpy of GaH_2 and GaH_3 is chosen too high. The enthalpy content per Ga-H bond is constant for the three hydrides. It is more likely however, that the bond strength increases as more H is attached, in analogy with the arsenic and silicon hydrides (table 1 and [8]). The entropy of GaH_2 is probably too high, on the other hand for AsH_2 it is thought to be too low. As the molecular weight of Ga and As is nearly the same, the translational and rotational contribution of the entropy is similar; comparable bond strengths and lengths will give almost equal vibration frequencies. Apart from the argument that the entropy is expected to be comparable, it is more logical to have an S°, which is increasing when more hydrogen is attached to Ga or As. So it is well possible that AsH_2 and GaH_3 are more abundant in the gas phase than presented in the following, for GaH_2 the enthalpy and entropy effect may cancel.

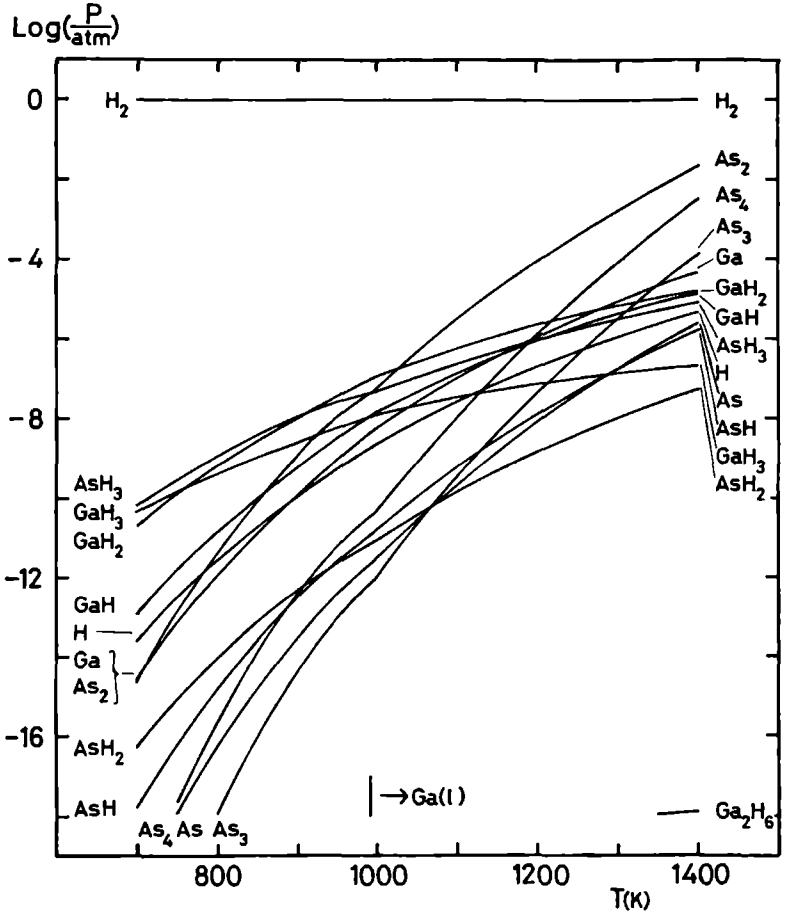

Fig. 9b Gas phase composition of GaAs in equilibrium with a hydrogen atmosphere at 1 atm total pressure as a function of temperature. P_{GaAs} has been omitted in this graph. Above 997 K liquid gallium is present.

In fig. 9b the evaporation of GaAs in a hydrogen ambient is presented. Compared with N_2 it is most noticable that the crystal is less gallium rich, the temperature where the Ga-liquidus is reached is shifted 200 degrees upwards to 997 K. This is in agreement with the prediction that the comparable reactivity of hydrogen towards arsenic and gallium favours especially the latter. For gallium the profit is

largest as instead of the monatomic species, now GaH_2 and GaH_3 can try to maintain the sublimation congruently. For arsenic, the effect of hydrogen is less pronounced, as the difference in stability with As_2 actually has to be considered.

Comparison with fig. 7 shows that already at 700 K the sublimation results in a depletion of arsenic for GaAs crystals, since even at this low temperature the As_2 pressure is lower than the stoichiometric value. At 700 K GaH_3 and AsH_3 are the major gallium and arsenic species, GaH_2 takes over at 750 K, with respect to gallium. As discussed, it could well be that GaH_3 actually is more important, the effect however on the temperature where liquid gallium starts to be formed, will not be very significant. The pressure of GaH_3 is then already 1 decade lower than that of GaH_2 and the temperature dependence of P_{As_2}, which is then the dominating arsenic species, is rather strong. At still higher temperatures the influence of arsenic hydrides becomes negligible. GaH_2 remains the dominant gallium species until 1270 K, where the monatomic species takes over. However the gallium hydrides cannot influence P_{Ga} or P_{As_2}, they only lessen the amount of gallium, which will be left behind on the crystal surface, in an evaporation process.

To prevent arsenic to leave GaAs, it is common practice to apply an arsenic pressure to the crystal. In fig. 10 the influence of 1% AsH_3 is shown, when the crystal is heated in a hydrogen atmosphere. A comparison of the calculated Ga (or As) pressure with the pressure in equilibrium with stoichiometric GaAs shows that up to 1200 K the arsine is able to suppress the formation of arsenic vacancies effectively, and fills more interstitial sites with arsenic. Below 672 K even the As-liquidus will be followed. It is indeed well-known that in MOCVD, despite the kinetic barriers in the arsine decomposition, an arsenic mirror is formed at the cold walls of the reactor tube. From 1200 to 1336 K the evaporation of arsenic is too strong to counteract and $[V_{As}]$ is increasing fast with temperature. Above 1336 K liquid gallium is formed and the gas phase composition is identical with fig. 9b.

It can be deduced from fig. 10 that, with respect to the stoichiometry in the GaAs crystal, it does not matter whether 1% AsH_3 is added in H_2 or 1% As in N_2. At high temperatures in both systems the

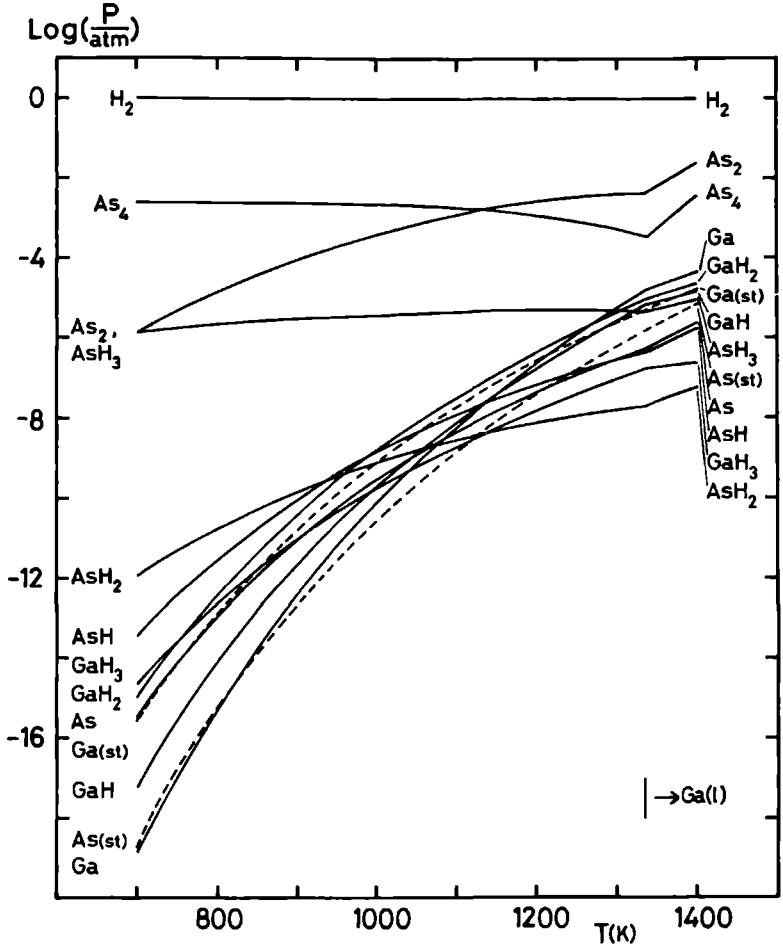

Fig. 10 Gas phase composition of GaAs in equilibrium with 1% AsH_3 in H_2 at 1 atm total pressure as a function of temperature.
P_{As_3}, P_{GaAs}, P_H and $P_{Ga_2H_6}$ have been omitted in this graph.
Above 1336 K liquid gallium is present.
The dashed lines indicate the partial pressure of As and Ga in equilibrium with stoichiometric GaAs.

dominating arsenic species are As_2 and As_4, the arsenic hydrides being negligible, thus resulting in equal pressures of monatomic arsenic and gallium. So already from the P-T plot of the phase diagram (fig. 8), it

could have been derived at which temperature the introduction of 1% As would have been insufficient to prevent formation of liquid gallium.

In fig. 10 also the unstable arsenic and gallium hydrides are presented. Though thermodynamically the stability of arsenic in the crystal is determined by the total arsenic pressure in the system, it could well be that in a dynamical CVD system, only sub-equilibria can be established. For such a system, it is concieved that perhaps not only monatomic gallium and arsenic determine the point defect equilibria in the solid, but all the adsorbed gallium and arsenic species. Then some hydrides, viz. GaH, GaH_2, AsH and AsH_2, become very important. Together with the monatomic species, they probably are bonded strongest, and determine the surface concentration [7]. In this case, this would result in the opinion that the suppression of the arsenic evaporation is, roughly, determined by the sum of the pressures of As, AsH and AsH_2. Giving a difference in stoichiometry of GaAs in H_2 and N_2.

3.5. Reactivity of GaAs towards Cl and O

So far the gas phase was relatively inert. The loss of material was primarily due to the tendency of the crystal to evaporate. However the sublimation mainly affects the arsenic sublattice. If HCl and H_2O are introduced in the gas phase, also the gallium is removed from the GaAs, but now in a chemical instead of physical way. Both etchants prefer reaction with gallium to removal of arsenic, thus counteracting the arsenic evaporation at intermediate temperatures. It will be shown that in H_2 the reactivity, as well as the selectivity towards gallium is larger for HCl than for H_2O. This is according to the expectation on the basis of electronegativities.

With the use of the thermodynamic data as presented in table 3, the influence of 100 ppm water is studied; fig. 11. It can be seen that in the whole temperature region the gallium oxides are far more important than the arsenic oxides. At 700 K the difference in partial pressure is more than 4 decades, decreasing to a factor 400 at 1400 K. It appears that the stable gallium oxides are GaOH and Ga_2O, the latter especially at high temperatures. For arsenic the corresponding AsOH and As_2O have

Table 3

Thermodynamic data for the Ga-As-O system

	$\Delta H^{\circ}_{f,298}$ (kcal/mol)	S°_{298} (cal/mol K)		$C_p = a + bT + cT^{-2} + dT^{2}$ (cal/mol·K) a	b×10³	c×10⁻⁵	d×10⁶	Ref.
Ga_2O	-21.7	68.7		12.808	1.486	-1.254	-0.543	[55]
GaO	66.8	55.2		7.694	2.158	-0.53	-1.054	[41,56]
GaOH	-35.4	58.0		12.496	0.434	-0.775	0.254	[55]
Ga_2O_3(s)	-260.3	20.31		26.98	3.69	-5.02		[37]
AsO	-7.9	54.0		7.4				[57]
AsO_2	-71.7	60.9		10.0				[57]
As_2O_3(s)	-156.16	29.33		8.37	48.6			[58]
As_2O_3(l)	-154.383	30.198		39.0				[54,58]
As_2O_3	-139.676	55.663		21.5				[54,58]
As_2O_5(s)	-221.05	25.191		32.94	11.06	-7.43		[41,59]
As_4O_6(s)	-314.0	51.2		45.72				[41]
As_4O_6	-295.81	91.0	T < 1200 K T >	40.7 55.6	22.8 0.02	-11.0 -30.4	-9.7	[41,60]
$GaAsO_4$(s)	-239.540	35.88		30.89	8.21	-4.51		[61,62]
O	59.554	38.468	T < 800 K T >	5.111 4.98	-0.27 -0.008	0.172 0.261	0.146 0.001	[40]
O_2	0.0	49.005	T < 800 K T >	5.16 7.96	5.312 0.774	0.422 -2.834	-2.209 -0.116	[40]
OH	9.318	43.89	T < 800 K T >	7.363 5.023	-1.333 2.471	0.075 2.754	1.315 -0.438	[40]
HO_2	5.0	54.383	T < 800 K T >	5.323 8.657	10.229 3.801	0.312 -2.491	-4.358 -0.844	[63]
H_2O	-57.798	45.106	T < 800 K T >	6.963 4.907	2.549 5.719	0.243 2.815	0.322 -1.057	[63]
H_2O_2	-32.53	55.66	T < 800 K T >	7.209 12.514	14.812 3.4	-0.601 -3.958	-7.3 -0.492	[63]

All species gaseous unless designated, (l): liquid, (s) solid

not been reported yet. The Ga-O bond strength is 110 and 106 kcal/mol for the hydroxide respectively, the suboxide (table 3). This has to be compared with a diatomic bond strenght (DABS) for AsO of not less than 140 kcal/mol. So at first sight the stability of the gallium oxides is remarkable, especially as the entropy loss in forming one bond with oxygen is for all three molecules equal: 26 cal/mol K. That P_{GaOH} is larger than P_{AsO} is due to great stability of OH compared with O and, to a lesser extent, to the higher pressure of P_{Ga} compared with that of monatomic arsenic. The stability of Ga_2O is mainly caused by the

formation of two Ga-O bonds per, hardly present, O-atom. As expected, the partial pressure of the monoxide of gallium is negligible compared with P_{AsO}. However it is well possible that the actual stability of GaO is larger than presented here, as there are no obvious reasons why the diatomic bondstrength is only 58 kcal/mol (table 3), only half of the value for GaOH or Ga_2O. The partial pressure of AsO on the other hand could be too high, as a lower DABS of 115 kcal/mol has been reported [41,54]. As can be seen in fig. 11 higher oxides such as As_2O_3, As_2O_5, As_2O_6 or $GaAsO_4$ are absent at a low water input. Only at high oxygen and arsenic pressures (and low temperatures) they are present in significant amounts.

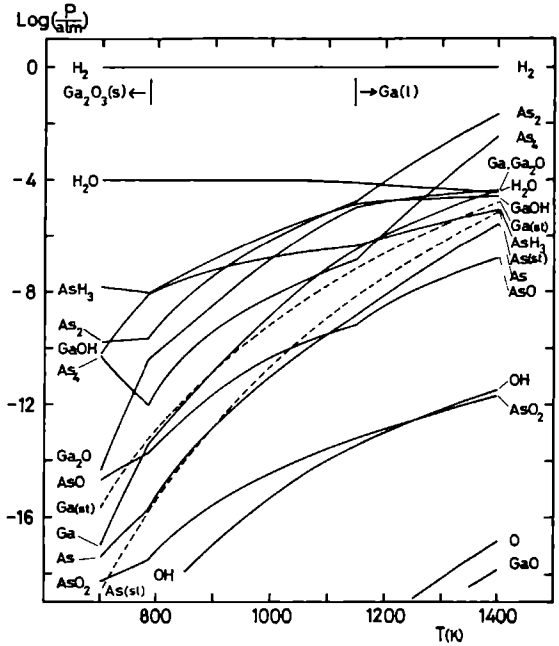

Fig. 11 Gas phase composition of GaAs in equilibrium with 100 ppm H_2O in H_2 at 1 atm total pressure as a function of temperature. Only the relevant pressures are indicated as well as the gallium and arsenic oxides. Below 785 K solid Ga_2O_3 is formed; above 1150 K liquid gallium is present. The dashed lines indicate the partial pressure of As and Ga in equilibrium with stoichiometric GaAs.

At low temperatures the water input is so high that solid Ga_2O_3 is formed. This is in analogy with Si, where oxide formation presents a serious problem in growth and etching [64]. However in comparison with the silicon system the conversion of H_2O is low, so the gaseous oxide, GaOH, is far less abundant than SiO. Likewise the solid oxide is far less stable. In case of 0.1 ppm H_2O, which is representative for growth systems, it has already disappeared at 592 K, to compare with 1138 K for silicon systems. As typical growth temperatures are 1000 K for GaAs with MOCVD [30,51] and 1300 K for Si from SiH_4 [65], it is obvious that proper crystal growth is more affected by oxygen in the latter system. It should be noticed that for GaAs growth in the absence of hydrogen, like in MBE systems, the presence of oxygen is far more notorious [66]. Then oxygen is all divided over the solid and gaseous gallium oxides, instead of being in the form of relatively inert water.

In general the amount of arsenic and gallium released into the gas phase, mainly in the form of AsH_3 and As_2, respectively GaOH, Ga_2O and Ga, is strongly increasing with temperature. For GaAs the tendency of arsenic to evaporate is more enhanced at higher temperatures than the etching of gallium, so the crystal has to become arsenic poorer with increasing temperatures to prevent, as far as possible, incongruent loss of Ga- and As-species. The rate of gallium enrichment, which affects the reactivity (and selectivity) of the etchant, can be inferred from a comparison of the increase of P_{Ga} relative to the rise of P_{Ga}(stoich.).

It can be seen in fig. 11 that first the arsenic content in the gas phase decreases with temperature. This is related to the amount of Ga_2O_3(s) which becomes less and can be compensated only partially by an enhanced formation of gaseous gallium species. Although this is accompanied by an increasing gallium content of GaAs, the crystal remains arsenic rich. At 785 K, where the last solid Ga_2O_3 has just disappeared, the arsenic pressure starts to rise abruptly, as then the gallium loss no longer decreases. This slows down the rate of the arsenic depletion. Thus it is only at 900 K that a stoichiometric composition is attained for a congruently etched GaAs crystal. Up to 1150 K the arsenic evaporation can be suppressed and the gallium oxidation promoted by increasing $[V_{As}]$. Then the limit of the existence

region is reached and liquid gallium is formed. The slope of the arsenic related pressures rises again, as there is no mechanism anymore to counteract the evaporation.

Table 4

Thermodynamic data for the Ga-As-Cl system

	$\Delta H^\circ_{f,298}$ (kcal/mol)	S°_{298} (cal/mol K)		$C_p = a + bT + cT^{-2} + dT^2$ (cal/mol·K) a	$b\times10^3$	$c\times10^{-5}$	$d\times10^6$	Ref.
GaCl	-17.1	57.236		8.847	0.233	-0.398	-0.049	[67,28]
$GaCl_2$	-39.0	71.668		13.794	0.133	-0.833	-0.041	[67,28]
$GaCl_3$	-102.4	77.515		19.463	0.567	-1.518	-0.212	[67,28]
Ga_2Cl_2	-56.1	83.681		19.521	0.548	-1.533	-0.233	[67]
Ga_2Cl_4	-148.5	103.031	T < 600 K T >	17.984 28.142	26.683 4.001	-1.511 -7.848	-15.748 -1.272	[67]
Ga_2Cl_6	-228.9	116.9		43.005	0.99	-3.406	-0.37	[67]
AsCl	28.0	66.264		8.019	1.252			[39]
$AsCl_2$	-15.0	71.952		13.469	0.138			[39]
$AsCl_3$(l)	-72.9	51.7		31.9				[41,37]
$AsCl_3$	-62.5	78.2		19.62	0.24	-1.42		[41,37]
Cl	28.989	39.454	T < 800 K T >	5.432 5.946	0.624 -0.809	-0.294 -0.247	-0.778 0.202	[68]
Cl_2	0	53.289	T < 800 K T >	8.271 8.896	1.453 0.168	-0.469 -0.903	-0.755 -0.017	[63]
HCl	-22.063	44.645	T < 800 K T >	7.168 5.04	-1.093 3.028	-0.015 1.646	1.56 -0.673	[63]

All species gaseous unless designated, (l): liquid

The Ga-As-H-Cl system is well studied [26-28], as chlorides are well suited to transport gallium from a hot to a cooler zone. The thermodynamic data for the gallium chlorides are recently reviewed and extended with digallium chlorides - comparable with the well-known aluminium dimeric species - by Chatillon and Bernard [67]. Especially the values for GaCl and $GaCl_3$, as presented in table 4, are reliable, as they are the most stable compounds at high respectively low temperatures. The accuracy of the data for the arsenic chlorides is obviously low: they are quite unstable. Only $AsCl_3$ is well-known at low temperatures, as the liquid is used as a source of As and Cl in epitaxy.

The low partial pressures of the arsenic chlorides (fig. 12) are caused by the smaller bond strength of As-Cl, 73 kcal/mol, compared to ~82 kcal/mol for Ga-Cl of $GaCl_2$ and $GaCl_3$. The monochloride of gallium is particularly stable (111 kcal/mol), as it contains a triple bond, analogous with BF or N_2. The stability of AsCl can be subject to discussion. The bond strength used in this paper, 73 kcal/mol, could be too low, as a more stable, double, bond is formed compared with the di- and trichloride. This is compensated by the entropy, which is most probably too low, as a value similar to that for GaCl is expected. The value of 107 kcal/mol reported for the DABS [54], is thought to be far too high.

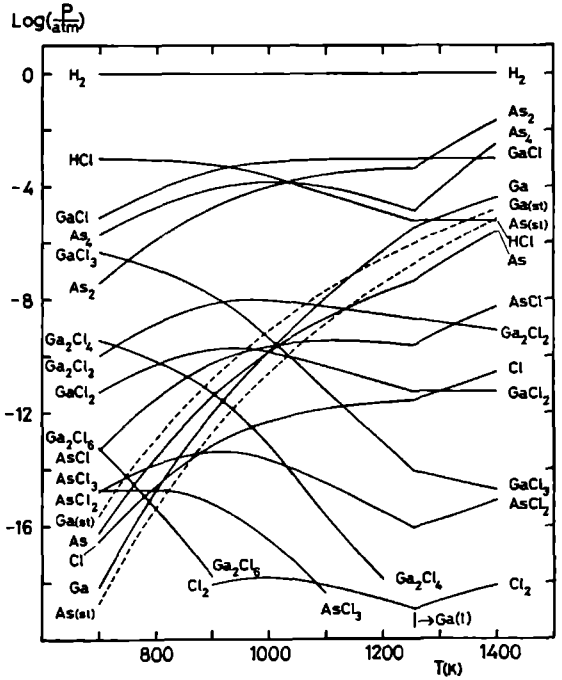

Fig. 12 Gas phase composition of GaAs in equilibrium with 0.1% HCl in H_2 at 1 atm total pressure as a function of temperature. Only the relevant pressures are indicated as well as the gallium and arsenic chlorides. Above 1256 K liquid gallium is present.
The dashed lines indicate the partial pressure of As and Ga in equilibrium with stoichiometric GaAs.

In fig. 12 the etching of GaAs with 0.1% HCl in H_2 is represented. At low temperatures only little HCl is converted into GaCl, however already at 930 K half of the hydrogen chloride has reacted, whereas at high temperatures gallium chloride is by far the major chloride species. This is illustrating the greater reactivity, in H_2, of HCl compared with H_2O, as the latter is just half converted at 1290 K. The selectivity to gallium is also larger; P_{GaCl} is 8 decades higher than P_{AsCl} at 700 K and still 5 decades at 1400 K. Thus the temperature where liquid gallium is segregated is only reached at 1256 K. Then the release of arsenic species into the gas phase is facilitated. As the rise of P_{Ga} with temperature then slows down and P_{GaCl} remains at its maximum value of 10^{-3} atm, the decrease of P_{HCl} is stopped. Therefore the gallium species, with more than one Cl bonded per Ga, are then relatively more abundant in the gas phase.

Table 5
Temperature limit for incongruent evaporation

System	T (K)
N_2	794
0.1% H_2 in N_2	825
0.1% H_2O in H_2	1240
0.1% HCl in H_2	1255.6
0.1% AsH_3 in H_2	1255.8

A comparison of the temperature, where the formation of liquid gallium starts, learns that the effectivity to maintain congruent loss of gallium and arsenic species in the gas phase, is increasing in the order $N_2 < H_2 << H_2O$ in $H_2 < HCl$ in $H_2 \simeq AsH_3$ in H_2. This efficiency is a combination of reactivity and selectivity towards gallium. If T_{crit} for an etchant is lower than 794 K, the value for an inert carrier gas, it reacts preferably with arsenic. Arsine is preventing most effectively liquid gallium formation. The introduced AsH_3 is a complete substitute for the arsenic which would otherwise evaporate. HCl and H_2O are the counterparts of arsine, as they allow congruent evaporation by

merely compensating, instead of only preventing, evaporation of arsenic, in the form of gallium chlorides and oxides. It can be seen that reactivity and selectivity of HCl is maximal, as only formation of GaCl is realistic in this temperature region. Though H_2O is only converted 40%, it is still quite effective to prevent gallium segregation, as it is very selective. H_2 is, though it reacts with gallium and arsenic, not really an etchant, on the other hand also not as inert as N_2.

4. Conclusion

Three aspects related with high-temperature processes, in particular gas phase etching and decomposition, are studied for GaAs.

The structure of the bare surface points to the fact that not only (111), but also (100) and perhaps (110), are F-faces, showing growth and etching via steps, if reconstruction and relaxation is taken into account. It is shown that for (100) the Ga-dimerization is unstable compared with the arsenic reconstruction. This results for the As stabilized structures in a connected net of strong bonds, making it indeed favourable to etch via steps. In etching (100) is not very eager to release As, and the top layer tries to remain arsenic rich. The stability of the As-As dimers has also consequences for the steps on (111)Ga. They will be very stable in comparison with the steps on (111)As, where the gallium dimerization is unlikely. So on (111)Ga pronounced steps will be present, whereas this is less probably on (111)As. On (110) the etching is fastest in the $[1\bar{1}0]$ direction, though it is possible that a stabilization in [001] is present. Then the influence of steps will be noticable.

Theoretically the existence region is extended to the As-rich side if Frenkel disorder on the arsenic sublattice (V_{As}-As_i) is assumed to be the dominant point defect equilibrium. The arsenic pressure which should be applied to obtain a stoichiometric crystal is low compared with the experimentally derived values. So kinetic barriers in the arsenic incorporation are likely to be present.

A thermodynamical study of the gas phase composition in the Ga-As system learns that arsenic is most eager to evaporate, leading to gallium droplets at already low temperatures. Adding hydrogen in the system shifts the occurence of droplets with 200 degrees as H forms compounds with gallium. In chlorine and oxygen containing systems, the most important chlorides and oxydes are GaCl, respectively GaOH and Ga_2O. These elements mainly react with gallium and with respect to stoichiometry, compensating for the arsenic loss due to evaporation. Of the two elements chlorine is most reactive and selective towards gallium

Acknowledgements

The present investigations have been carried out under the auspices of the Netherlands Foundation for Chemical Research (SON) with financial support from the Netherlands Organization for the advancement of pure Research (ZWO). I am indebted to Professor L.J. Giling for the many fruitful discussions. I would like to thank Mrs. W.P.J.H. Jacobs and K.E.P. v Bommel for performing calculations and Mrs. A.F. Lourens and J. H. Janssen for the illustrations.

REFERENCES

[1] S.N.G. Chu, C.M. Jodlauk and W.D. Johnston, J. Electrochem. Soc. 130 (1983) 2398
[2] C.T. Foxon, J.A. Harvey and B.A. Joyce, J. Phys. Chem. Solids 34 (1973) 1693
[3] C.Y. Lou and G.A. Somorjai, J. Chem. Phys. 55 (1971) 4554
[4] R. Bhat, B.J. Baliga and S.K. Ghandhi, J. Electrochem. Soc. 122 (1975) 1378
[5] E.I. Givargizov and R.A. Babasian, J. Electr. Mat. 9 (1980) 883
[6] S. Dorschchand, L. Däweritz and H. Berger, Crystal Res. Technol. 18 (1983) 1359
[7] J.G.E. Gardeniers, H.H.C. de Moor and W.P.J.H. Jacobs, to be published
[8] H.H.C. de Moor, this thesis, ch. 2
[9] H.H.C. de Moor, this thesis, ch. 3
[10] H.C. Gatos and M.C. Lavine, J. Electrochem. Soc. 107 (1960) 427
[11] H.D. Barber and E.L. Heasell, J. Phys. Chem. Solids 26 (1965) 1561
[12] D.H. Reep and S.K. Ghandhi, J. Crystal Growth 61 (1983) 449
[13] D.W. Shaw, J. Crystal Growth 31 (1975) 130
[14] L. Hollan and J.M. Durand, J. Crystal Growth 46 (1979) 665

[15] R. Cadoret in: Current Topics in Materials Science, Vol. 5, ch. 2, Ed. E. Kaldis, (North-Holland, Amsterdam, 1980)
[16] R.C. Sangster in: Compound Semiconductors, Vol. 1, p. 241, Ed. R.K. Willardson and H.L. Goering (Reinhold, New York, 1962)
[17] W.J.P. van Enckevort and L.J. Giling, J. Crystal Growth 45 (1978) 90
[18] D.J. Chadi, Phys. Rev. Letters 52 (1984) 1911
[19] F. Hottier and J.B. Theeten, J. Crystal Growth 48 (1980) 644
[20] K. Jacobi, Surface Sci. 132 (1983) 1
[21] J.H. Neave and B.A. Joyce, J. Crystal Growth 44 (1978) 387
[22] D.J. Chadi, C. Tanner and J. Ihm, Surface Sci. 120 (1982) L425
[23] A. Kahn, Surface Sci. Reports 3 (1983) 193
[24] R. Chang and W.A. Goddard III, Surface Sci. 144 (1984) 311
[25] C. Astaldi, L. Sorba, C. Rinaldi, R. Mercuri, S. Nannarone and C. Calandra, Surface Sci. 162 (1985) 39
[26] D.W. Shaw, J. Phys. Chem. Solids 36 (1975) 111
[27] K.-H. Bachem and M. Heyen, J. Crystal Growth 55 (1981) 330
[28] J.L. Gentner, Philips J. Res. 38 (1983) 37
[29] J. Bloem, Y.S. Oei, H.H.C. de Moor, J.H.L. Hanssen and L.J. Giling, J. Electrochem. Soc. 132 (1985) 1973
[30] J. van de Ven, J.L. Weyher, H. Ikink and L.J. Giling, to be published in J. Electrochem. Soc.
[31] M.A. DiGiuseppe, A.K. Chin, F. Ermanis and L.J. Peticolas, J. Crystal Growth 73 (1985) 311
[32] R.F. Brebrick, Met. Trans. 8A (1977) 403
[33] M.B. Panish, J. Crystal Growth 27 (1974) 6
[34] M. Tmar, A. Gabriel, C. Chatillon and I. Ansara, J. Crystal Growth 69 (1984) 421
[35] J.R. Arthur, J. Phys. Chem. Solids 28 (1967) 2257
[36] V.V. Rakov, B.D. Lainer and M.G. Mil'vidskii, Russ. J. Phys. Chem. 44 (1970) 922
[37] I. Barin, O. Knacke and O. Kubaschewski, Thermochemical Properties of Inorganic Substances (Supplement) (Springer, Berlin 1977)
[38] G. De Maria, L. Malaspina and V. Piacente, J. Chem. Phys. 52 (1970) 1019
[39] P. Klima, J. Silhavy, V. Rerabek, I. Braun, C. Cerny and R. Holub, J. Crystal Growth, 32 (1976) 279
[40] JANAF Thermochemical Tables, 1982 Supplement, J. Phys. Chem. Ref. Data 11 (1982) 695
[41] D.D. Wagman, W.H. Evans, V.B. Parker, R.H. Schumm, I. Halow, S.M. Bailey, K.L. Churney and R.L. Nuttal, "NBS tables of chemical thermodynamic properties", J. Phys. Chem. Ref. Data 11 (1982) supplement 2
[42] M. Tirtowidjojo and R. Pollard, J. Crystal Growth 77 (1986) 200
[43] A.N. Morozov, V.Y. Bublik and O.Yu. Morozova, Cryst. Res. Technol. 21 (1986) 749
[44] D.T.J. Hurle, J. Phys. Chem. Solids 40 (1979) 613
[45] H.H.C. de Moor, this thesis, ch. 6

[46] J. Nishizawa, H. Otsuka, S. Yamakoshi and K. Ishida,
Japan. J. Appl. Phys. 13 (1974) 46
[47] J. Nishizawa, Y. Okuno and H. Tadano, J. Crystal Growth 31 (1975) 215
[48] P.D. Dapkus, H.M. Manasevit, K.L. Hess, T.S. Low and G.E. Stillman,
J. Crystal Growth 55 (1981) 10
[49] J.A. Van Vechten, J. Electrochem. Soc. 122 (1975) 419
[50] V.T. Bublik, M.G. Mil'vidskii and V.B. Osvenski, Sov. Phys. J. 23 (1980) 1
[51] T. Nakanisi, J. Crystal Growth 68 (1984) 282
[52] P. Skeath, C.Y. Su, I. Lindau and W.E. Spicer, J. Crystal Growth 56 (1982) 505
[53] C.D. Thurmond, J. Phys. Chem. Solids 26 (1965) 785
[54] Handbook of Chemistry and Physics, 60th ed., Ed. R.C. Weast
(CRC Press, Cleveland, OH, 1979-80)
[55] D. Battat, M.M. Faktor, I. Garrett and R.H. Moss,
J. Chem. Soc. Faraday Trans. I 70 (1974) 2280
[56] V. Raziunas, G.J. Macur and S. Katz, J. Chem. Phys. 39 (1963) 1161
[57] G. Dittmer and U. Niemann, Philips J. Res. 37 (1982) 1
[58] I. Barin, O. Knacke and O. Kubaschewski, Thermochemical Properties of Inorganic
Substances (Springer, Berlin, 1973)
[59] L.G. Gorokhova and M.Zh. Makhmetov, Deposited Doc. 1974, VINITI 2381-74
[60] B.I. Noläng, Svensk Energidata, University of Uppsala (1985)
[61] L.G. Gorokhova, V.P. Malyshev, M.Zh. Makhmetov and E.A. Buketov,
Deposited Doc. 1974, VINITI 711-74
[62] L.G. Gorokhova and M.Zh. Makhmetov, Deposited Doc. 1974, VINITI 466-74
[63] JANAF Thermochemical Tables 2nd ed., NSRDS-NBS 37
(Natl. Bur. Std. US, Washington, DC, 1971)
[64] H.J. Rijks, J. Bloem and L.J. Giling, J. Crystal Growth 47 (1979) 397
[65] J. Bloem and L.J. Giling, in: Current Topics in Materials Science
Vol. 1, ch. 4, Ed. E. Kaldis, (North-Holland, Amsterdam, 1978)
[66] P.D. Kirchner, J.M. Woodall, J.L. Freeouf and G.D. Pettit,
Appl. Phys. Lett. 38 (1981) 427
[67] C. Chatillon and C. Bernard, J. Crystal Growth 71 (1985) 433
[68] JANAF Thermochemical Tables, 1974 Supplement,
J. Phys. Chem. Ref. Data 3 (1974) 311

In this thesis three subjects relevant for CVD of semiconductor crystals are discussed:

1. Adsorption on crystal surfaces
2. Near equilibrium growth
3. Trapping of dopants

In the first part of this thesis a better understanding is attained of the crystal growth processes taking place on a semiconductor surface. The notion that growth units adsorb on the surface and diffuse to steps is given a theoretical basis. Up to now, no conclusive model is presented explaining step growth on a Si(100) surface. In this study a consistent view is given on Si(100), based on the intrinsic properties of the surface and on adsorption of growth units and impurities on that surface.

In chapter 2 an adsorption model is presented, based on Langmuir chemisorption, for the attachment, of all gas phase species present in the Si-H system, on a Si(111) surface. It is outlined how to calculate the adsorption energy in terms of enthalpy and entropy. Together with the partial pressures in the gas phase this allows calculation of the surface coverage. It is discussed that in particular the strong dependence of the surface coverage on the bond strength is a problem in the adsorption calculations. An inaccaracy of only 10% can drastically change the picture, one obtains of the surface coverage. This is illustrated on the basis of the coverage with hydrogen (H). Dependent on the choice of the bond strength the surface can be fully covered or merely bare at high temperatures. Taken into account the experimental observation of step growth, it can be concluded that at low temperatures the surface is fully covered with H, whereas at elevated ones the surface is essentially bare. A comparison with the transition between poly- and monocrystalline growth, as a function of total H_2 pressure, confirms this view and demonstrates the benefit of working under reduced pressures.

It is shown that only the formation of chemical bonds leads to appreciable surface coverages. The important consequence is that SiH_4 can not be regarded as a growth unit which incorporates at the step. It will either decompose on the surface or in the gas phase to SiH_2, what is shown to be the dominant adsorbed growth species. Thus radicals should be considered more in gas phase calculations

In chapter 3 the adsorption model is applied to the Si(100) surface to describe the growth from silane. It is demonstrated that starting from a reconstructed surface the coverage with growth units is not significantly higher than on Si(111). Though silicon species have the possibility to form two bonds, the stability of the surface is increased so much by the dimerization that the tendency to adsorb is only low. This points to the fact that one should be very careful not to overestimate the coverage of semiconductor surfaces, as they all are stabilized, either by forming new bonds (reconstruction) or rearrangements (relaxation). In all these cases where the adsorption process removes this stabilization, the adsorbing species must raise this energy.

For a reconstructed surface, the adsorption model must take into account the structure of the surface and the way the species adsorb. For a Si(100) surface it is assumed that no dimer bond can be present adjacent to a double-bonded adsorbate. This model directly explains step growth. It tells that silicon must always break dimer bonds upon adsorption, whereas in case of hydrogen attachment the reconstruction can be maintained. It also gives the clue to a model where simultaneous attachment of two single-bonded adsorbates lead to step growth. So dimerization of a (100) surface leads to a low surface coverage at high temperatures and to a mechanism which makes it favourable to attach adjacent to a step.

Chapters 4 and 5 illustrate very nicely the use of thermodynamics in calculating the gas phase composition. A method is devised which makes it possible to grow epitaxial silicon layers in a furnace with a constant growth rate. To overcome the depletion, which is in a furnace enhanced by the depostion on the hot walls, a system is used where the

supersaturation remains low. To obtain a constant supply of silicon, the total silicon content introduced is high. The low supersaturation is then achieved by an accurate balancing of reactions which deposit silicon and other which etch it. By favouring the silicon forming reactions as the gas proceeds in the reactor, a constant supply of silicon can be obtained. Two systems are studied, one containing Cl the other I. For the first it is demonstrated that indeed the thermodynamical predictions come out and a constant growth rate could be achieved. It is demonstrated that the iodine system has advantages when working under reduced pressures, as the solubility of silicon then decreases with temperature.

In chapter 6 the incorporation of sulfur in GaAs is studied. The experiments, available in literature, could well be explained by assuming that for too high growth rates, the dopants are buried: subsurface trapping. Then the equilibrium incorporation breaks down and an excess will be built in. This is shown to be a general phenomenon for III-V compounds as the diffusion is rather slow. The trapping leads to an orientation dependence; it is indicated that the incorporation of dopants is decreased by reconstruction and relaxation of the semiconductor surface.

In chapter 7 a theoretical basis is given for high-temperature processes of GaAs, in particular etching and thermal decomposition. A study of the surface structure of GaAs learns that (111)A, (111)B, but also (100) and (110) are F-faces, with growth and etching via steps. The formation of As-As dimers gives a great stabilization of the (100) surface and of the {100} type steps on (111)Ga. It is unlikely that gallium is able to show reconstruction due to its low electron density. Therefore (100) will try to be arsenic-rich. The {100} type steps on (111)As are unstable, as no Ga-Ga-stabilization occurs. A study of the relation between stoichiometry and gas phase composition gives a whole new idea about the existence region of GaAs. It leads also to the idea that the III/V ratio in the bulk is in growth experiments determined by kinetics. Thermodynamical calculations on the Ga-As-H and Ga-As-H-Cl and Ga-As-H-O systems conclude this thesis and give on good idea on the reactivity of gallium versus arsenic in different etching environments.

In dit proefschrift zijn drie onderwerpen bestudeerd die van belang zijn voor CVD van halfgeleider kristallen:

1. Adsorptie aan kristaloppervlakken
2. Groei bij bijna-evenwicht
3. Het begraven van dotering

In het eerste deel van dit proefschrift wordt tot een beter begrip gekomen van de kristalgroei-processen die zich afspelen op het oppervlak van een halfgeleider. Aan de opvatting dat groeideeltjes adsorberen op het oppervlak en naar de stappen diffunderen wordt een theoretisch fundament gegeven. Tot nu toe, is er nog geen sluitend model gepresenteerd dat stappengroei op een Si(100) oppervlak kan verklaren. In dit boekje wordt een konsistente kijk op Si(100) gegeven dat gebaseerd is op de intrinsieke eigenschappen van het oppervlak en de adsorptie van groei-eenheden en verontreinigingen op dat oppervlak.

In hoofdstuk 2 wordt een adsorptiemodel gegeven, gebaseerd op Langmuir chemisorptie, voor het hechten van alle in het Si-H systeem aanwezige deeltjes, op een Si(111) oppervlak. Een methode wordt gepresenteerd waarmee de adsorptie-energie wordt uitgerekend uitgaande van de enthalpie en entropie. Samen met de partiele drukken in de gasfase maakt dit het mogelijk om de bedekkingsgraad uit te rekenen. Er wordt aangegeven dat met name het feit dat de bedekking sterk afhangt van de bindingssterkte een probleem is in adsorptie-berekeningen. Een onnauwkeurigheid van slechts 10% kan het beeld dat men heeft van de bedekking drastisch veranderen. Dit is geillustreerd aan de hand van de waterstof-bedekking. Afhankelijk van de keuze van de bindingssterkte is het oppervlak volledig bedekt of vrij leeg bij hoge temperatuur. Met meename van de experimenteel waargenomen stappengroei, kan gekonkludeerd worden dat bij lage temperaturen het oppervlak volledig bedekt is met H, terwijl het bij hoge in principe leeg is. Een vergelijking met de overgang tussen poly- en éénkristallijne groei, als funktie van de totale H_2-druk, bevestigt deze kijk en geeft tevens het voordeel aan van het werken bij lage druk.

Het wordt aangetoond dat alleen vorming van, sterke, chemische bindingen kan leiden tot merkbare oppervlakte-bedekkingen. Het belangrijke gevolg hiervan is dat SiH_4 niet kan worden beschouwd als een groeideeltje dat aan de stap inbouwt. Het ontleedt of op het oppervlak of in de gasfase tot SiH_2, dat het belangrijkste geadsorbeerde groeideeltje blijkt te zijn. Bijgevolg moeten radikalen zeker niet worden vergeten in gasfase berekeningen.

In hoofdstuk 3 wordt het adsorptiemodel toegepast op een Si(100) oppervlak om de groei met silaan te beschrijven. Het wordt aangetoond dat uitgaande van een gerekonstrueerd oppervlak, de bedekking met groeideeltjes niet wezenlijk hoger is dan op Si(111). De stabiliteit van het oppervlak is zoveel vergroot door de dimerisatie dat, ofschoon silicium deeltjes in principe twee bindingen kunnen vormen, de neiging om te adsorberen klein is geworden. Dit geeft aan dat men op moet passen om de bedekking van halfgeleider oppervlakken niet te hoog in te schatten. Ze zijn namelijk gestabiliseerd door het vormen van nieuwe bindingen (rekonstruktie) of door relaxatie. In al die gevallen dat adsorptie deze stabilisatie verwijdert, moeten de adsorberende deeltjes deze opbrengen.

Voor een gerekonstrueerd oppervlak moet het adsorptiemodel rekening houden met de struktuur van het oppervlak en de wijze waarop de deeltjes adsorberen. Voor een Si(100) oppervlak wordt aangenomen dat geen dimeer binding aanwezig kan zijn naast een dubbel gebonden adsorbaat. Dit model verklaart meteen de stappengroei. Het geeft aan dat silicium altijd een binding moet verbreken om te adsorberen, terwijl in geval van H-adsorptie de rekonstruktie gehandhaafd kan blijven. Het geeft ook de direkte aanzet tot een model waar simultane aanhechting van twee enkelgebonden adsorbaten tot stappengroei leidt. Zodoende leidt dimerisatie van een (100) oppervlak tot een lage oppervlakte-bedekking bij hoge temperaturen en tot een mechanisme dat het aanhechten aan een stap bevoordeelt boven willekeurige aangroei.

De hoofdstukken 4 en 5 zijn een mooie illustratie van het gebruik van thermodynamika om gasfase samenstellingen te berekenen. Er is een methode bedacht om epitaxiale silicium lagen in een oven te groeien bij een konstante groeisnelheid. Om depletie te voorkomen, die in een oven versterkt wordt door depositie op de hete wanden, is er bij lage oververzadiging gewerkt. Om een konstante aanvoer van silicium te krijgen, is de totale input van silicium groot. De lage oververzadiging wordt dan bereikt door een zorgvuldig manipuleren met elkaar

tegenwerkende reakties, nl. enkele die silicium vormen en andere die het wegnemen. Door de siliciumvormende belangrijker te laten worden naarmate het gas verder in de reaktor komt, kan een konstante aanvoer van silicium bereikt worden. Er zijn chloor- en jodium-houdende systemen bekeken. Voor het eerste systeem is aangetoond dat de thermodynamische voorspellingen inderdaad prachtig uitkomen en een konstante groeisnelheid kon bereikt worden. Het jodium system heeft voordelen bij gereduceerde druk, aangezien de oplosbaarheid van silicium hier daalt met de temperatuur.

In hoofdstuk 6 is de inbouw van zwavel bestudeerd. De in de literatuur beschikbare experimenten konden goed verklaard worden door aan te nemen dat voor te hoge groeisnelheden, de doterings-elementen begraven worden. Dan wordt het inbouw-evenwicht verbroken en een overmaat ingebouwd. Dit is een algemeen verschijnsel voor III-V verbindingen, aangzien diffusie daarin langzaam is. Het begraven leidt tot een orientatie-afhankelijkheid. De inbouw van dotering wordt verminderd door relaxatie en reconstruktie van het halfgeleider oppervlak.

In hoofdstuk 7 wordt een theoretisch fundament gelegd voor hoge temperatuur processen van GaAs, in het bijzonder etsen en thermische ontleding. Een studie van de oppervlakte-struktuur van GaAs geeft aan dat (111)A, (111)B, maar ook (100) en (110) F-vlakken zijn, waar groeien en etsen plaatsvinden via stappen. De vorming van As-As dimeren geeft een aanzienlijke stabilisatie van het (100) oppervlak en van {100}-achtige stappen op (111)Ga. Het is onwaarschijnlijk dat gallium ook rekonstruktie te zien geeft, t.g.v. zijn lage elektronendichtheid. Dientengevolge zal (100) arseen-rijk proberen te zijn. De {100}-achtige stappen zijn instabiel t.g.v. het ontbreken van Ga-Ga-stabilisatie. Een studie naar de relatie tussen stoichiometrie en samenstelling van de gasfase geeft een heel andere kijk op het bestaansgebied van GaAs. Het leidt ook tot de konklusie dat de III/V verhouding in het kristal bij groei-experimenten wordt bepaald door kinetiek. Evenwichtsberekeningen aan Ga-As-H, Ga-As-H-Cl en Ga-As-H-O systemen besluiten dit proefschrift en geven een goed beeld van de reaktiviteit van gallium t.o.v. arseen in verschillende ets-omgevingen.

CURRICULUM VITAE

Hugo de Moor werd op 19 augustus 1956 geboren te Tilburg, alwaar hij in 1974 zijn eindexamen atheneum B haalde aan het Cobbenhagen college.
In datzelfde jaar begon hij aan de Katholieke Universiteit te Nijmegen met de studie scheikunde. Na het behalen van het kandidaatsexamen S3 in 1977, studeerde hij af in december 1981. Zijn doktoraal examen omvatte de hoofdrichtingen vaste stof chemie (Prof. Dr. J. Bloem) en molekuulspektroskopie (Prof. Dr. E. de Boer) alsmede het kaputkollege chemische technologie (Prof. Dr. C. van Heerden).
In het kader van het hoofdvak vaste stof chemie werd 1 jaar als student-assistent gewerkt aan een projekt dat als doel had goedkope foto-voltaische zonnecellen te ontwikkelen. Tevens werd geassisteerd bij diverse praktika. Daarnaast was hij drie jaar penningmeester van de scheikunde-studenten vereniging Sigma en aktief in het raadswerk.
Van 1 januari '82 tot '86 was hij als wetenschappelijk ambtenaar in dienst van ZWO/SON verbonden aan de afdeling Vaste Stof Fysika III en werd het in dit proefschrift beschreven onderzoek uitgevoerd onder leiding van Prof. Dr. J. Bloem en Prof. Dr. L.J. Giling.
Tijdens de promotieperiode assisteerde hij bij het natuurkundepraktikum en verzorgde hij de werkkolleges chemie en samenleving en algemene chemie.
Sinds 1 oktober 1986 is Hugo de Moor in de dienst van Philips (Elcoma) te Nijmegen. Hij heeft daar een taak in de ontwikkeling van de groei, m.b.v. MOCVD, van epitaxiale GaAs-AlGaAs lagen voor solid state lasers.

STELLINGEN

1. Ten onrechte wordt voor kristallen met een zinkblende- of diamantstruktuur rekonstruktie van het (100)-oppervlak niet meegenomen.

   - Dit proefschrift
   - R. Cadoret in: Current Topics in Materials Science Vol. 5, ch. 2 Ed. E. Kaldis, (North-Holland, Amsterdam, 1980)

2. De stoichiometrie van een, m.b.v. MOCVD gegroeide, GaAs-laag kan beter beschreven worden, door van de adsorbaten de III/V-verhouding te nemen, in plaats van, zoals gebruikelijk, van de gasfase deeltjes.

   - T. Nakanisi, J. Crystal Growth 68 (1984) 282

3. Bij hoge zink-dotering van GaAs is het zinvol om de vorming van $ZnAs_2$ en Zn_3As_2 mee te nemen.

   - R.W. Glew, J. Crystal Growth 68 (1984) 44

4. De evenredigheid van de doterings-inbouw met de partiaaldruk van het mono-atomaire element, is een indikatie dat er een goede uitwisseling is van de ingebouwde dotering met het kristaloppervlak.

5. De thermische ontleding van III-V verbindingen vertoont een kinetisch gelimiteerde sublimatie van de V-komponent. Dit wordt pas, ten dele, opgeheven als het III-element als een vloeibare laag op het oppervlak aanwezig is, zodat dán ook een SLV-mechanisme valt waar te nemen.

   - S.N.G. Chu, C.M. Jodlauk en W.D. Johnston Jr., J. Electrochem. Soc. 130 (1983) 2398

6. De aard van een dislokatie is van wezenlijk belang in een diskussie over het verband tussen dislokaties en het funktioneren van een chip.

   - B.O. Kolbesen en H.P. Strunk in: VLSI Electronics: Microstructure Science Vol. 12 ch. 4, Eds. N.G. Einspruch en H.R. Huff, (Academic Press, 1985)

7. De bruine kleur van de "$Cr_2O_7^{2-}$-Cl^--oplossing" van Adachi en Oe is het gevolg van reduktie van het bichromaat tot Cr^{3+} door het chloride. Deze degradatie maakt de oplossing ongeschikt om groeven te etsen.

   - S. Adachi en K. Oe, J. Electrochem. Soc. 131 (1984) 126

8. De huidige bezuinigingen in het hoger onderwijs leiden op langere termijn tot grote kosten.

9. De volkswijsheid dat mei-regen doet groeien is toe aan herwaardering.

10. Het idee dat een tekstverwerker tijd bespaart is onjuist.

    - Dit proefschrift.

Hugo de Moor
28 januari 1987